ANALYSIS OF LIPIDS FROM *CHROMULINA FREIBURGENSIS* FOR THEIR POTENTIAL USE AS BIOFUELS

by

Amanda Mondloch

A thesis submitted in partial fulfillment of the
requirements for the degree of

Interdisciplinary Master of Science

Montana Tech of The University of Montana

2012

Abstract

Many uncertainties concerning energy availability exist for the future. Finding environmentally friendly, alternative energy sources is a pressing issue, especially for countries that do not have obtainable oil resources. Energy consumption is currently at an all-time high and is expected to increase by 50% by 2020. The world consumes 84.2 million barrels of oil per day and 18.7 million barrels are used by the United States alone. Fifty-seven percent (57%) of the United States' crude oil is imported and 8.9 million barrels a day are used for motor vehicles. It is uncertain how long the oil reserves will last and therefore it is imperative to find economically viable, renewable energy sources with reduced waste emissions. Biofuels are renewable sources that have received much attention in recent years because they have potential to be environmentally friendly and readily available. Microalgae are a source of biofuels that have many advantages over other biofuel sources. Algae do not require agricultural land to grow and can grow in waste water. Algae fix atmospheric carbon which makes them nearly carbon neutral and their fuel products do not contain sulfur or many other toxins that can be harmful to the environment.

Chromulina freiburgensis is a species of algae that was isolated from the water of the Berkeley Pit in Butte, Montana and has not yet been characterized in terms of biofuel potential. The goal of this project was to isolate and grow *C. freiburgensis*, and to extract, characterize, and quantify the lipids produced from this alga. Fatty acid methyl esters were extracted and quantified via transesterification. Using the growth conditions presented in this study, *C. freiburgensis* did not produce an adequate amount of lipids to be considered a potential biofuel source.

Keywords: algae, biofuels, lipids, *Chromulina freiburgensis*

Dedication

I would like to thank my family, especially Dan, for their patience and support throughout my education.

Acknowledgements

Thank you, Dr. Doug Cameron, for all of your assistance and guidance. I also appreciate all of the help from Dr. Marisa Pedulla and Dr. Grant Mitman. I would also like to say thanks to the Chemistry and Geochemistry Department at Montana Tech and the National Center for Research Resources for funding this project. “The project described was supported by Award Number P20RR016455 from the National Center For Research Resources. The content is solely the responsibility of the authors and does not necessarily represent the official views of the National Center For Research Resources or the National Institutes of Health.”

Table of Contents

List of Tables

List of Figures

Introduction

Finding alternative sources of energy has been an important topic since the oil crisis in the 1970's [1]. Not only is oil availability a concern for the future, but its combustion has a negative impact on the environment in terms of greenhouse gas emissions [2-4]. Microalgae have received much attention worldwide in recent years because they have many advantages over other natural energy sources. Algae grow almost everywhere including sea water, freshwater, sewage, and in waste lands [5]. Algae also grow especially well in areas where carbon dioxide is present in abundance for example near coal fired power plants. Algae can also grow in industrial settings where carbon is deficient but nitrogen and phosphorous are abundant [6]. Algae are capable of multiplying very quickly and can produce high neutral lipid and polysaccharide yields as byproducts of photosynthesis under the appropriate conditions [2, 7].

Based on previous research, several species of algae have proven to be abundant producers of oils and lipids and have been investigated as biofuel sources. Lipids comprise up to 50% of the dry mass of *Chlorella sp.*, *Chlamydomonas sp*, and *Neochloris oleoabundans* [5, 6]. Some species of algae such as *Caulerpa racemesa* and *Pterocladia capillacea* also have high polysaccharide contents [8]. Polysaccharides can be extracted from the biomass and used to make ethanol for fuel or feedstock.

1. Background

1.1. Biofuels

Biofuels are solids, liquids, or gases that are made from recent biomass [9-11]. Biofuels are originally produced from photosynthesis. Biofuels are alternative fuel sources made from a

variety of natural crops including corn, rapeseed, soybean, sunflower, flax, and hemp. They can also be produced from waste vegetable oils and microalgae oils.

Biofuels are classified as 1st, 2nd, 3rd, or 4th generation [13, 14, 15, 16]. First generation biofuels are made from feedstocks that have been used as food such as sugar, starch, or vegetable oil. Second generation biofuels are fuels that are made from non-food feedstocks such as lignocellulose from grasses, agricultural residues, and wood and forestry residues [12]. Third generation biofuels are also made from non-food feedstocks, but the fuel is identical to their petroleum counterparts and they are carbon neutral. Algae are a third generation biofuel source and are considered carbon neutral because they use sunlight and carbon dioxide for photosynthesis and therefore the amount of carbon used for growth essentially equals the amount of carbon released into the atmosphere when these fuels are burned. Fourth generation biofuels are made from genetically engineering third generation biofuels and are designed to be carbon negative.

The major forms of biofuels today are biodiesel and bioethanol [12]. Bioethanol can be used as an additive to gasoline to make mixtures of E15 (15% ethanol, 85% gasoline) and E85 (85% ethanol, 15% gasoline). Lignocellulosic ethanol is a second generation biofuel that is produced from non-food residual biomass such as stems, leaves, wood chips, and non-food crops including switchgrass and algae, however, the major feedstocks for bioethanol are sugarcane and corn [13, 14, 15, 16]. Bioethanol is a particulate free burning fuel source that combusts cleanly with oxygen [1]. Greenhouse gases may be reduced 12% by production and combustion of ethanol versus conventional fuel sources [13]. Ethanol can also be used to make biodiesel.

Biodiesel is an alternative to diesel, and many engines can use 100% biodiesel. Biodiesel is produced from vegetable oil, plant oil, and animal fats. The majority of biodiesel feedstock is soybean, canola seed, rapeseed, sunflower, and palm oil.

1.1.1. Advantages of Biofuels

The world's petroleum reserves are expected to be depleted in less than 50 years at the current rate of consumption [1, 14]. Biofuels are a biodegradable, renewable energy source that can, in principle, be sustainably supplied. Biofuels are environmentally friendly; they create no net increase in carbon dioxide released into the atmosphere, have no aromatic compounds, and have no sulfur content which makes burning biofuels 90% less toxic compared to common diesel sources [1]. Biofuels have better efficiency than conventional diesel fuel in terms of flash point and biodegradability, and they have economic potential due to the ever increasing prices of non-renewable fossil fuels.

When algal biofuels are produced via lipid extractions, a residue is left as waste. The residue from these extractions can be used as aquaculture feed, animal food supplements, or a source of pharmaceuticals [3].

1.2. Algae and its Evolution

The tree of life has three primary domains; bacteria, archaea, and eukaryotes. Bacteria and archaea are prokaryotes. Eukaryotes and prokaryotes differ in size, complexity, structure and function. First, eukaryotes are generally larger than prokaryotes with an average cell size of 10-100 microns and 0.1-0.2 microns, respectively [15]. Prokaryotes are mostly single celled individuals while eukaryotes may be unicellular or multicellular organisms. Not only are eukaryotes larger, they are much more complex than prokaryotes. Eukaryotes have membrane bound organelles such as mitochondria, chloroplasts, Golgi apparatus, and endoplasmic

reticulum [15, 16]. Prokaryotes do not have membranous organelles, a cytoskeleton, or a nuclear envelope that separates their DNA from the cytoplasm. Also, eukaryotes have multiple chromosomes consisting of linear DNA molecules and prokaryotes contain a single circular piece of DNA.

It is thought that mitochondria and chloroplasts in eukaryotes evolved from endosymbiotic bacteria. Mitochondria were originally aerobic heterotrophic prokaryotes that developed an endosymbiotic relationship with a bacterium which eventually became eukaryotic cells [15, 16]. Plant and algal chloroplasts were originally photosynthetic prokaryotes and evolved later, involving a second endosymbiotic event [15]. It is thought that there were several symbiotic events thereafter, which accounts for the diversity of plastids in algal groups [15]. Algal groups are separated taxonomically by their 18S ribosomal RNA. 18S rRNA is part of the small subunit of eukaryotic ribosomes. This particular piece of RNA is used as a target for polymerase chain reaction and phylogenetic studies because it is easily accessible and highly conserved flanking regions.

Algae are plant-like, photosynthetic, eukaryotic organisms. Algae are typically autotrophic and have a membrane bound nucleus and plastids but do not have roots, stems, leaves, or vascular tissue (Figure 1) [5]. They have relatively simple reproductive structures but can reproduce via asexual cell division or through complex sexual reproduction.

Algae are separated taxonomically into seven different divisions based on several factors such as the pigments they use for photosynthesis, storage carbohydrates, cell wall components, and flagella. The seven divisions are Euglenophyta, Chrysophyta, Pyrrophyta, Chlorophyta, Rhodophyta, Phaeophyta, and Xanthophyta [16]. They range in size from single celled

microorganisms to complex multi-cellular life forms such as giant kelps which can grow to 65 meters in length [16].

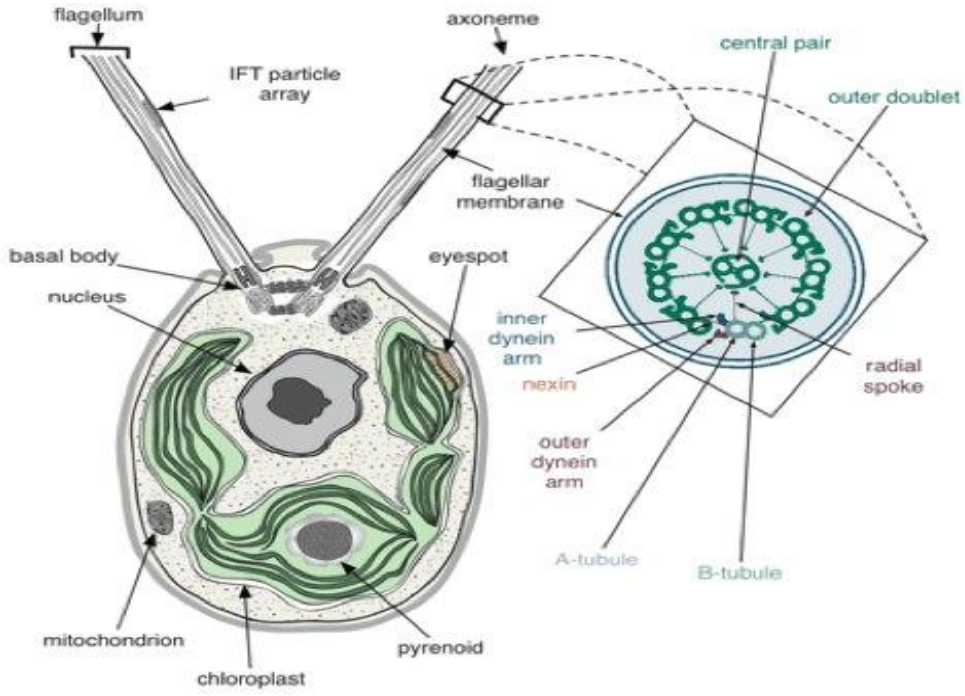

Figure 1: *Chlamydomonas* cell [17].

Algae are found in salt water, fresh water, and waste water around the world. They can be cultivated under difficult climatic conditions and produce a wide variety of commercially interesting byproducts including oils, fats, sugars, and functional bioactive compounds [5].

Algae are a very important species because they produce a large amount of the world's photosynthetic oxygen. Algae are at the base of the food chain and they are a food source for many animals. Importantly, algae may also have the potential to become large producers of biodiesel.

There are many advantages to using algae as a source of biodiesels such as:

1. They fix carbon dioxide from the atmosphere and thus reduce the amount of atmospheric CO_2 which is currently considered a global environmental problem [5, 9, 12].
2. Algal biofuels are non-toxic, biodegradable and contain no sulfur.
3. Algae can grow in conditions that may otherwise be considered unsuitable for conventional plants.
4. They provide much higher yields of biodiesel fuel than other energy sources.
5. They have higher photosynthetic efficiencies and growth rates compared to other crops.
6. Microalgal oils are more similar to conventional fuels than oils from other biofuel sources and are more stable based on their flash point values.
7. Algae can be grown in photobioreactors (better growth control) or open ponds (cheaper). The carbon source for algae growing in open ponds may come from coal fired power plants; the CO_2 and wastewater are therefore recycled.

1.3. *Lipid Metabolism in Algae*

Lipid metabolism has been extensively studied in plants and animals but little is known about the key enzymes and biochemical pathways involved in the biosynthesis of lipids in microalgae, especially *Chromulina.* Lipid metabolism is a complex process and many of the key lipid metabolizing enzymes that have been identified in algae are based on orthology to fungi and plants [18]. Most of this work has been done on the reference organism, *Chlamydomonas reinhardtii*, which may or may not represent the lipid metabolizing enzymes or products found in the same class, let alone division [19]. Genetic approaches have been used to determine the

essential genes involved in the synthesis of lipids [19]. Algal mutants have been used to determine the functions and physiological roles of lipids and metabolizing enzymes *in vivo*.

1.4. *Chromulina freiburgensis*

Chromulina freiburgensis is a single-celled golden brown alga and is a member of the class Chrysophyta [20, 21]. Members of Chrysophyta are mostly found in fresh water at a slightly acidic pH. Their cell walls tend to have a high concentration of silica and their main energy storage product is laminarin. Brown algae contain chlorophylls a and c in addition to carotenes and xanthophylls [22]. Carotenes are unsaturated hydrocarbons that aid in photosynthesis and protect algal tissues. Xanthophylls are similar in structure to carotenes but they contain oxygen. Xanthophylls absorb light wavelengths that are not absorbed by cholorophylls.

C. freiburgensis exhibits two life stages, a non-motile coccoid state and a flagellated state [20, 21]. Cells in the coccoid life stage are round in shape with a diameter ranging from 5-10 µm. Flagellated cells are 7-15 µm in length with a 3-5 µm flagellum [15, 20]. In uncontaminated environments, *C. freiburgensis* is most commonly found in the flagellated state. The strain of *C. freiburgensis* examined was isolated from the surface water of the Berkeley Pit in Butte, Montana [14]. The Berkeley Pit is an acidic mine waste lake that contains heavy metals such as iron, zinc, manganese, and copper.

2. Methods

2.1. Isolation of *Chromulina freiburgensis*

2.1.1. Initial Algal Culture

All glassware, tubes, filters, and fertilizer were autoclaved. One tablespoon of Osmocote fertilizer (ammonium nitrate, ammonium phosphate, calcium phosphate, and potassium

phosphate), 936 mL of Berkeley Pit surface water, and 10 mL of $NaNO_3$ (5.0 g/200 mL) were mixed together in an aspirator bottle [23]. A previously grown *C. freiburgensis* colony from a 1% modified acid medium (MAM) agar plate was used to inoculate the medium. The aspirator bottle was connected to continuous air flow, a constant light intensity of 100 µmol/m^2/s, and was kept at a temperature of 9.8°C in the Percival Scientific culture chamber.

2.2. Growth of Algae

2.2.1. MAM [24]

Ten mL of the initial algal culture (IAC) of *C. freiburgensis* (Figure 2) grown was used to inoculate 1000 mL of MAM in an aspirator bottle. The bottle was placed in the Percival Scientific culture chamber with constant air flow, a light intensity of 100 µmol/m^2/s, and a temperature of 9.8°C.

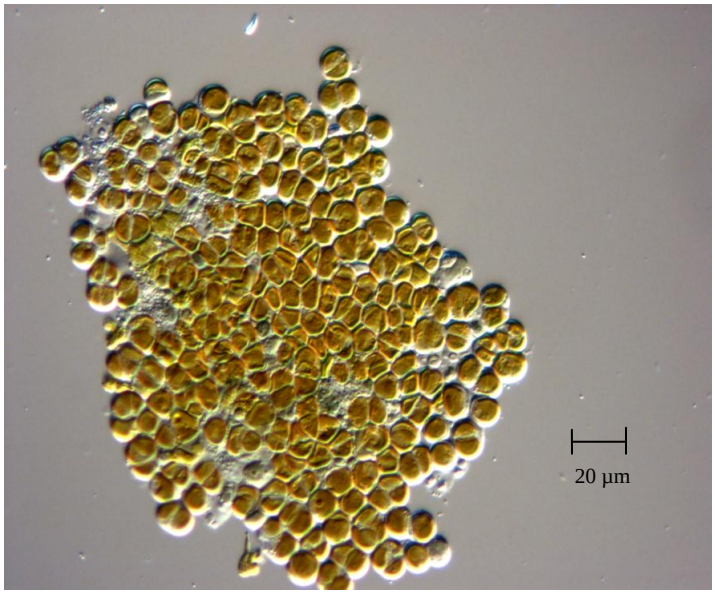

Figure 2: Light Micrograph of *Chromulina freiburgensis*

As the algal culture was used for analysis, MAM was added to the aspirator bottles allowing for a continuous supply of culture. Each culture was analyzed under the Nikon Eclipse E800 microscope to make sure it was not contaminated.

2.2.2. Berkeley Pit Water, $NaNO_3$, Osmocote Fertilizer

One tablespoon of Osmocote fertilizer, 936 mL of Berkeley Pit water, and 10 mL of $NaNO_3$ (5.0 g/200mL) were combined in a 1000 mL aspirator bottle. The medium was inoculated with 10 mL of IAC and placed in the Percival Scientific culture chamber with constant air flow, a light intensity of 100 µmol/m^2/s and a temperature of 9.8°C.

2.2.3. Acidified Bold's Basal Medium

Bold's Basal Medium (BBM) was acidified to pH 2.5 with A.C.S. reagent grade sulfuric acid obtained from JT Baker [25]. 1000 mL of Acidified Bold's Basal Medium was placed in an aspirator bottle. The medium was inoculated with 10 mL of IAC, placed in the Percival Scientific culture chamber with constant air flow, a light intensity of 100µmol/m^2/s, and a temperature of 9.8°C.

2.2.4. Algal Counts

Twenty µL of the culture was placed on a Petroff-Hausser counting slide (Figure 3) and magnified at 20x under the Nikon Eclipse E800 microscope. Five boxes in the center grid were arbitrarily selected and the algal cells were counted. The mean number of cells was calculated and inserted into the following formula to determine the number of cells/mL (1).

$$(n_1 + n_2 + n_3 + n_4 + n_5/5) \times (25) \times (50{,}000) = \#\ \text{cells/mL} \qquad (1)$$

N = the number of cells per small box
25 = the number of larger boxes in the center of the grid
50,000 = dilution factor

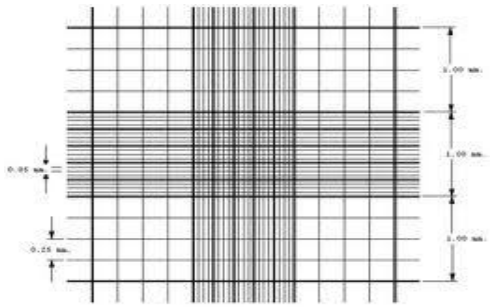

Figure 3: Petroff Hausser Counting Chamber

2.3. Lipid Extraction

2.3.1. Ether/Water Reflux

The algal culture (~500 mL) was dried in a drying oven at 70° C for 24 hours. The dried biomass (~1.0 g) was weighed and placed in a 250 mL glass round bottom flask. Thirty-five mL of reagent grade 99.8% diethyl ether obtained from Acros Organics was added to the flask and the mixture was refluxed for five hours. The solvent phase was decanted into a 45 mL glass vial for esterification. Thirty-five mL of deionized water was added to the 250 mL round bottom flask containing the solid residue and refluxed for another five hours. The aqueous solvent was filtered and concentrated by gentle heating (60°C). The concentrated aqueous extract was transferred to a glass 5 mL vial for analysis [26]. All extracts were stored in the refrigerator at a temperature of 5°C.

2.3.2. Bligh and Dyer Lipid Extraction [27]

The algal culture was dried in a drying oven at 70°C for 24 hours. The dried biomass (~1.0 g) was massed and ground into a fine powder. Three mL of A.C.S. grade chloroform:methanol (2:1) obtained from Fisher Scientific was added to the biomass. The mixture was agitated for 20 minutes at room temperature. The solvent phase was recovered by centrifugation and the whole solvent was evaporated. The organic material was re-dissolved in

98.5% hexane (Sigma Aldrich) for analysis via gas chromatography mass spectrometry (GC-MS).

2.3.3. Transesterification of Microalgae Lipids

C. freiburgensis was dried via a drying oven and a freeze dryer. The drying oven was set at 80°C and the algae were placed in it for 24 hours [28]. A dry weight was obtained (~0.5 g). The dried biomass was placed in a 50 mL glass round bottom flask where it was ground into a fine powder. Two and a half mL of A. C. S. reagent grade 2.5% sulfuric acid in methanol was added to the flask. The mixture was heated at 60°C for two hours with constant stirring. Then, the mixture was vacuum filtered and the solution containing the supernatant was transferred to a separatory funnel. Three mL of hexane was added and mixed well for 15 minutes and the hydrophobic layer was transferred to a new vessel (repeated three times). The hydrophobic layer was then washed with three mL of de-ionized water and transferred to a 45 mL vial. A.C.S. reagent grade anhydrous sodium sulfate obtained from JT Baker was added to the hydrophobic layer to remove all remaining water. Gentle heat was applied to the hydrophobic layer to concentrate.

2.4. Esterification of Lipids [26]

2.4.1. Method I-Esterification of Lipids from Bligh and Dyer Extraction

Five mL of 2.5% sulfuric acid in methanol was added to the vial containing the Bligh and Dyer lipid extract. The mixture was heated at 80°C for three hours with constant stirring. The mixture was removed from the heat and an equal volume of de-ionized water and hexane was added to the vial. The vial was mixed and the organic layer was recovered for further analysis.

2.4.2. Method II-Esterification of Lipids from Ether Reflux

Five mL of 2.5% sulfuric acid in methanol was added to the ether reflux ether extract and placed in the drying oven at 80°C for 80 minutes. Five mL of hexane were added and mixed well. The mixture was centrifuged for two minutes and the top (organic) layer was recovered. The process was repeated three times. The organic layer was further analyzed.

2.5. Polysaccharide Extraction

One liter of algae was dried in the drying oven at 80°C for 24 hours [29]. A dry weight was obtained. The dried biomass was placed in a 250 mL round bottom flask. Fifty mL of ethyl alcohol obtained from Aldrich was added to the flask. The mixture was heated for two hours at 80°C. The flask was cooled and the supernatant was removed. Fifty mL of 25°C de-ionized water was added to the flask. The mixture was stirred for two hours. The supernatant was transferred to a 150 mL beaker and all water was evaporated. Twenty mL of ethanol was added to the beaker, mixed well, and transferred to a vial. The addition of ethanol was repeated four times. The ethanol volumes were combined, centrifuged, and concentrated for analysis via liquid chromatography mass spectrometry (LC-MS).

2.6. Characterization of Lipids

2.6.1. GC-MS Method

One µL of a C_4-C_{24} standard fatty acid methyl ester (FAME) mixture catalog number 18919-1AMP (100 mg/mL hexane) obtained from Sigma Aldrich was injected via the heated needle technique into the Thermo Scientific Trace GC Ultra Model No. K24300000000080 coupled to an ITQ 1100 Mass Spectrometer (see Table 3.2.1). The FAME standard was analyzed via electron ionization (EI) and chemical ionization (CI). The GC-MS parameters used for all analyses are listed in Table 1.

Table 1: GC-MS Parameters

Trace GC Ultra Oven Parameters	
Initial Temperature	100°C (hold 1.0 minute)
Ramp #1	2°C/min until 250°C (hold 1.0 min)
Ramp #2	15°C/min until 280°C (hold 1.0 min)
Carrier Gas	Helium
Constant Flow	1.0 mL/min
PTV Mode	Splitless Injection
PTV Inlet Parameters	
Initial Temperature	280°C
Inject	0.1 min
Transfer Rate	14.5°C/sec to 280°C (hold 5 min)
ITQ 1100 MS Parameters (EI)	
Source Temperature	280°C
Start Time	3 min
Damping Gas Flow	0.3 mL/min
Microscans	3
Maximum Ion Time	25 ms
Tune File	Autotune
Full Scan	100-550 amu
Electron Lens	10 V
Electron Energy	70 eV
Emission Current	200 µamp
ITQ 1100 MS Parameters (CI)	
Source Temperature	280°C
Start Time	3 min
Damping Gas Flow	0.3 mL/min
Microscans	3
Maximum Ion Time	25 ms
Tune File	Autotune
Full Scan	100-550 amu
Electron Lens	10 V
Electron Energy	120 eV
Emission Current	200 µamp

*Acetonitrile was used as the reagent gas for all positive ion CI analyses.
Column- Restek Rxi-5MS, 30 m x 0.25 mm i. d. x 0.25 µm film thickness

The positive ion-source pressure was set by adjusting the ratio between the 1-methyleneimino-1-ethenylium ion and the adduct ion. The oven was heated to 280°C for one hour between analyses to ensure no compounds adsorbed to the column. One µL of sample from all extractions was injected, and the data were analyzed with XCalibur version 2.0 software.

2.7. Quantification of Lipids

2.7.1. Internal Standard

102.8 mg naphthalene (obtained from Sigma Aldrich) /mL hexane was made as a stock solution for an internal standard. The stock solution was diluted to make the internal standard (ISS). Ten µL of the stock solution was diluted to one mL with hexane.

The transesterification method was performed on 1.3 g of dried algae. The final volume of product dissolved in hexane after concentration was 2.5 mL. Ten µL of the ISS was added to one mL of transesterification sample. One µL was analyzed via EI and CI GC-MS.

2.7.2. Calibration Curve

Two hundred µL of the C_4-C_{24} FAME standard mixture and five µL of ISS were combined. One µL of this solution was analyzed via EI GC-MS. A series of standards were then made by serially diluting the ISS (C4-C24 FAME standard mixture with internal standard) by a factor of five with hexane. Calibration curves were developed to determine the concentration of the lipids in the transesterification extract.

2.8. Characterization of Polysaccharides

2.8.1. Standard Solutions

Standard solutions of glucose and sucrose obtained from Fisher Scientific and Sigma Aldrich, respectively were made by adding 50 µg of each to 100 mL of de-ionized water. LC-MS analyses were performed with an Agilent 1100 Series LC coupled with a Bruker Esquire 4000

APCI mass spectrometer. The column used was an Eclipse XDB-C18 column (5 µm x 4.6 µm x 150 mm). All LCMS analyses were performed using this instrument. Fifteen µL of each standard solution was injected. An isocratic elution with 50:50 methanol:water as the solvent was performed with a flow rate of 1 mL/min.

2.8.2. Polysaccharide Analysis

The concentrated sucrose standard was analyzed via negative ion atmospheric pressure chemical ionization mass spectrometry (APCI MS/MS) with a vaporizer temperature of 400°C. The standard was injected with a syringe pump.

3. Results and Discussion

3.1. Isolation of *Chromulina freiburgensis*

C. freiburgensis was successfully isolated and grown in pure culture (Figure 4). The MAM proved to be the best medium for the *C. freiburgensis* in terms of growth rate [20]. All algal cultures reported in this thesis were grown with MAM.

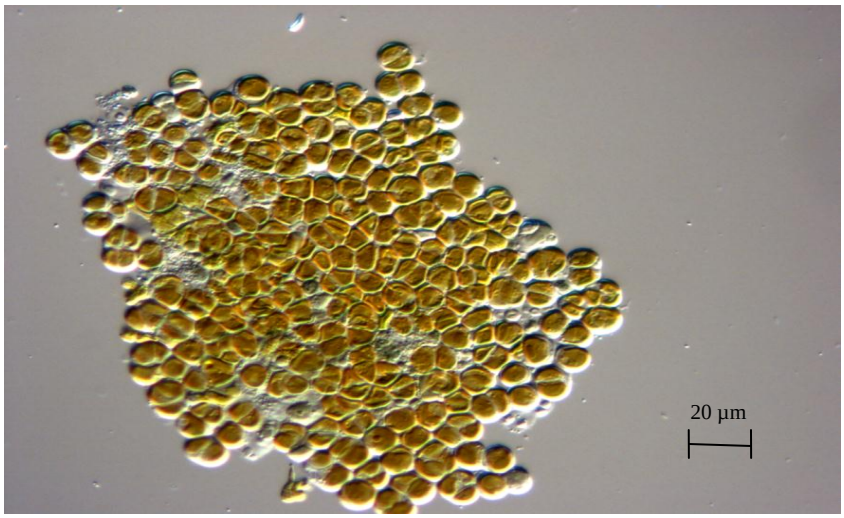

Figure 4: ***C. frieburgensis*** **colony**

3.2. Characterization of Lipids

Figure 4 is a representative chromatogram of an EI GC-MS analysis of the C_4-C_{24} FAME standard mixture. This chromatogram shows separation for most of the fatty acid methyl esters present. High temperatures at the end of the analysis caused column bleed, and the resolution at the tail end (retention time of 60 minutes and greater) was poor. Table 2 lists all of the analytes, their weight percent, and their retention times (RT).

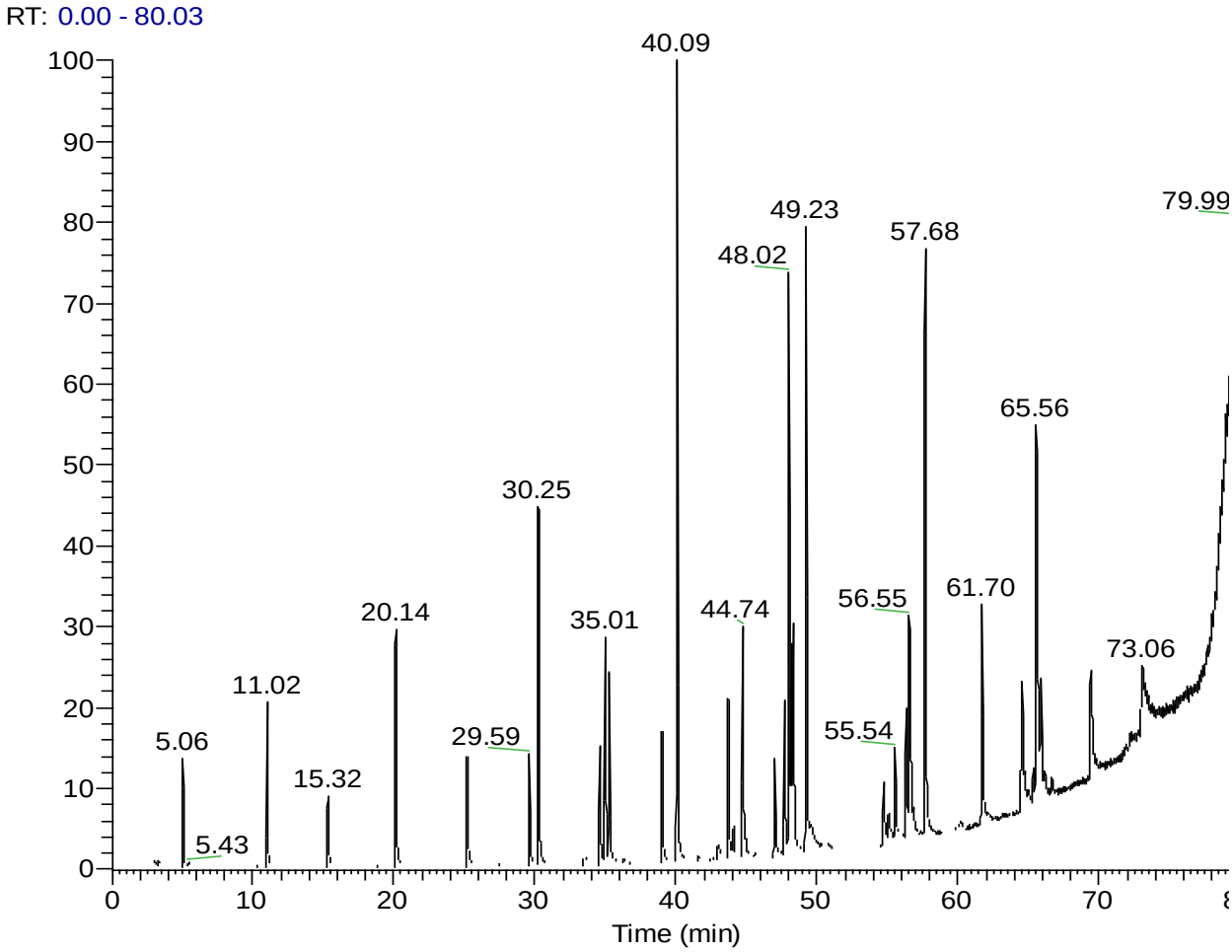

Figure 5: EI Chromatogram of C4-C24 Fatty Acid Methyl Ester Standard Mixture

Table 2: C_4-C_{24} FAME Standard Analytes

C4-C24 FAME Standard Mixture							
Analyte	**Wt %**	**Formula**	**RT**	**Analyte**	**Wt %**	**Formula**	**RT**
Methyl butyrate	4.00	C:4:0	**	Methyl linoleate	2.00	C:18:2	*
Methyl hexanoate	4.00	C:6:0	**	Methyl linolenate	2.01	C:18:3	*
Methyl octanoate	3.98	C:8:0	5.06	Gamma-linolenic acid methyl ester	2.02	C:18:3	*
Methyl decanoate	3.99	C:10:0	11.02	Methyl arachidate	4.02	C:20:0	57.68
Methyl undecanoate	1.99	C:11:0	15.32	Methyl eicosenoate	2.04	C:20:1	*
Methyl laurate	3.98	C:12:0	20.14	Cis-11,14-eicosadienoic acid methyl ester	2.00	C:20:2	*
Methyl tridecanoate	2.01	C:13:0	25.19	Cis-11,14,17-eicosatrienoic acid methyl ester	2.05	C:20:3	*
Methyl myristate	3.98	C:14:0	30.25	Cis-8,11,14-eicosatrienoic acid methyl ester	1.99	C:20:3	*
Myristoleic acid methyl ester	1.99	C:14:1	29.59	Methyl Cis-5,8,11,14-Eicosatetraenoic acid methyl ester	1.99	C:20:4	*
Methyl pentadecanoate	2.00	C:15:0	35.24	Methyl Cis-5,8,11,14,17-Eicosapentaenoic acid	2.01	C:20:5	54.75
Cis-10-Pentadecenoic acid methyl ester	1.99	C:15:1	35.01	Methyl heneicosanoate	2.00	C:21:0	61.70
Methyl palmitate	6.02	C:16:0	40.09	Methyl behenate	4.00	C:22:0	65.56
Methyl palmitoleate	1.99	C:16:1	39.02	Methyl erucate	2.00	C:22:1	64.55
Methyl heptadecanoate	2.00	C:17:0	44.74	Cis-13,16-docosadienoic acid methyl ester	1.99	C:22:2	*
Cis-10-heptadecenoic acid methyl ester	2.04	C:17:1	43.72	Cis-4,7,10,13,16,19-Docosahexaenoic acid methyl ester	1.99	C:22:6	*
Methyl stearate	3.98	C:18:0	49.23	Methyl tricosanoate	1.99	C:23:0	69.44
Cis-9-oleic methyl ester	3.98	C:18:1	*	Methyl lignocerate	3.99	C:24:0	73.06
Trans-9-elaidic methyl ester	2.05	C:18:1	48.33	Methyl nervonate	2.00	C:24:1	*
Linolelaidic acid methyl ester	1.99	C:18:2	*				

* C_{18}-C_{24} unsaturates could not be resolved because a non-polar column was used. ** C:4:0 and C:6:0 fatty acid methyl esters were not of interest because they were not in the transesterification extract. These compounds eluted prior to acquisition of MS data using the chromatographic procedure described in Section 2.6.1.

Figure 6 is a representative chromatogram of an EI GC-MS analysis of the *C. freiburgensis* extract from the Bligh and Dyer method. This method was repeated three times and there were not any detectable free fatty acids present in any of the analyses. There are some small peaks present (ex. RT 17.56, 40.37, and 70.68), but based on the NIST MS Library Search 2.0 the peaks were determined to be polysiloxanes from the column because these peaks were also present in the control runs. The tail end of the chromatogram has poor resolution due to column bleed from high temperatures similar to the FAME standard chromatogram.

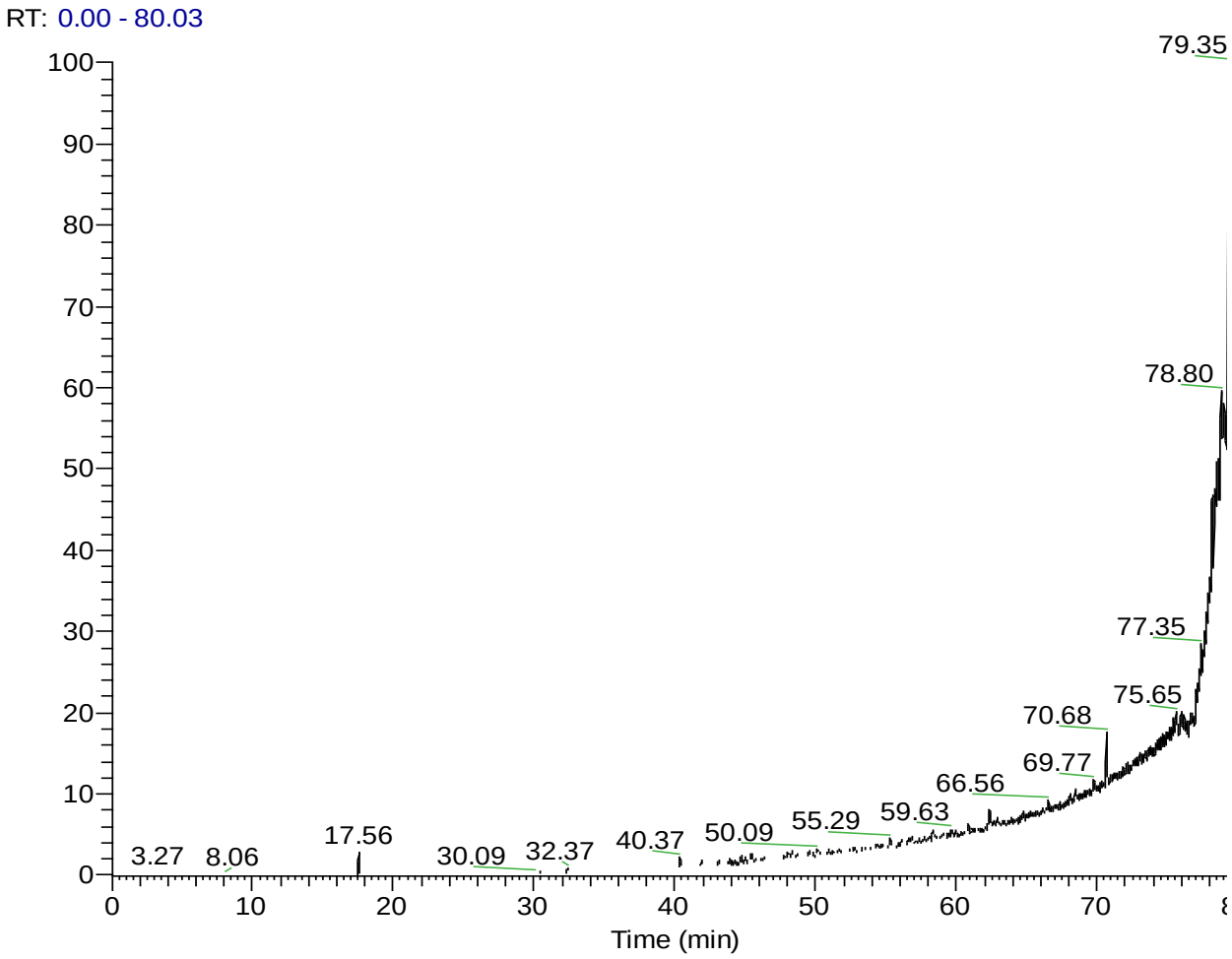

Figure 6: EI Chromatogram of *C. freiburgensis* extract- Bligh and Dyer Method

Figure 7 is a chromatogram of an EI GC-MS analysis of the *C. freiburgensis* extract from the ether reflux method. As in the analysis of the extract using the Bligh and Dyer method, there were no detectable free fatty acids present. The few small peaks present are concluded to be polysiloxanes.

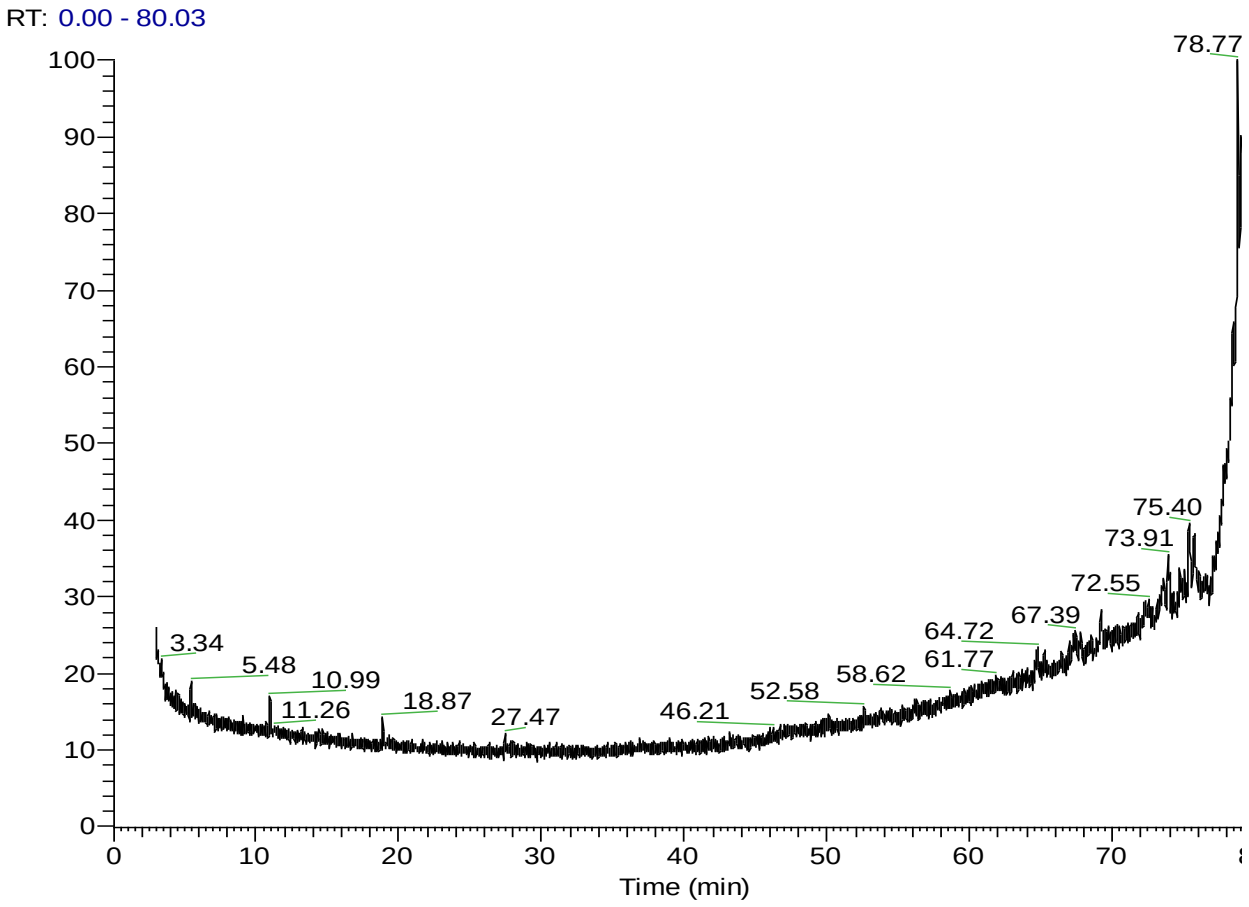

Figure 7: **EI Chromatogram of *C. freiburgensis* extract- Ether Reflux Method**

Figures 8 and 9 are representative EI and CI chromatograms for the *C. freiburgensis* transesterification extract. The retention times of the FAME's in the EI and CI analysis were reproducible. Tetradecanoic acid methyl ester, hexadecanoic acid methyl ester, octadecanoic acid methly ester, and eicosanoic acid methyl ester and their corresponding unsaturates were the most

abundant and will therefore be the only lipids discussed. The other FAME EI and CI chromatograms and mass spectra that had a relative abundance of at least 2% of the major peak (C:18:1, RT 48.31) in the chromatogram from the transesterification extraction are listed in Appendix A.

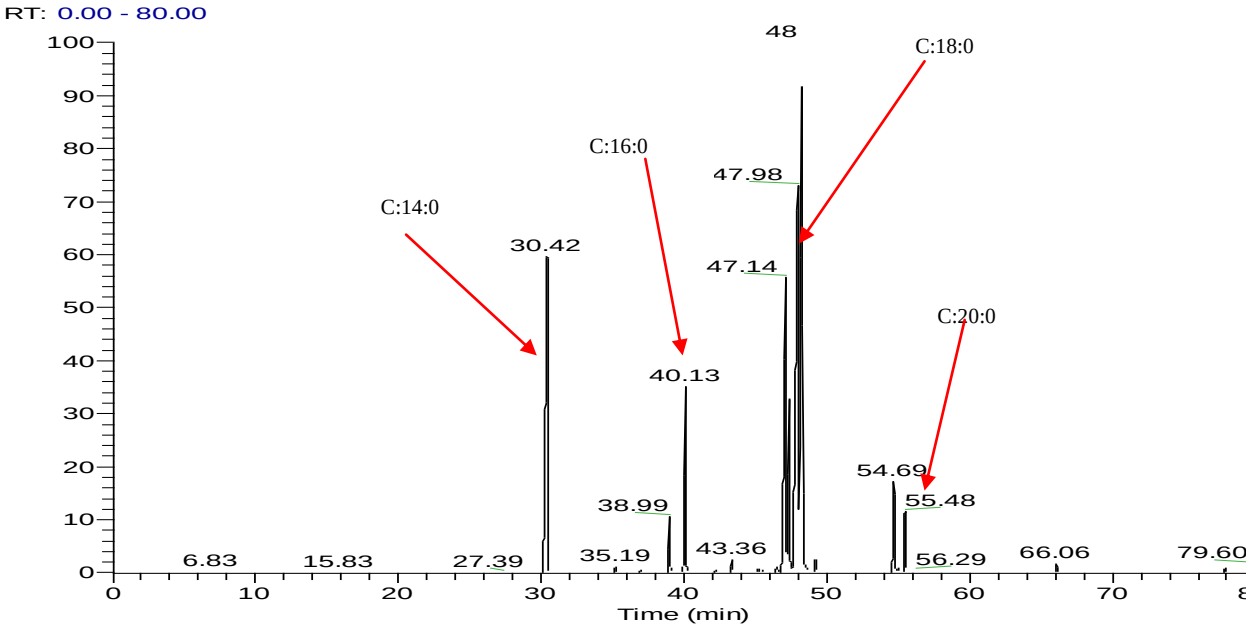

Figure 8: EI Chromatogram of Transesterification Extract from *C. freiburgensis*

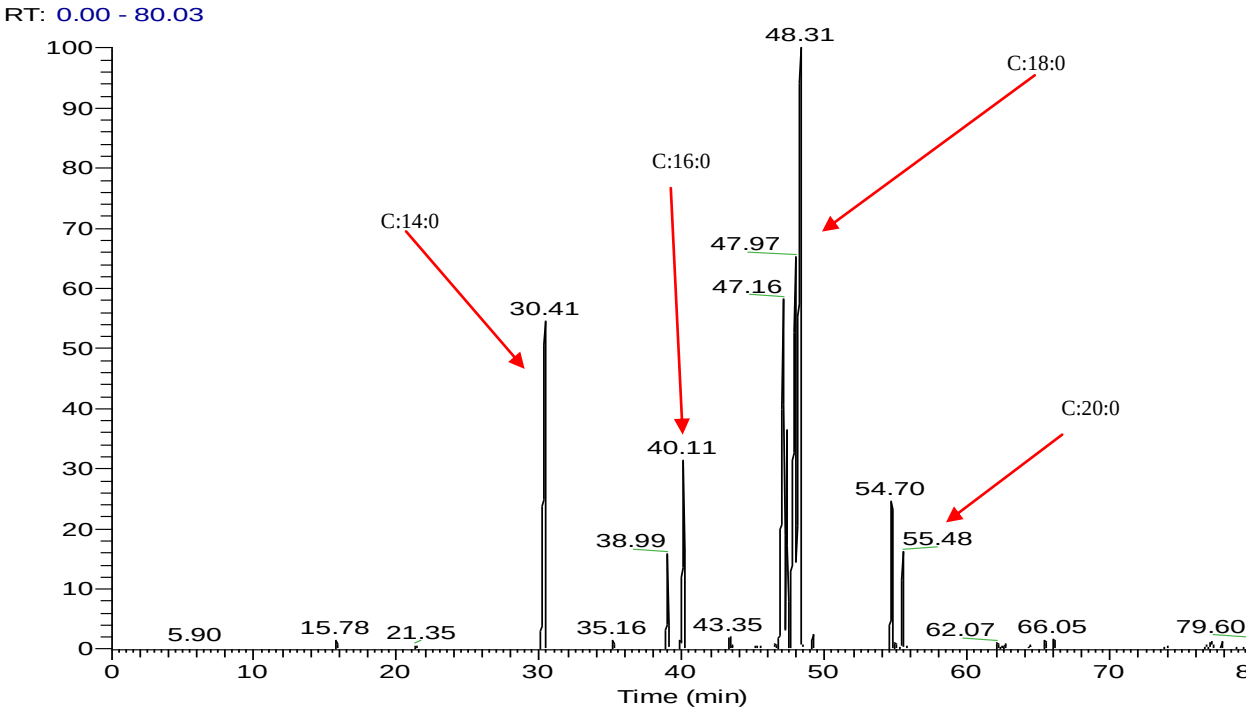

Figure 9: CI Chromatogram of Transesterification Extract from *C. freiburgensis*

3.3. Identification of Lipids

Retention times for each peak varied slightly with each analysis of the transesterification extract. The volatile compounds were affected most. The variation was likely due to the reproducibility achievable from manual sample injection. Table 3 compares the retention times for the C_4-C_{24} FAME (Figure 5) standard to the transesterification extract (Figure 8).

Table 3: C_4-C_{24} Standard Mixture vs. EI Transesterification Extract Lipid Retention Times

Retention Time	Transester-ification Compounds	Retention Time	Standard Compounds
15.78	C:8:2	N/A	N/A
16.47	C:9:1	N/A	N/A
20.06	C:12:0	20.14	C:12:0
30.41	C:14:0	30.25	C:14:0
35.16	C:15:0	35.24	C:15:0
38.99	C:16:1	39.02	C:16:1
40.11	C:16:0	40.09	C:16:0
43.36	C:17:0	44.74	C:17:0
47.16	C:18:3	46.99	C:18:3
47.39	C:18:4	N/A	N/A
47.97	C:18:2	48.02	C:18:2
48.31	C:18:1	48.33	C:18:1
49.19	C:18:0	49.23	C:18:0
54.70	C:20:5	54.75	C:20:5
55.48	C:22:4	57.68	C:20:0

The presence of peaks in the EI transesterification extract chromatogram at approximately the same retention times as peaks in the EI C_4-C_{24} FAME standard mixture chromatogram is strong evidence that lipids are present in the transesterification extract. A CI GC-MS analysis was performed on the transesterification extract in order to elucidate which compounds were present. The mass spectra for each peak in the chromatograms were analyzed using Xcalibur version 2.0 software. The mass spectra were used to identify the lipids in the extracts and an NIST MS Routine Library Search 2.0 routine confirmed the presence of FAMEs.

Figures 10 and 11 are the EI chromatograms of retention time 45 to 50 minutes of the C_4-C_{24} FAME standard and transesterification extract, respectively. All of the C:18 unsaturates could not be resolved because a non-polar column was used.

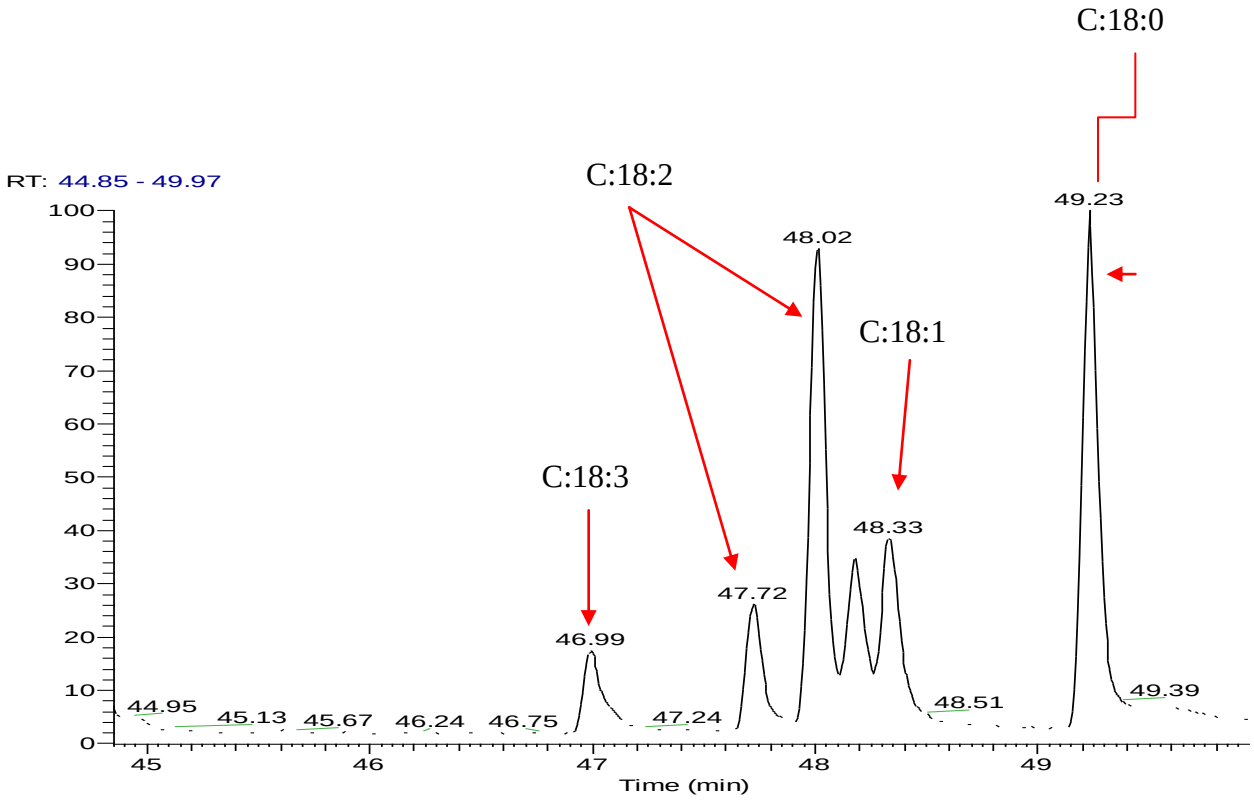

Figure 10: EI Chromatogram for the Retention Time that Includes 45-50 minutes from C_4-C_{24} FAME Standard Mixture

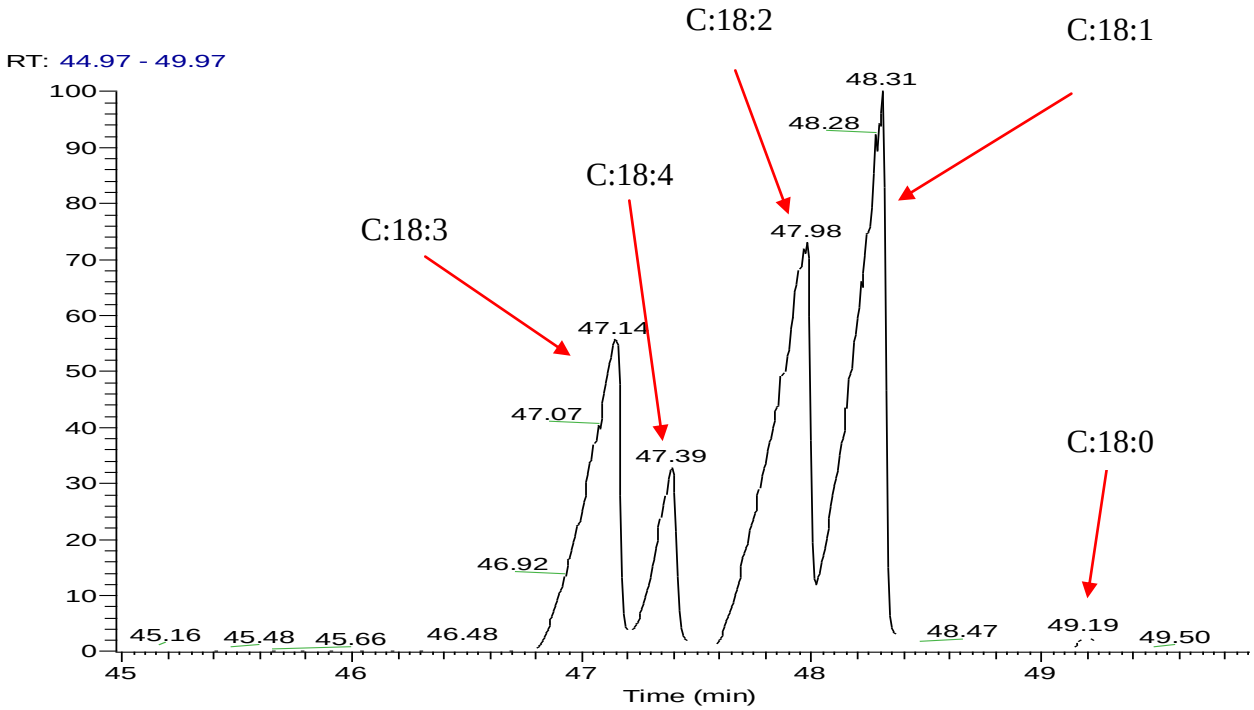

Figure 11: EI Chromatogram for the Retention Time that includes 45-50 minutes from the Transesterification Extract

Figures 12 and 13 are the CI and EI chromatograms of the transesterification extracts, respectively. There is no significant difference in retention times for octadecanoic acid methyl ester and its unsaturates.

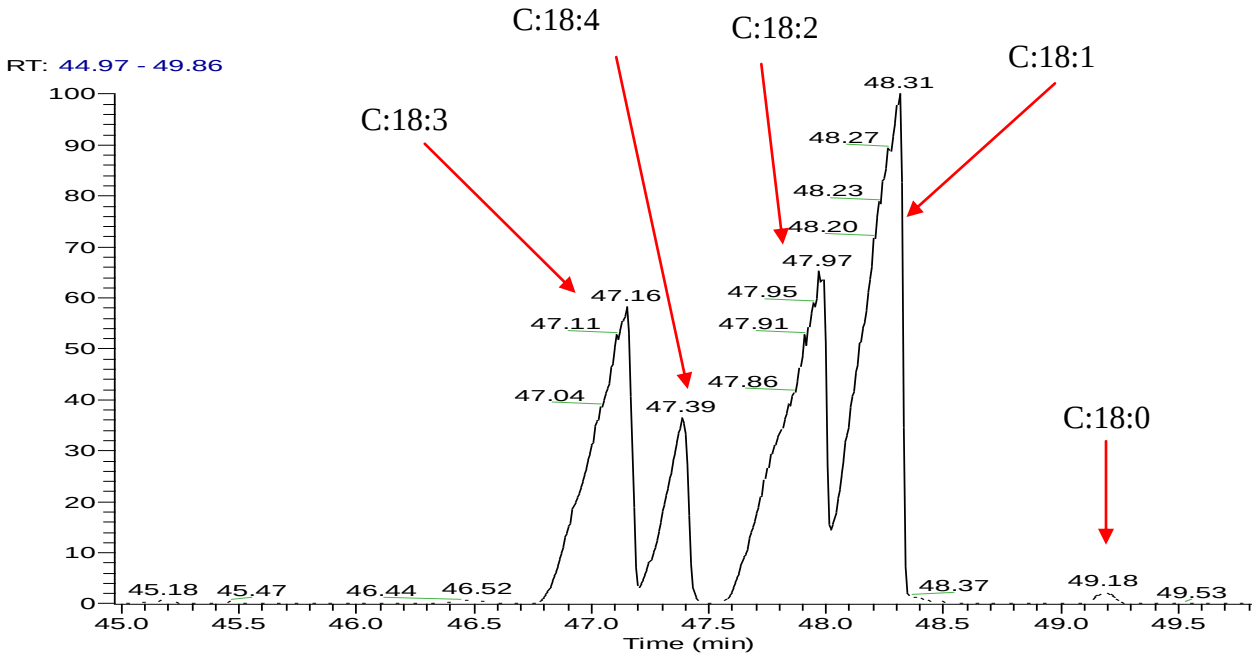

Figure 12: CI Chromatogram for the Retention Time that includes 45-50 minutes from the Transesterification Extract

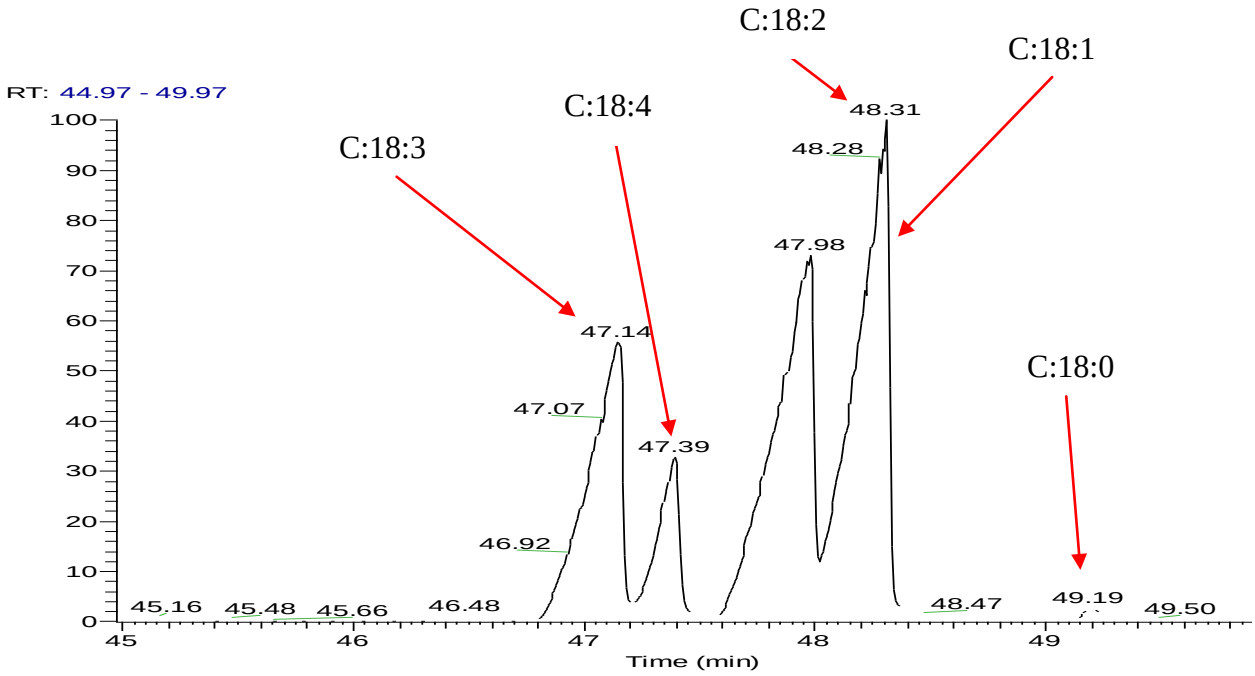

Figure 13: EI Chromatogram for the Retention Time that includes 45-55 minutes from the Transesterification Extract

Figure 14 shows the EI mass spectra from the transesterification extract compound eluting at retention time 49.19 minutes and the C_4-C_{24} FAME standard mixture chromatogram peak at retention time 49.23 minutes. In EI mass spectrometry, a 70 eV beam of electrons interact with the sample in the ion trap and gives the sample molecules excess energy [30, 31]. An electron is knocked off the sample molecule forming a positive ion called the molecular ion (M^+). The molecular ion is energentically unstable and further fragments into smaller pieces. The molecular ion in the figures below is at m/z=298 and the base peak is at m/z=143. The base peak is the most abundant peak in the spectrum and it represents the most abundant fragmentation ion (Note: the mass spectrometer was not set to trap and detect ions with m/z less than 100). The following two spectra (Figure 14) are essentially identical which is strong evidence that there is C:18:0 fatty acid methyl ester present in the transesterification extract. A library search was done using NIST Xcalibur software version 2.0 to confirm the presence of C:18:0.

Figure 15 is the CI mass spectrum from the transesterification extract at retention time 49.19 minutes. Acetonitrile was used as the reagent gas for all of the CI analyses. When doing CI analyses, ionized, gaseous acetonitrile is present in abundance in the ion trap and it collides with the sample molecules producing the molecular ion plus H^+ ($M+H^+$), and characteristic adduct ion ($M+CH_2CN^+$) that is equal to the molecular ion plus 40 mass units $(M + 40)^+$. The abundance of this ion in the spectrum varies with the reagent gas pressure.

Ionized acetonitrile also collides with neutral acetonitrile molecules to produce the 1-methyleneimino-1-ethenylium ion ($H_2C+NC=CH_2$) and creates an ion in the spectrum that is equal to the molecular ion plus 54 mass units $(M+54)^+$ in unsaturated fatty acids [31]. The $(M+H)^+$ and the $(M+40)^+$ ions are found for the the saturated and unsaturated FAMES. The $(M+54)^+$ion is only found for the unsaturated FAMES. CI is a lower energy process than EI, which results in less fragementation compared to the EI spectra. The mass spectrum for the compound eluting at retention time 49.19 minutes is characteristic of C:18:0 with the $M+H^+$ peak at m/z=299. The peak at m/z=338 is the $(M+40)^+$ adduct ion peak. CI spectra also produce molecular weight information that alson confirms the identification of the various FAMES.

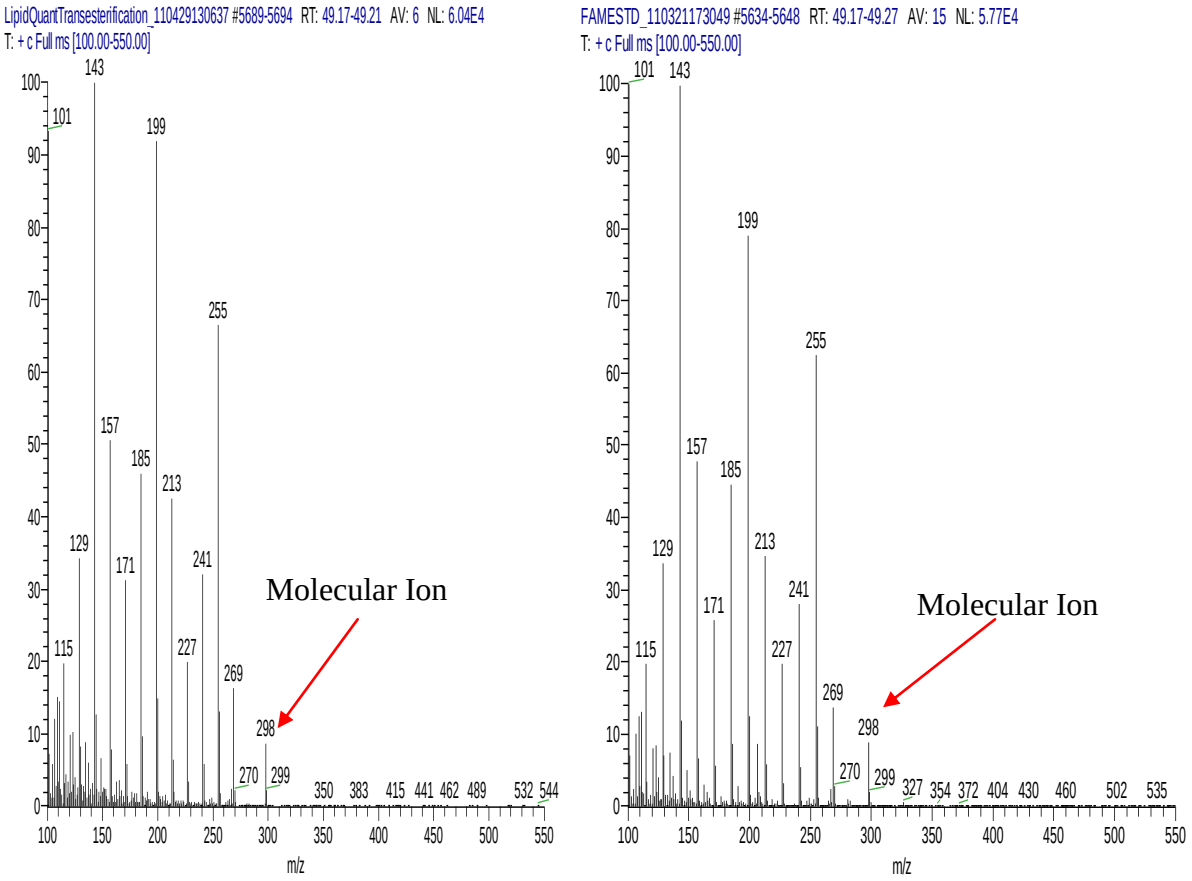

Figure 14: Transesterification Mass Spectrum RT 49.19 minutes vs. C_4-C_{24} FAME Standard Mass Spectrum RT 49.23 minutes

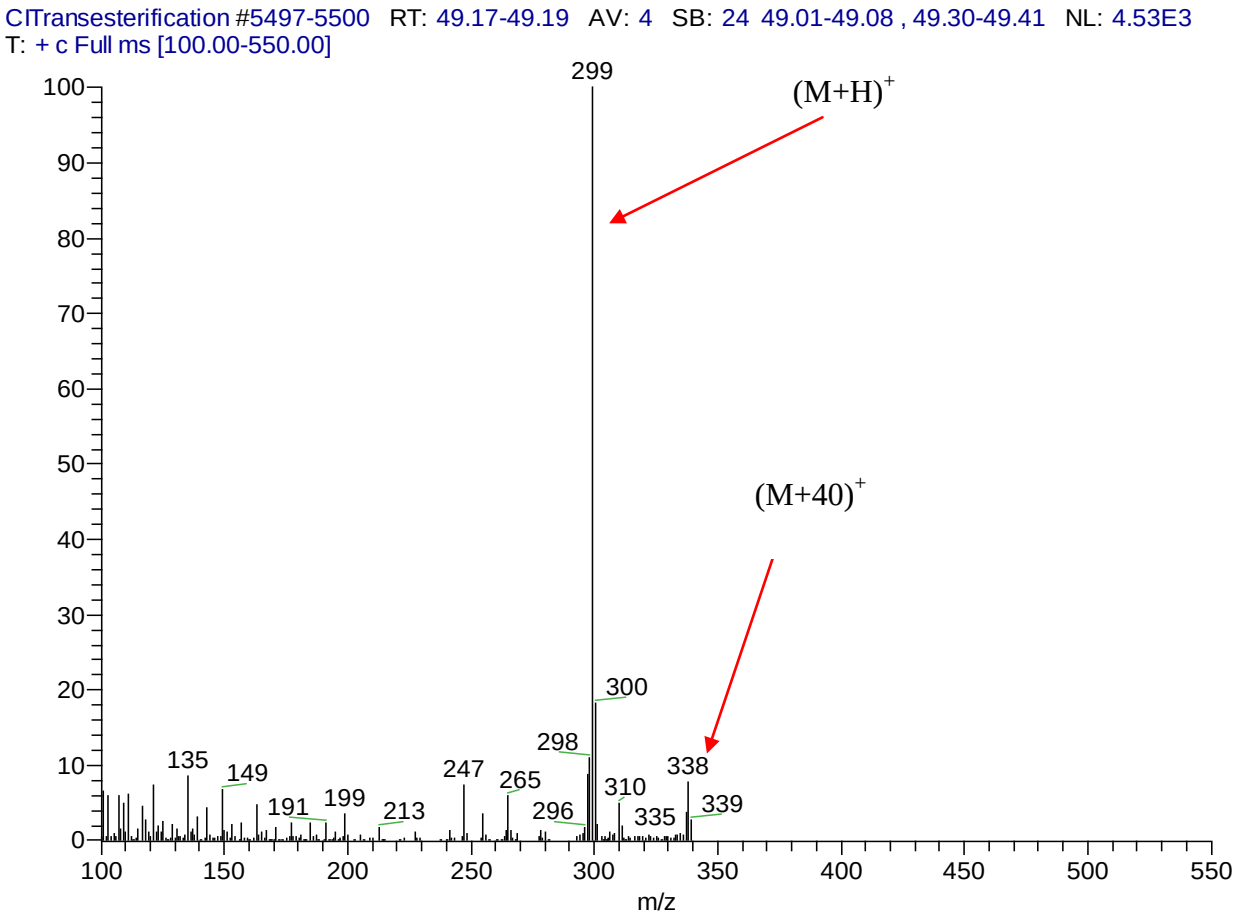

Figure 15: CI Mass Spectrum of Transesterification Extract at Retention Time 49.19 (C:18:0)

Figure 16 shows the mass spectra from the transesterification extract for the compound eluting at retention time 48.31 minutes and the C_4-C_{24} FAME standard compound eluting at retention time 48.33 minutes. These mass spectra are equivalent indicating that there is C:18:1 fatty acid methyl ester present in the transesterification extract. A library search was performed using Xcalibur software version 2.0 to confirm the presence of C:18:1. The molecular ion is at m/z=296.

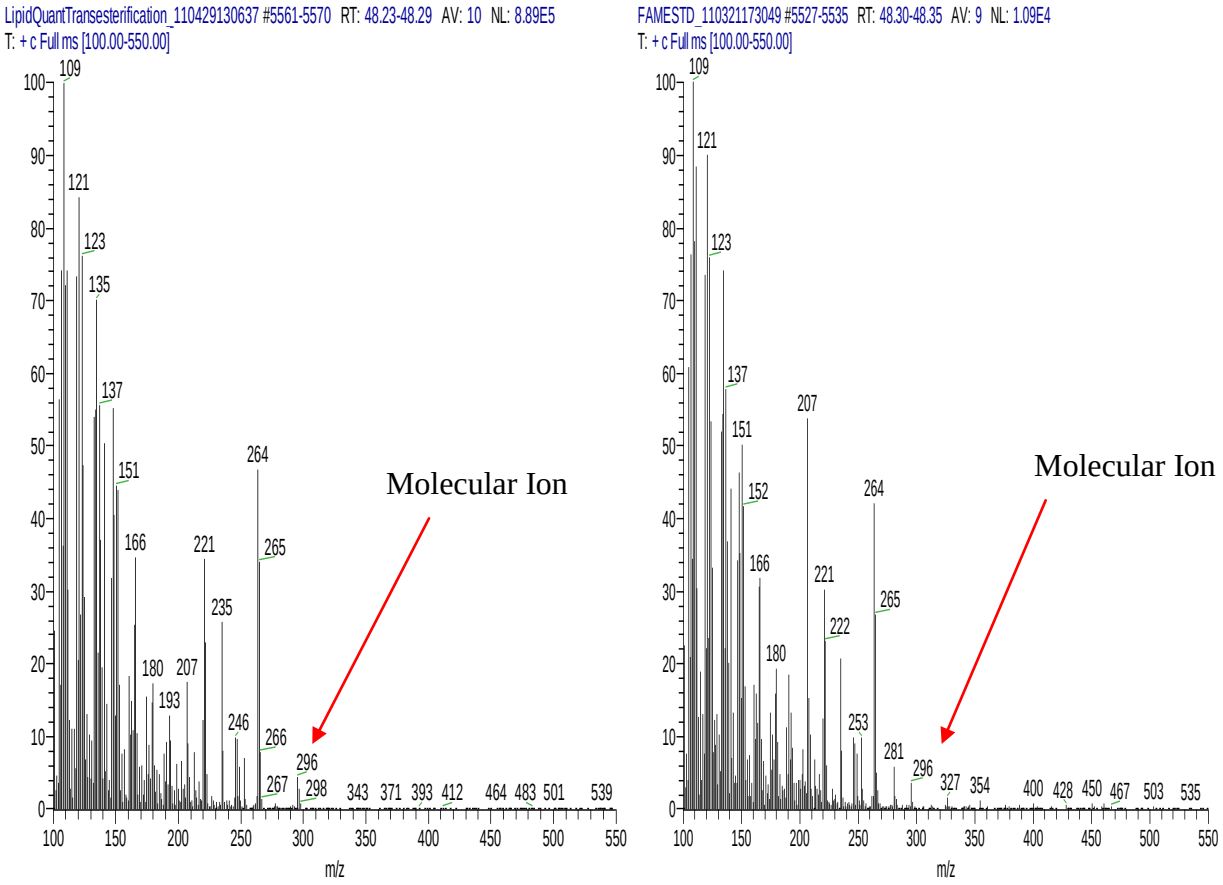

Figure 16: Transesterification Mass Spectrum RT 48.31 vs. C_4-C_{24} FAME Standard Mixture Mass Spectrum Comparison of Peak at RT 48.33

Figure 17 shows the CI mass spectra for the compound eluting at retention time 48.31 minutes in the transesterification extract. The ion at m/z=297 is a result of the molecular ion plus hydrogen $(M+H)^+$. The ion at m/z=336 is due to the molecular ion plus the adduct ion $(M + CH_2CN^+)$. The ion at m/z=350 is the $(M+54)^+$ peak $(M+HC+NC=CH_2)$, which is the result of acetonitrile reacting with itself.[31] The presence of these three ions is strong evidence C:18:1 is present.

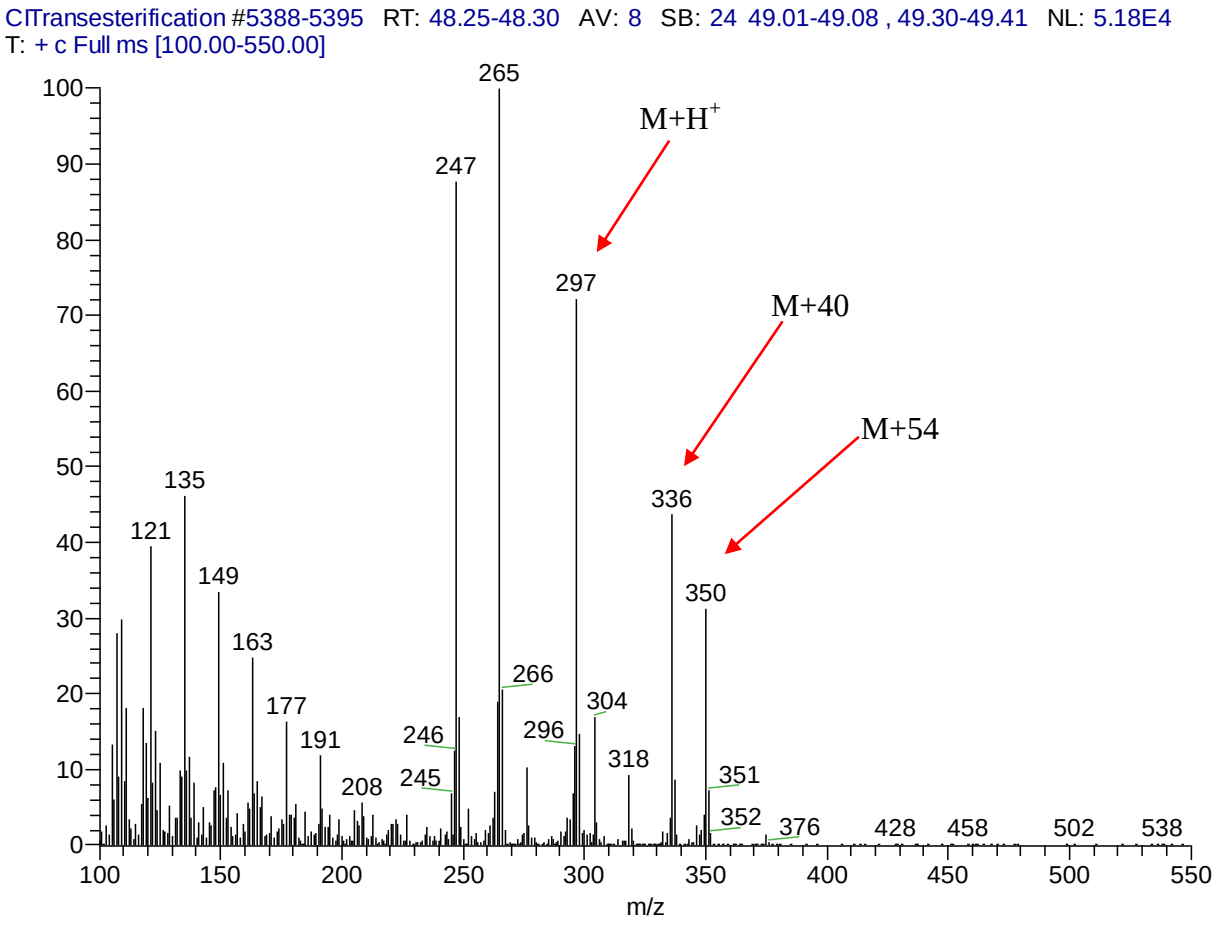

Figure 17: Transesterification CI Mass Spectrum of Retention Time 48.31 Minutes (C:18:1)

Figure 18 is a comparison of the mass spectrum for the compound eluting in the transesterification extract at retention time 47.97 minutes to the mass spectrum for the compound eluting in the C_4-C_{24} FAME standard at retention time 48.02 minutes. The fragmentation pattern in the two spectra are nearly the same indicating that C:18:1 is present. The molecular ion peak is at m/z=294 and the base peak is at m/z=135. A library search was also performed to confirm the presence of oleic acid.

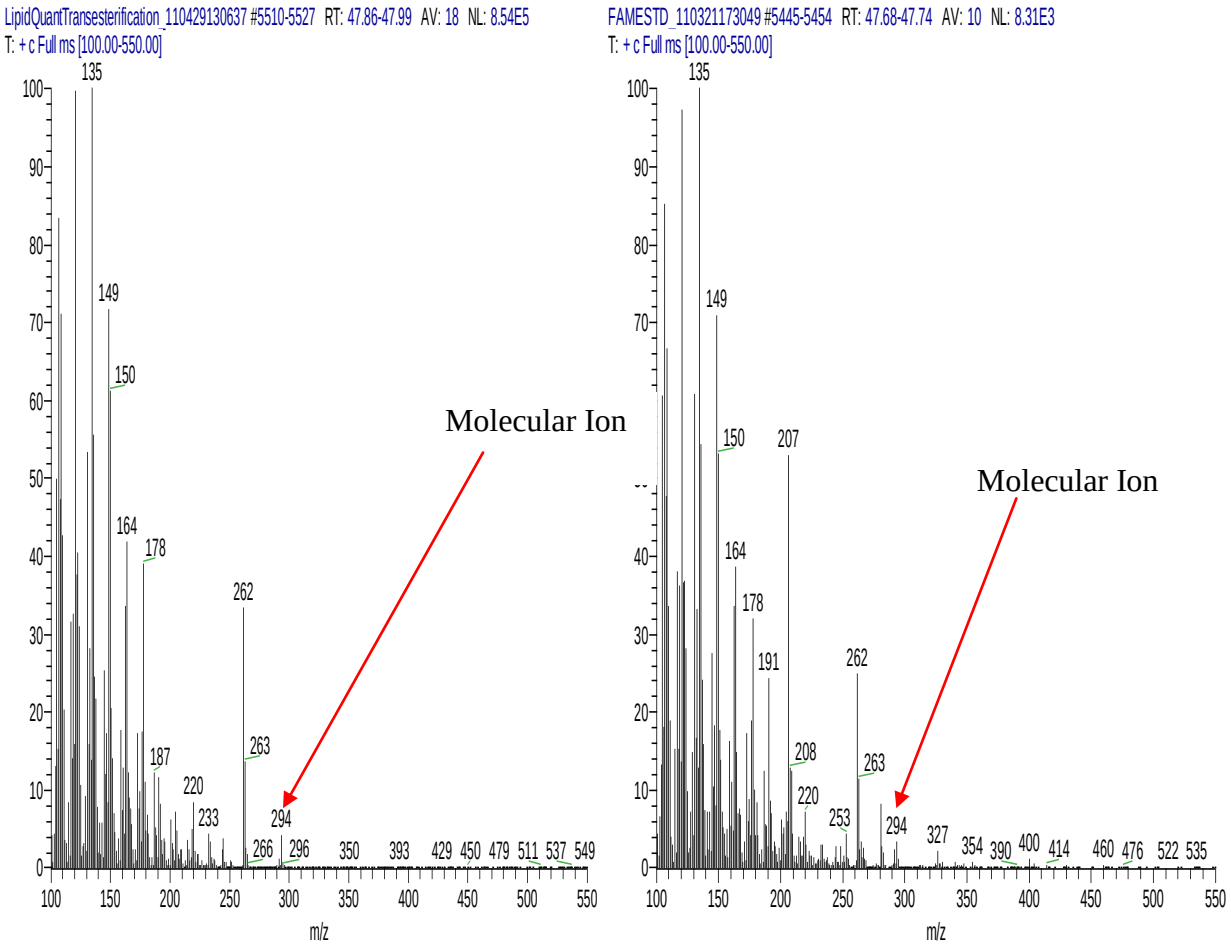

Figure 18: Transesterification Mass Spectrum RT 47.97 minutes vs. C4-C24 FAME Standard Mixture Mass Spectrum Comparison of Peak at RT 47.72 minutes

Figure 19 is the CI mass spectrum for peak at retention time 47.97 minutes in the chromatogram of the transesterification extract. The ion at m/z=348 is due to the molecular ion plus 1-methyleneimino-1-ethenylium ion $(M+54)^+$ and the ion at m/z=334 is the molecular ion plus the adduct ion. The $M+H^+$ ion at m/z=295, the adduct ion at m/z=348, and the 1-methyleneimino-1-ethenylium ion at m/z=348 suggests that C:18:2 is present.

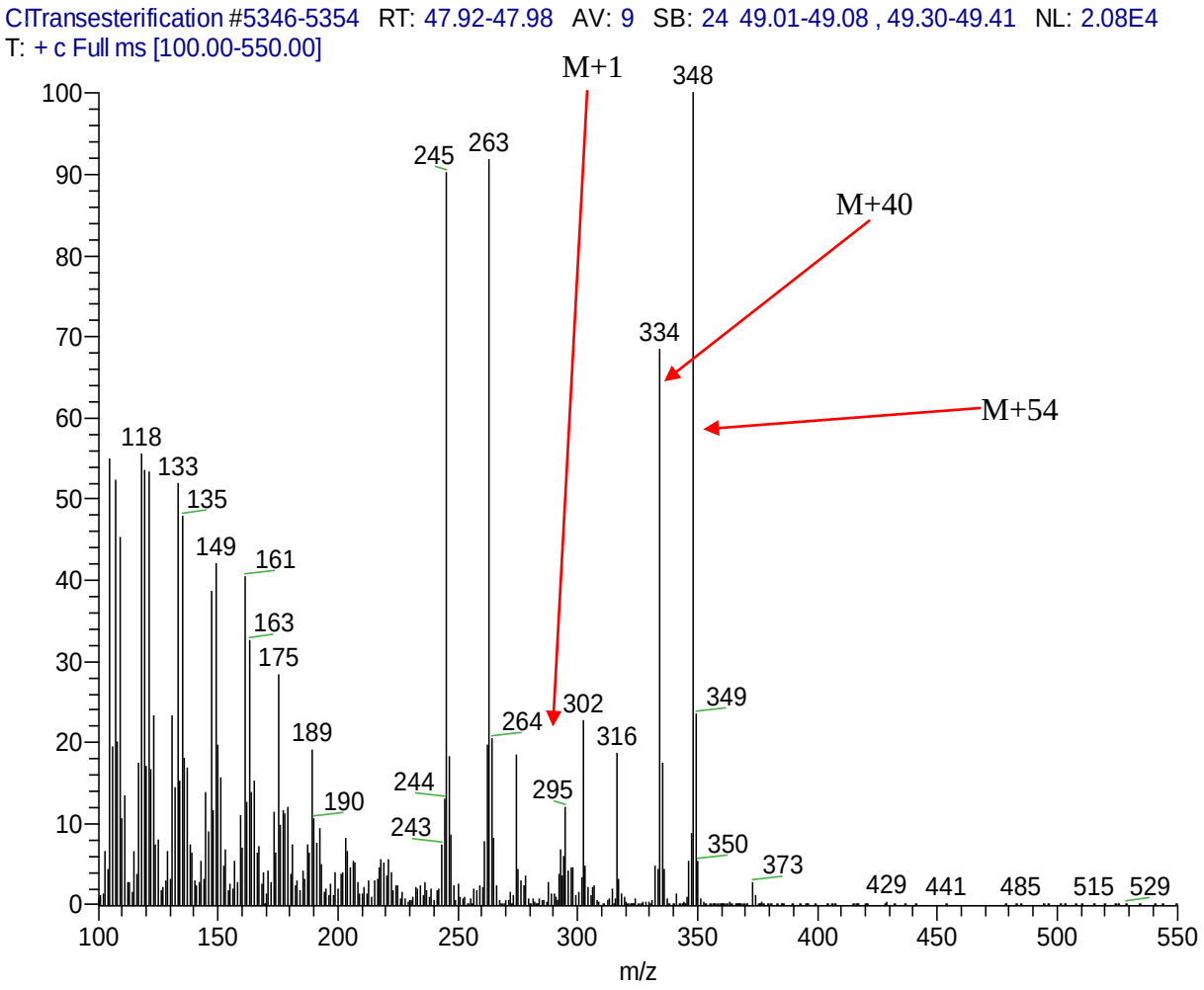

Figure 19: Transesterification CI Mass Spectrum of Retention Time 47.97 (C:18:2)

Below, the EI transesterification extract mass spectrum for the compound eluting at retention time 47.14 minutes is compared to the EI C_4-C_{24} FAME standard spectrum for the compound eluting at retention time 46.99 minutes (Figure 20). The fragmentation pattern in each spectrum is very similar. The molecular ion is present at m/z=292 and the base ion at m/z=121. A library search was performed on the transesterification extract confirming the presence of C:18:3.

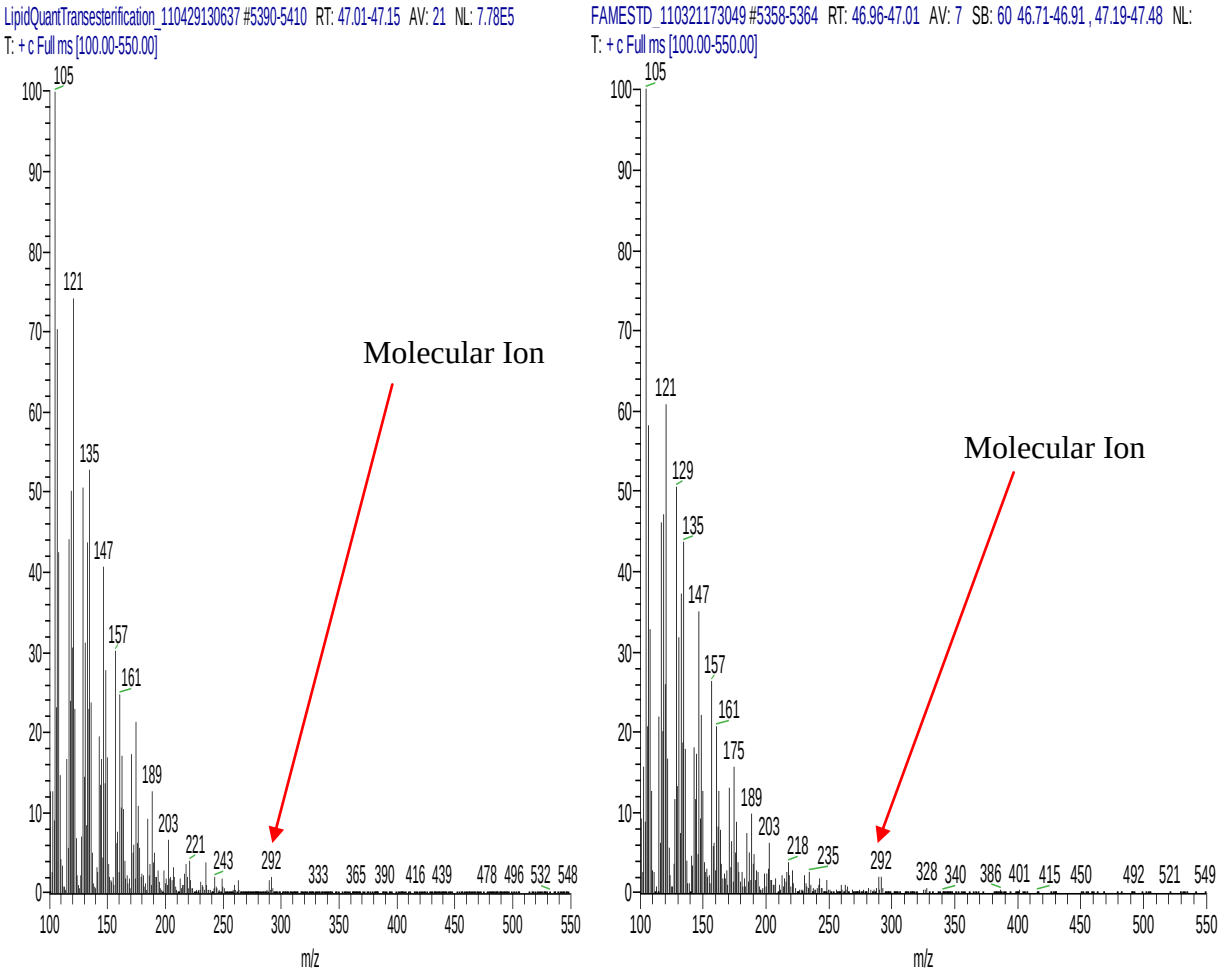

Figure 20: Transesterification Mass Spectrum RT 47.14 minutes vs. C_4-C_{24} FAME Standard Mixture Mass Spectrum Comparison of Peak at RT 46.99 minutes

The mass spectrum in Figure 21 is the results of the CI analysis of the transesterification extract at retention time 47.16 minutes. The $M+H^+$ ion at m/z= 293, the adduct ion at m/z=332, and the 1-methyleneimino-1-ethenylium ion at m/z=346 suggests that C:18:3 is present.

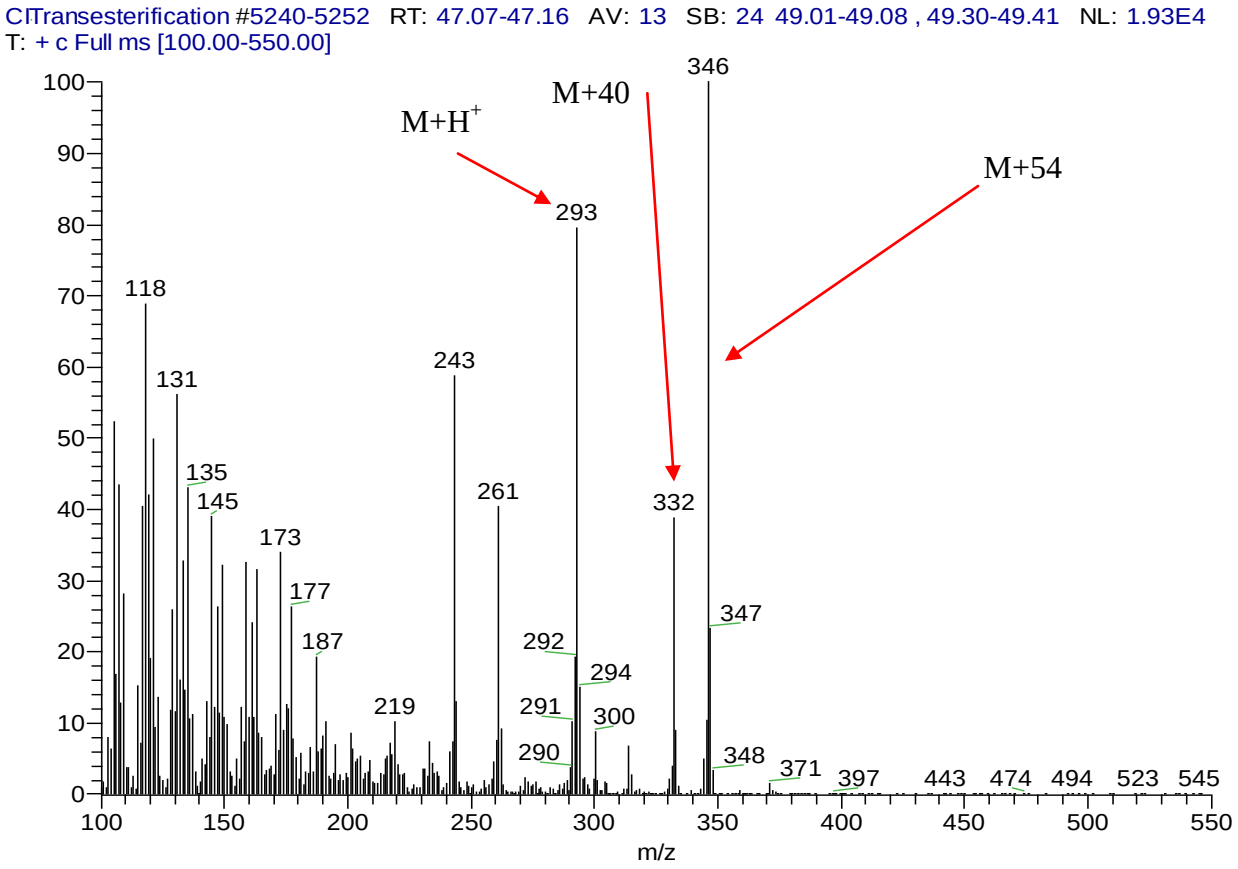

Figure 21: Transesterification CI Mass Spectrum of Retention Time 47.14 minutes (C:18:3)

Figures 22 and 23 are the EI and CI mass spectra for the compound eluting at retention time 47.39 minutes. The $M + H^+$ ion at m/z=291, the adduct ion at m/z=330, and the M+54 ion at m/z=344 in the CI analysis confirms that there is C:18:4 in the transesterification extract. There is not C:18:4 present in the C_4-C_{24} FAME standard so a comparison between the EI spectra could not be made.

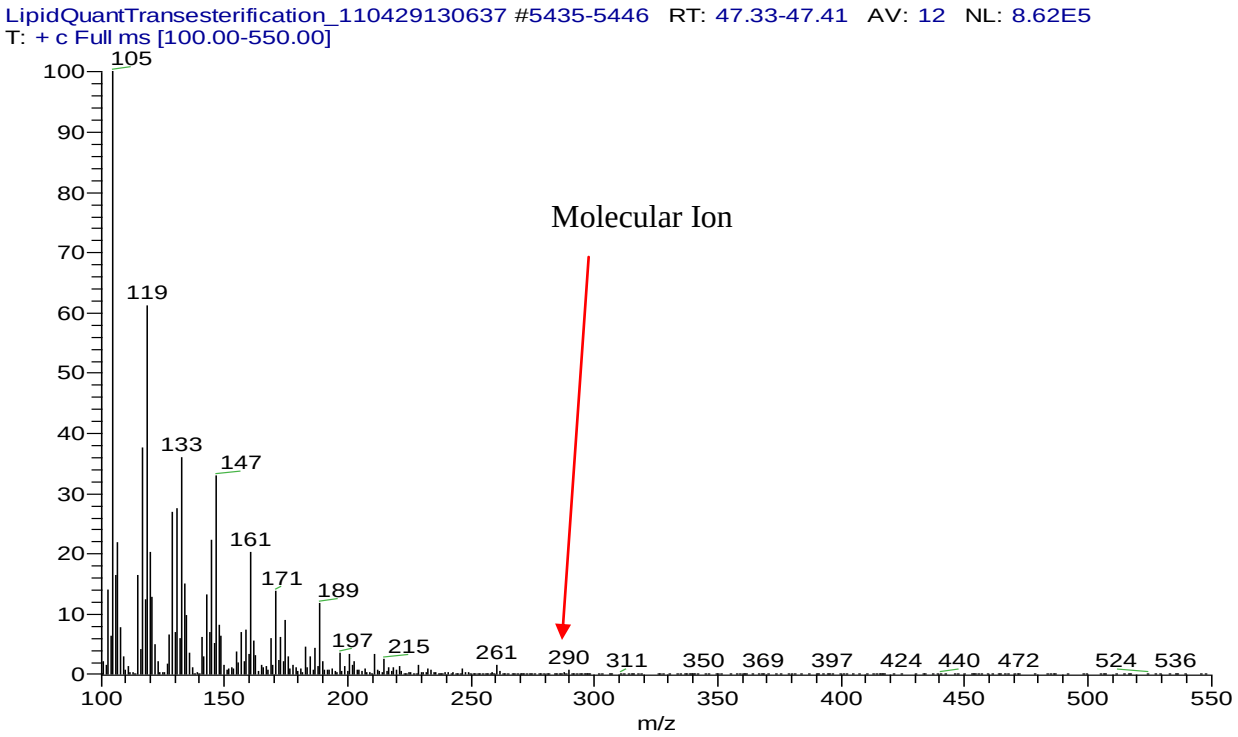

Figure 22: EI Transesterification Mass Spectrum at Retention Time 47.39

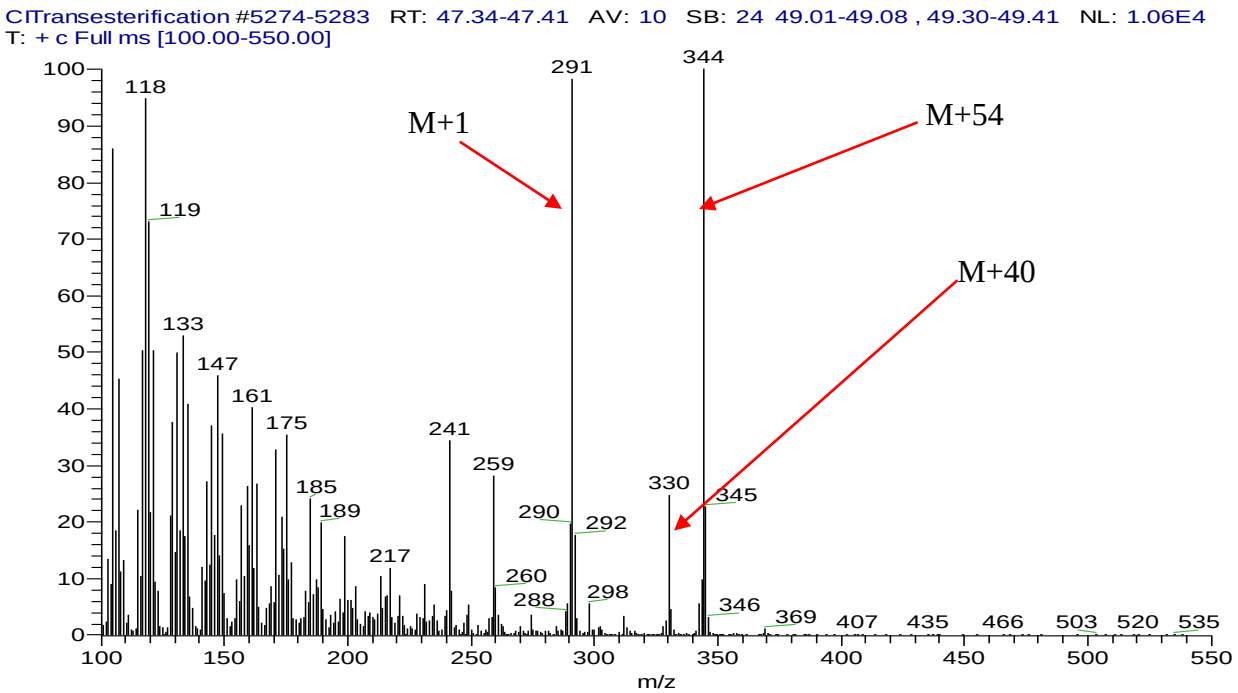

Figure 23: Transesterification CI Mass Spectrum of Retention Time 47.39 (C:18:4)

3.4. Quantification of Lipids

To quantify the lipids in the transesterification extract, an internal standard (naphthalene) was added to the C_4-C_{24} FAME standard and four serial dilutions were made (see Section 2.7). The concentrations and areas of the peaks in the C_4-C_{24} FAME standard and the areas of the peaks in the transesterification extract were used to calculate the concentrations of the fatty acid methyl esters in the transesterification sample. Below, the FAME standard chromatogram (Figure 24) and a table (Table 4) corresponding to the pertinent analytes are shown.

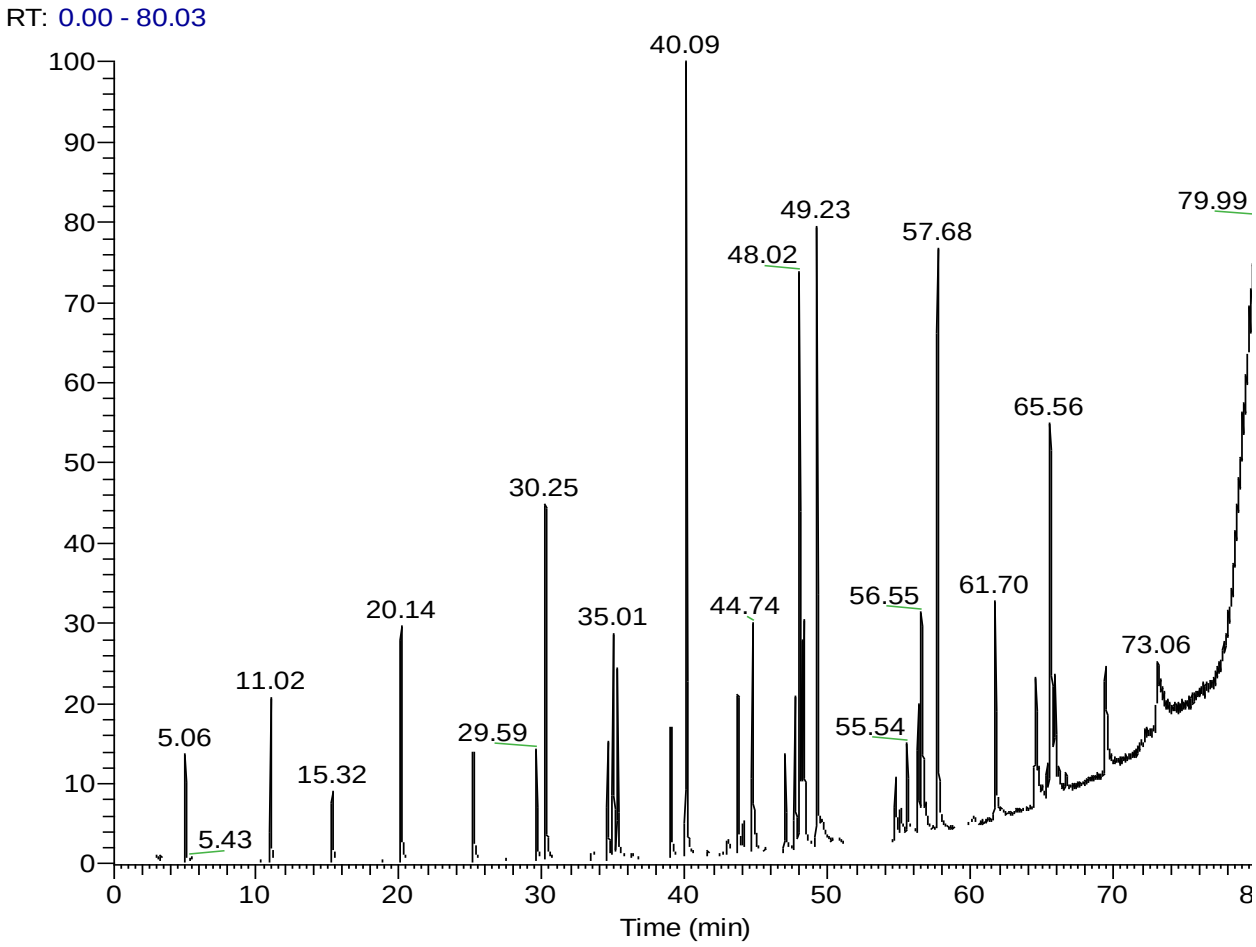

Figure 24: EI Chromatogram of C_4-C_{24} Fatty Acid Methyl Ester Standard Mixture

Table 4: C_4-C_{24} Standard FAME Mixture Areas and Concentrations

RT (min)	Compound	Area of Peak	Conc. in standard (mg/ml hexane)	Amount on Column (µg)
20.14	C:13:0	1.34E+06	2.0	0.2
29.59	C:14:1	6.96E+05	2.0	0.2
30.25	C:14:0	2.18E+06	4.0	0.4
35.24	C:15:0	1.22E+06	2.0	0.2
39.02	C:16:1	8.55E+05	2.0	0.2
40.09	C:16:0	4.75E+06	6.0	0.6
44.74	C:17:0	1.64E+06	2.0	0.2
46.99	C:18:3	7.54E+05	2.0	2.0
47.72	C:18:2	8.98E+05	2.0	2.0
48.02	C:18:2	3.45E+06	4.0	0.4
48.18	C:18:1	1.33E+06	2.0	0.2
48.33	C:18:1	1.49E+06	4.0	0.4
49.23	C:18:0	3.91E+06	4.0	0.4
54.75	C:20:5	4.99E+05	2.0	0.2
57.68	C:20:0	3.96E+06	4.0	0.4
61.7	C:21:0	1.62E+06	2.0	0.2

*The C:18 and C:20 unsaturates were unable to be resolved in the FAME standard. The exactretention time for each unsaturate is unknown. The concentration of these species will be estimated based on the RF values for the resolved analytes in the FAME standard.

Table 5: C_4-C_{24} Standard FAME with Internal Standard Serial Dilutions

C:12:0			C:13:0			C:14:0		
Dilution	Area	Conc. (mg/mL)	Dilution	Area	Conc. (mg/mL)	Dilution	Area	Conc. (mg/mL)
1	1.45E+07	0.8	1	1.45E+07	0.4	1	2.29E+07	0.8
2	2.45E+06	0.16	2	2.45E+06	0.08	2	3.94E+06	0.16
3	4.35E+05	0.032	3	4.35E+05	0.016	3	7.30E+05	0.032
4	n/a	0.0064	4	n/a	0.0032	4	n/a	0.0064
C:14:1			**C:15:0**			**C:16:0**		
Dilution	Area	mg/mL	Dilution	Area	mg/mL	Dilution	Area	mg/mL
1	8.86E+06	0.4	1	1.34E+07	0.4	1	5.02E+07	1.20
2	1.43E+06	0.08	2	2.28E+06	0.08	2	8.68E+06	0.24
3	2.07E+05	0.016	3	3.81E+05	0.016	3	1.56E+06	0.05
4	n/a	0.0032	4	n/a	0.0032	4	7.54E+04	0.01
C:16:1			**C:17:0**			**C:18:0**		
Dilution	Area	mg/mL	Dilution	Area	mg/mL	Dilution	Area	mg/mL
1	1.17E+07	0.4	1	1.82E+07	0.4	1	4.39E+07	0.80
2	1.82E+06	0.08	2	3.06E+06	0.08	2	7.61E+06	0.16
3	2.50E+05	0.016	3	4.70E+05	0.016	3	1.35E+06	0.03
4	n/a	0.0032	4	n/a	0.0032	4	5.90E+04	0.01
C:18:1 (RT 48.18)			**C:18:1 (RT 48.33)**			**C:18:2 (RT 47.72)**		
Dilution	Area	mg/mL	Dilution	Area	mg/mL	Dilution	Area	mg/mL
1	1.03E+07	0.4	1	1.17E+07	0.8	1	1.41E+07	0.4
2	2.56E+06	0.08	2	2.79E+06	0.16	2	2.21E+06	0.08
3	3.47E+05	0.016	3	5.29E+05	0.032	3	1.18E+06	0.016
4	n/a	0.0032	4	2.78E+04	0.0064	4	n/a	0.0032
C:18:3 (RT 46.99)			**C:20:0**			**C:20:5**		
Dilution	Area	mg/mL	Dilution	Area	mg/mL	Dilution	Area	mg/mL
1	1.33E+07	0.4	1	5.40E+07	0.80	1	1.35E+07	0.4
2	1.86E+06	0.08	2	9.75E+06	0.16	2	1.76E+06	0.08
3	1.98E+05	0.016	3	1.59E+06	0.03	3	1.56E+05	0.016
4	n/a	0.0032	4	6.97E+04	0.01	4	n/a	0.0032
C:21:0								
Dilution	Area	mg/mL						
1	2.78E+07	0.4						
2	4.61E+06	0.08						
3	5.62E+05	0.016						
4	2.29E+04	0.0032						

*5 µL of napthalene was added to Dilution 2, 3, and 4 after the serial dilution.

The calibration curves (Figures 25-41) were made via Microsoft® Excel using the method described in Section 2.7.2. The linearity over the range measured was selected based on the areas of the peaks in the transesterification extracts. The limit of dectection (LOD) can only be estimated based on the information obtained from the serial dilutions of the C_4-C_{24} FAME standard. The LOD for C:12:0 and C:14:0 is greater than 0.0064 mg/mL but less than 0.032 mg/mL. The LOD for C:13:0, C:14:1, C:15:0, C:16:1, C:17:0, and C:20:5 is less than 0.016 mg/mL but greater than 0.0032 mg/mL. The LOD for C:16:0, C:18:0, C:20:0, and C:21:0 is less than 0.0096mg/mL, 0.0064 mg/mL, 0.0064 mg/mL, and 0.0032 mg/mL, respectively.

The calibration curves shown in Figures 25-41 were used to estimate the concentration of each fatty acid methyl ester (FAME) in the transesterification extact.

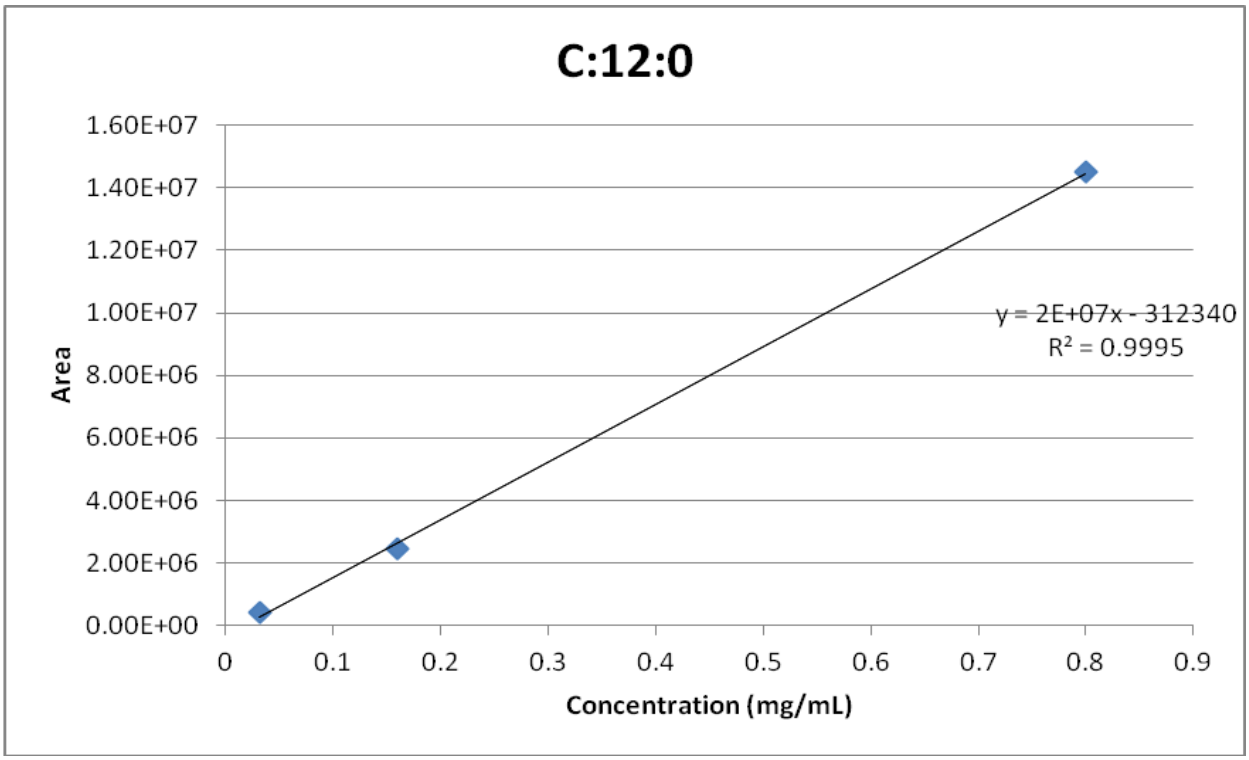

Figure 25: C_4-C_{24} Standard FAME C:12:0 Calibration Curve

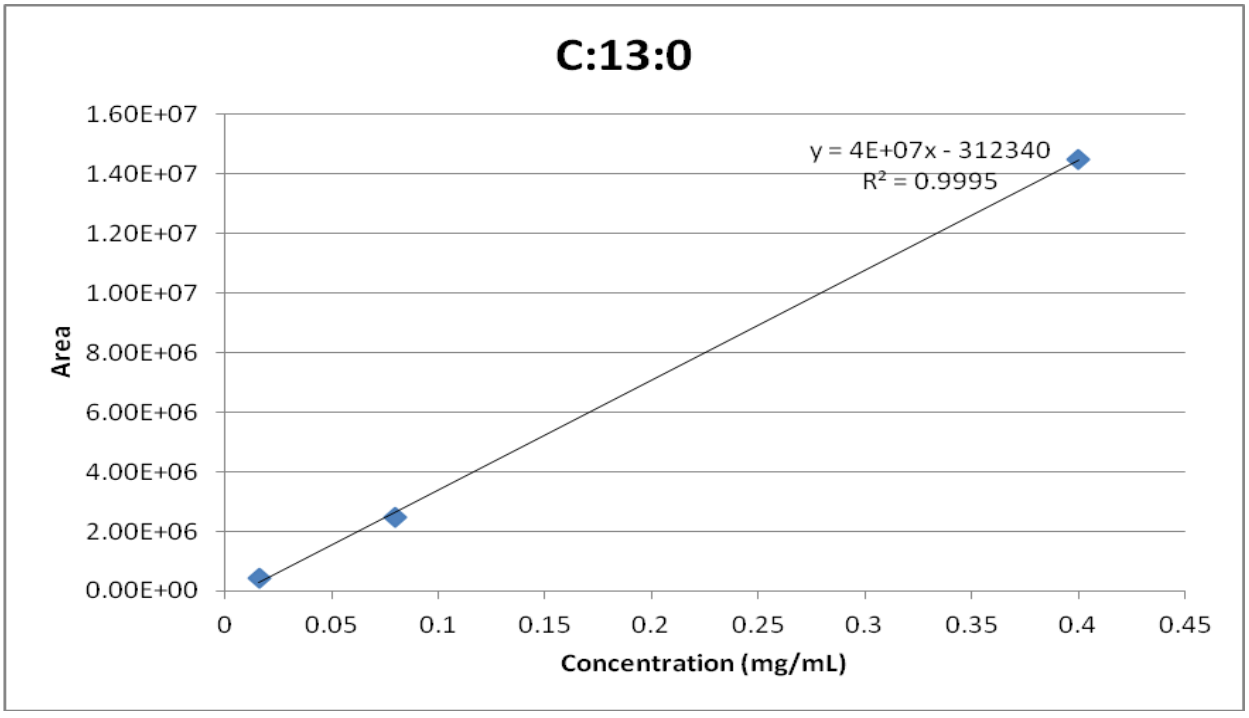

Figure 26: C_4-C_{24} Standard FAME C:13:0 Calibration Curve

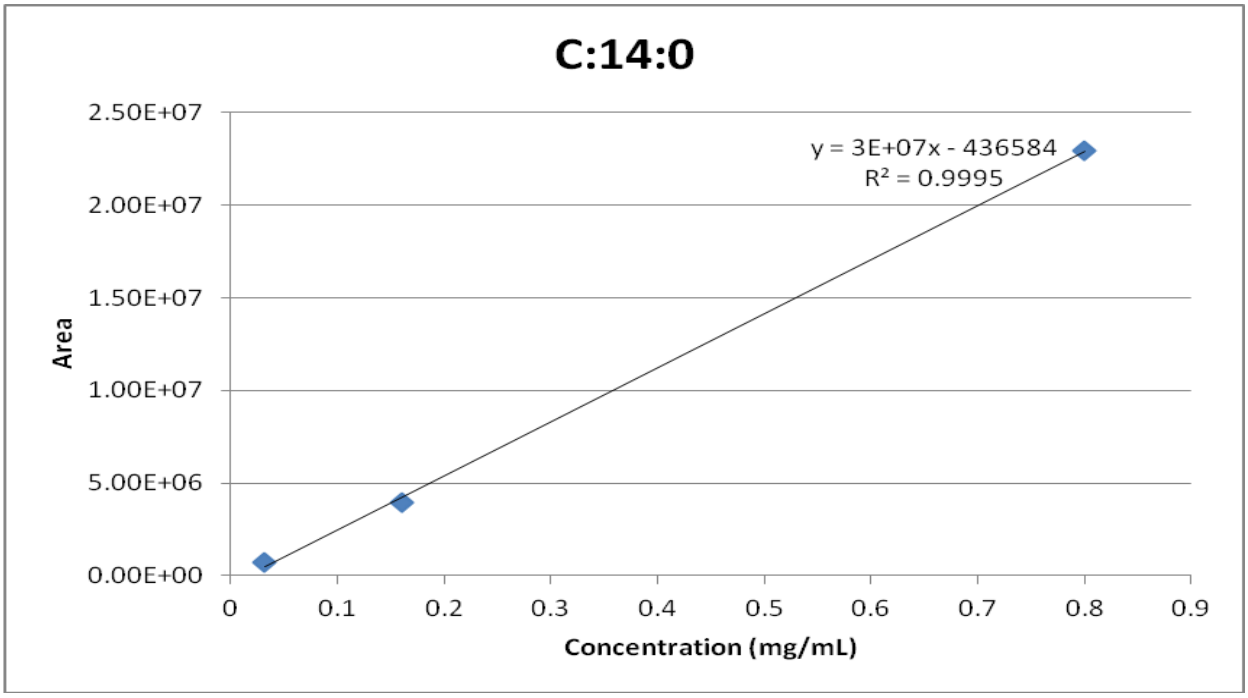

Figure 27: C_4-C_{24} Standard FAME C:14:0 Calibration Curve

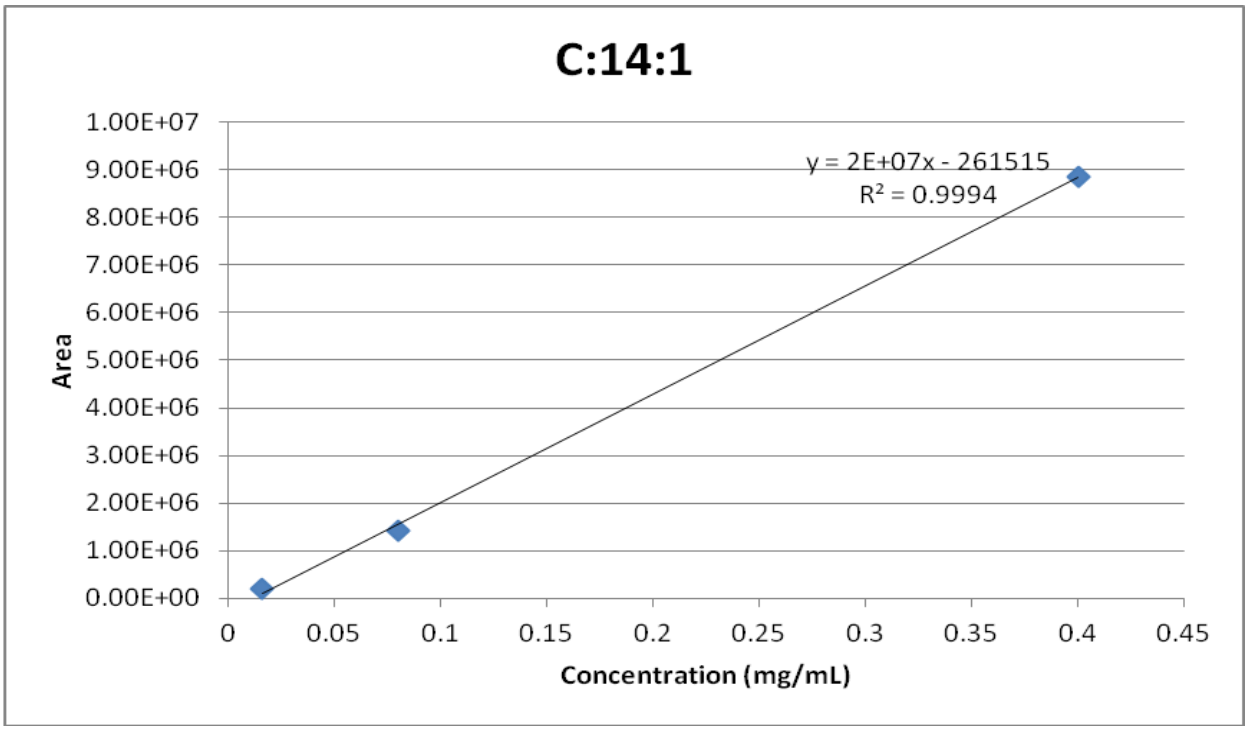

Figure 28 :C_4-C_{24} Standard FAME C:14:1 Calibration Curve

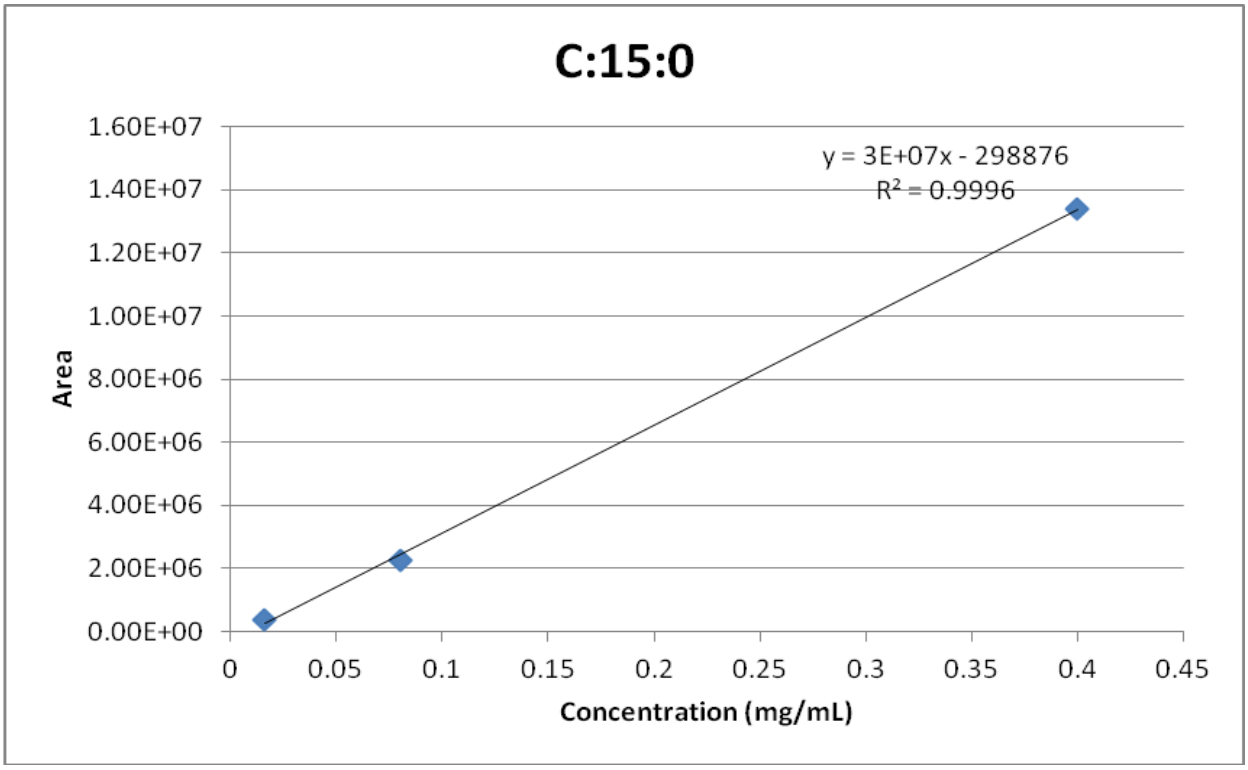

Figure 29: C_4-C_{24} Standard FAME C:15:0 Calibration Curve

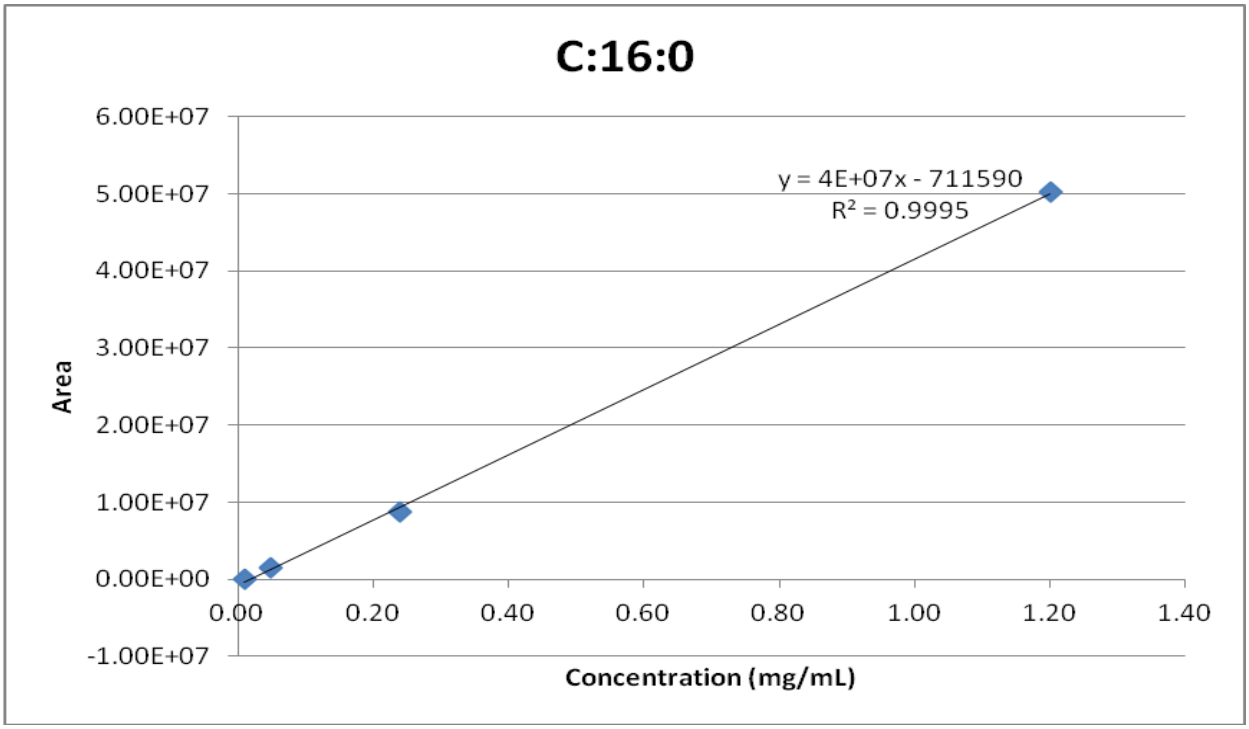

Figure 30: C_4-C_{24} Standard FAME C:16:0 Calibration Curve

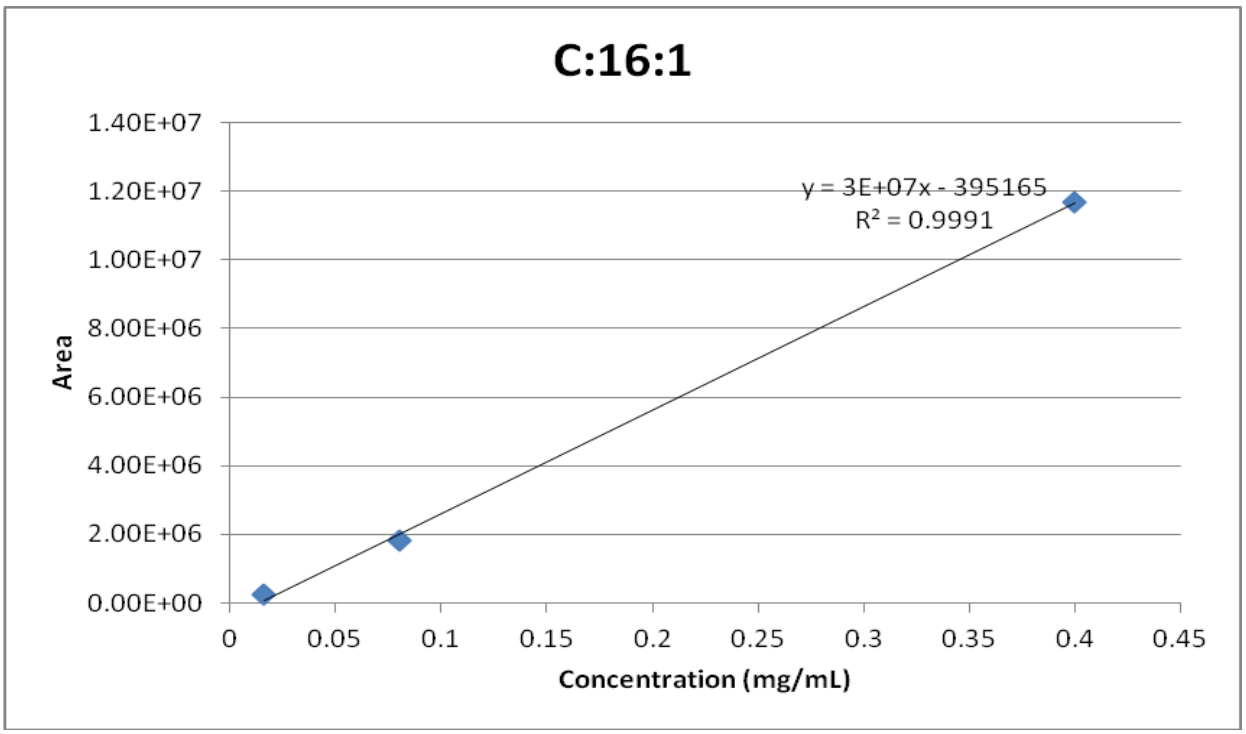

Figure 31: C_4-C_{24} Standard FAME C:16:1 Calibration Curve

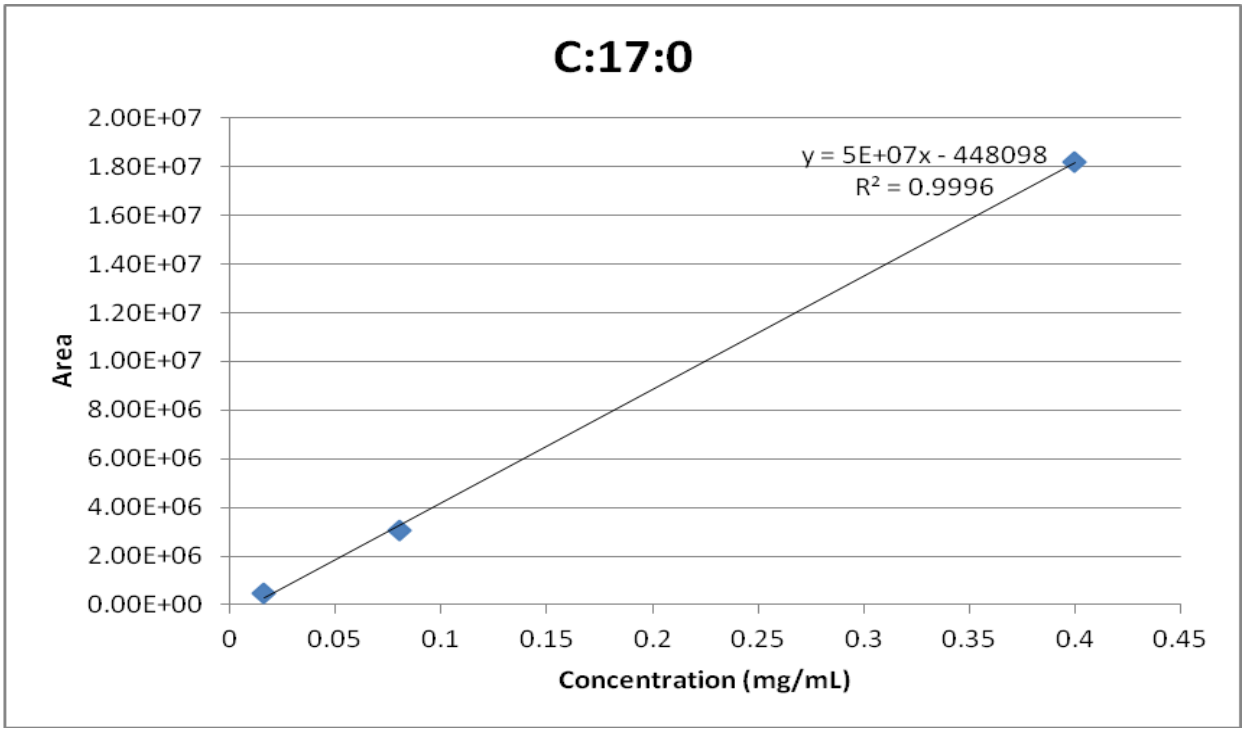

Figure 32: C_4-C_{24} Standard FAME C:17:0 Calibration Curve

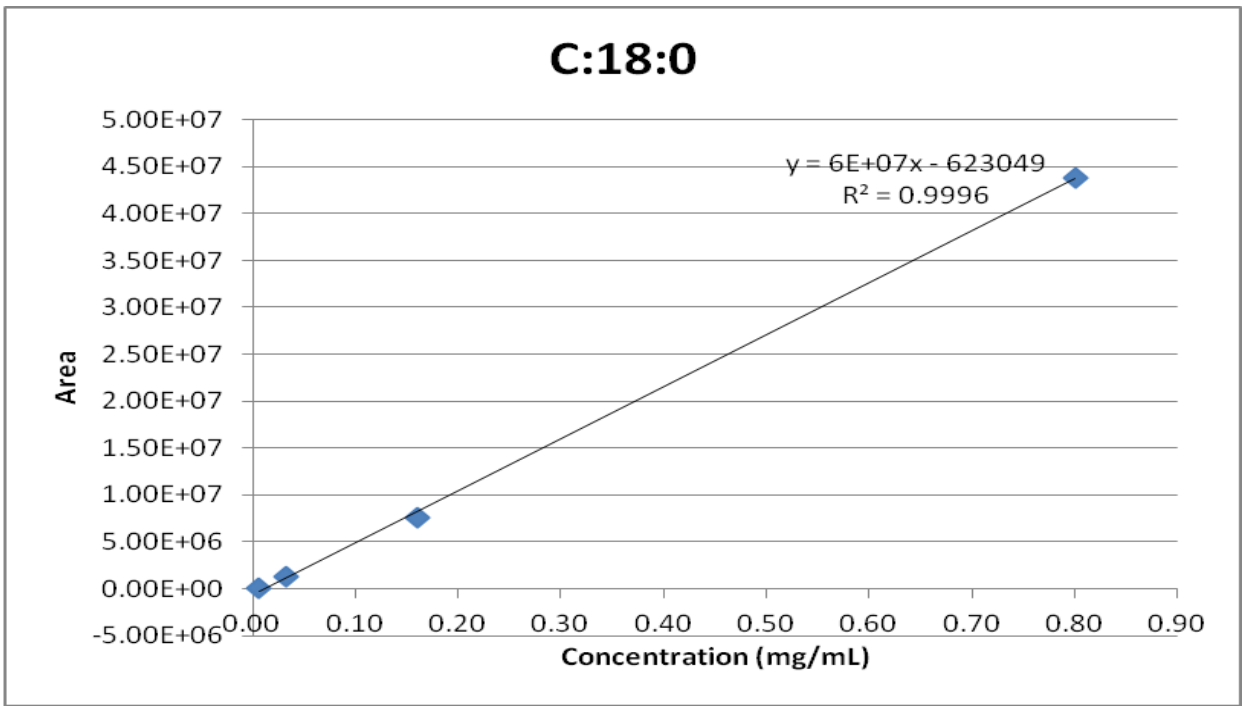

Figure 33: C_4-C_{24} Standard FAME C:18:0 Calibration Curve

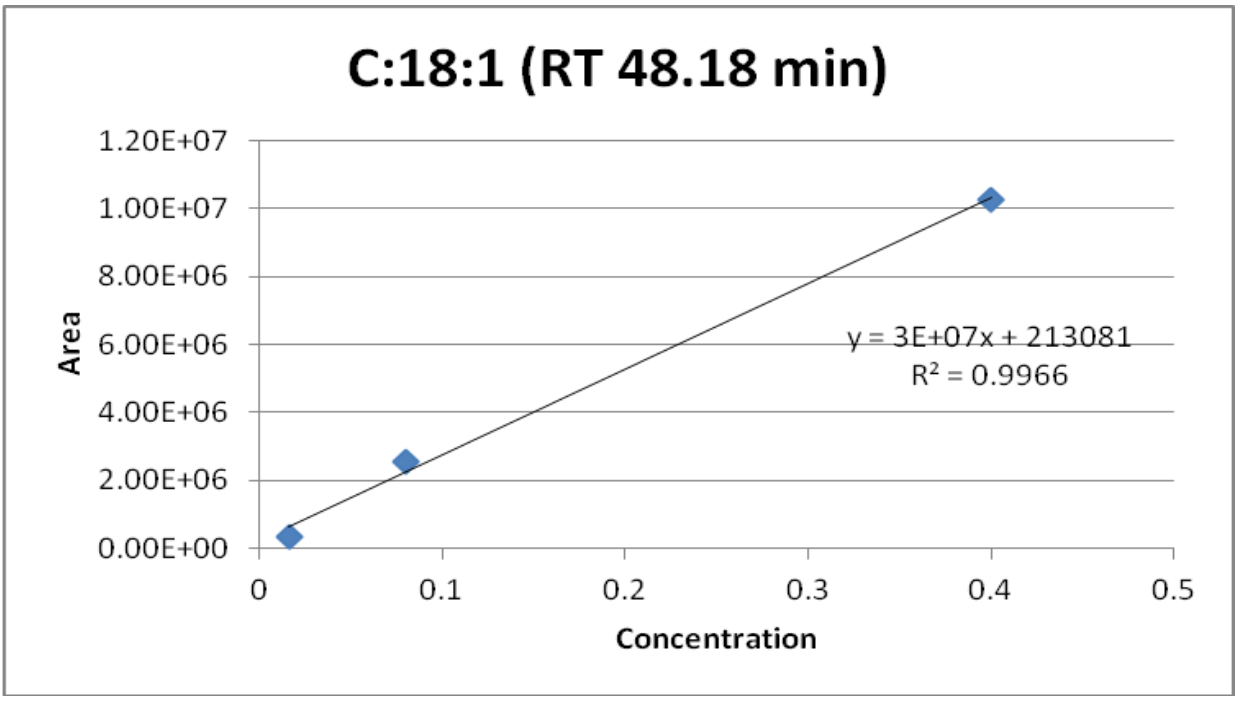

Figure 34: C_4-C_{24} Standard FAME C:18:1 (RT 48.18 min) Calibration Curve

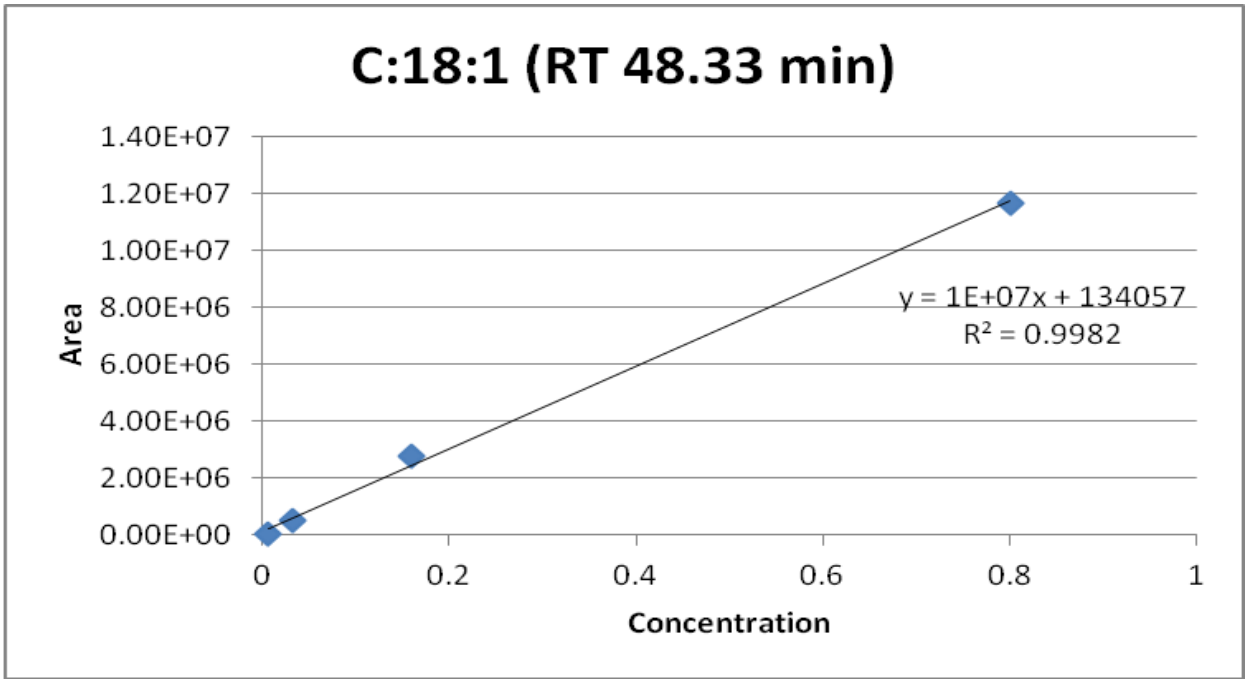

Figure 35: C_4-C_{24} Standard FAME C:18:3 Calibration Curve

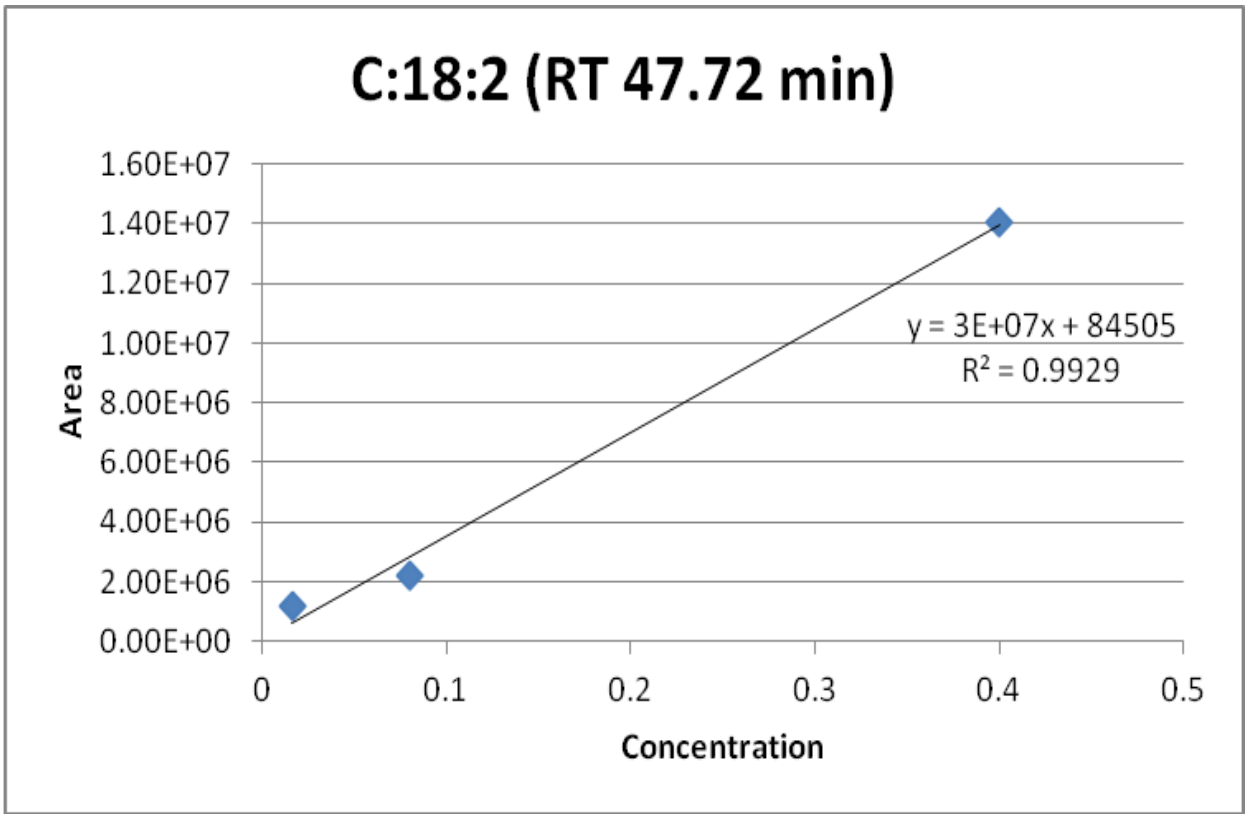

Figure 36: C_4-C_{24} Standard FAME C:18:2 (RT 47.72 min) Calibration Curve

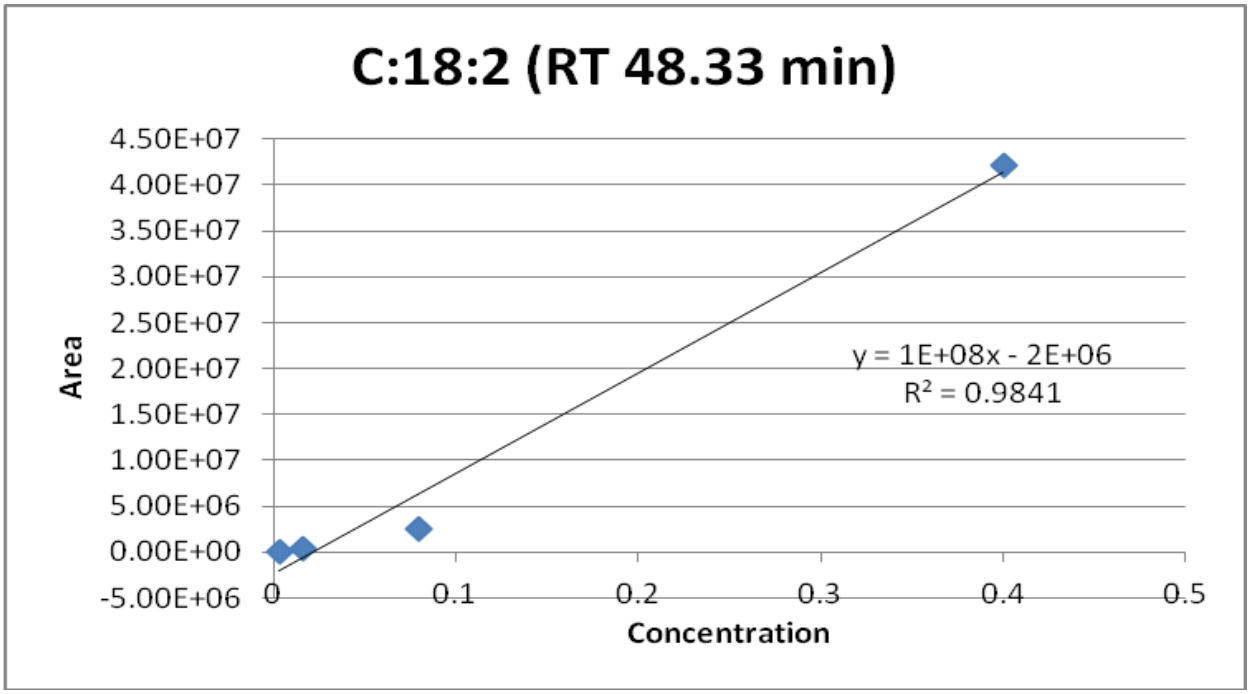

Figure 37: C_4-C_{24} Standard FAME C:18:2 (RT 48.33 min) Calibration Curve

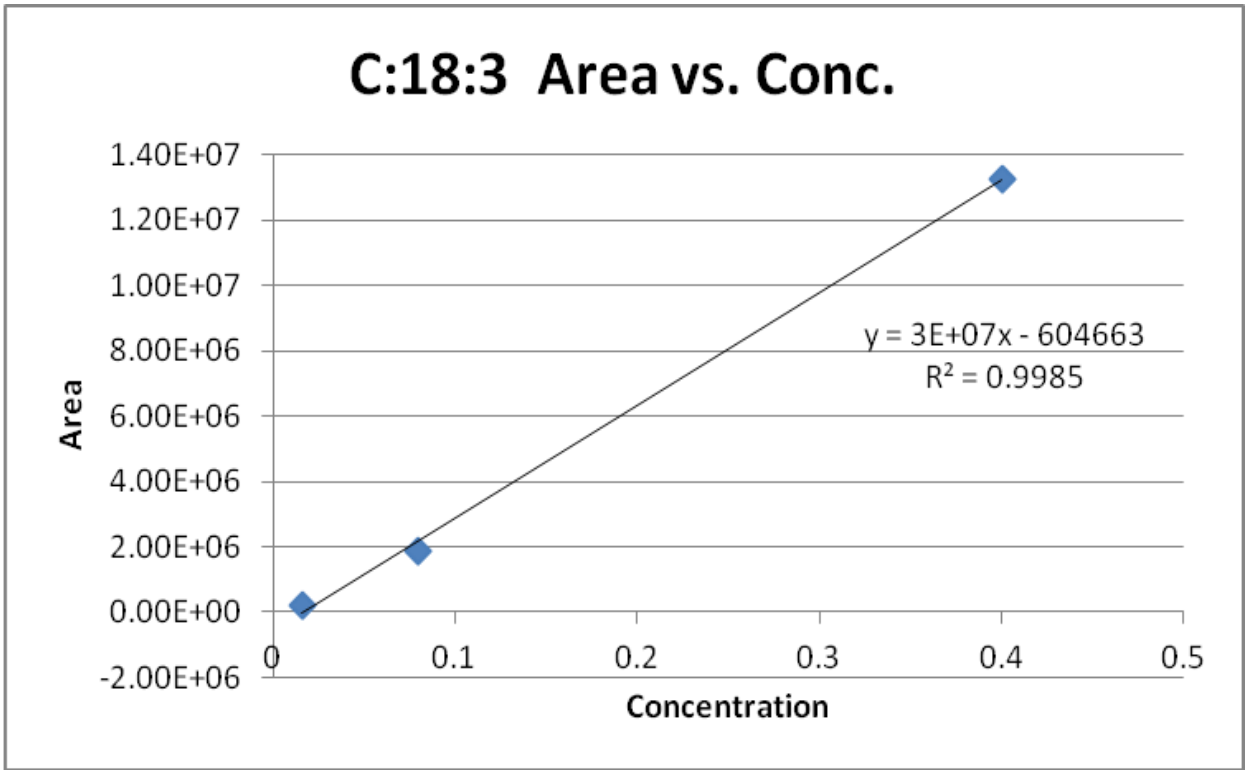

Figure 38: C_4-C_{24} Standard FAME C:18:3 Calibration Curve

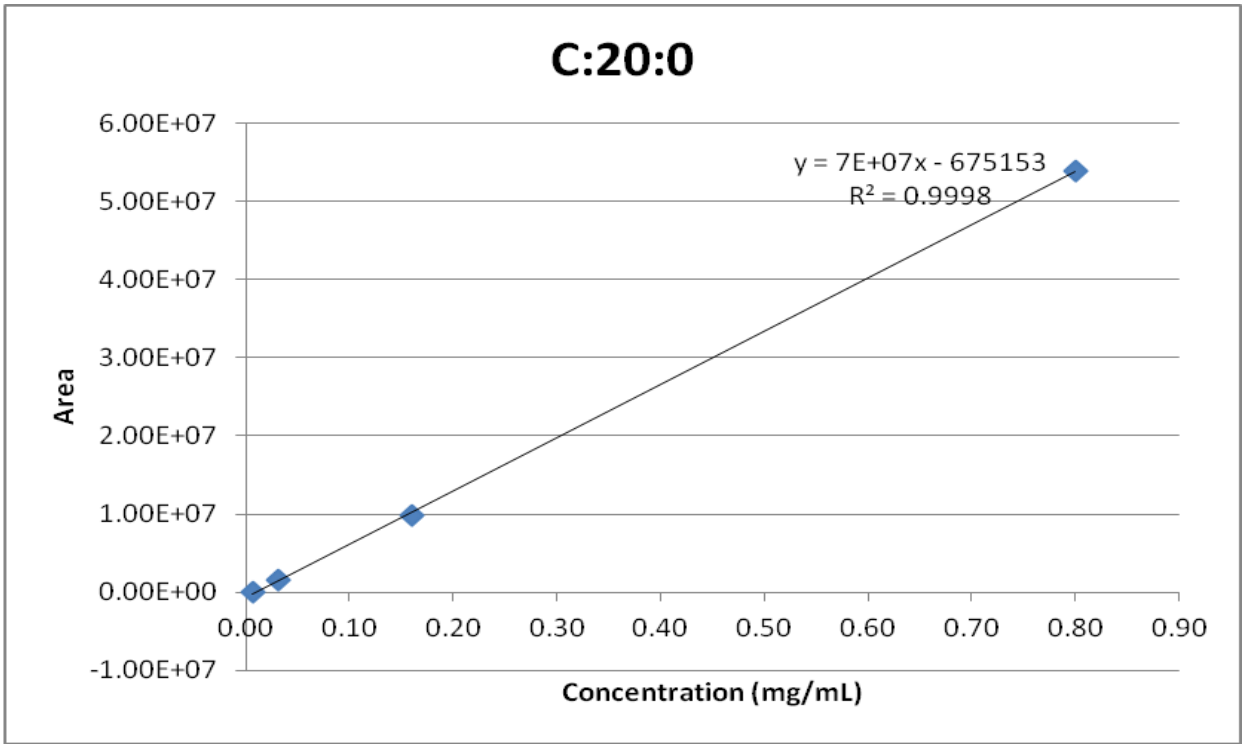

Figure 39: C_4-C_{24} Standard FAME C:20:0 Calibration Curve

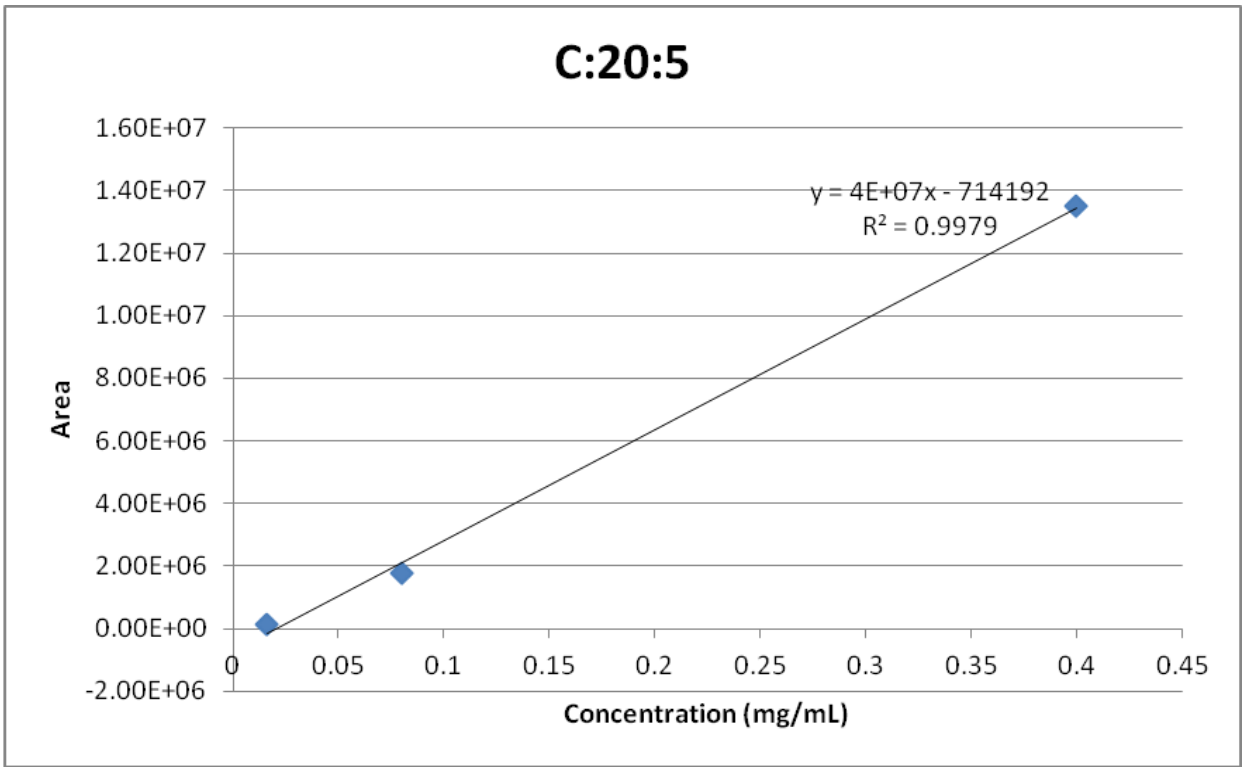

Figure 40: C_4-C_{24} Standard FAME C:20:5 Calibration Curve

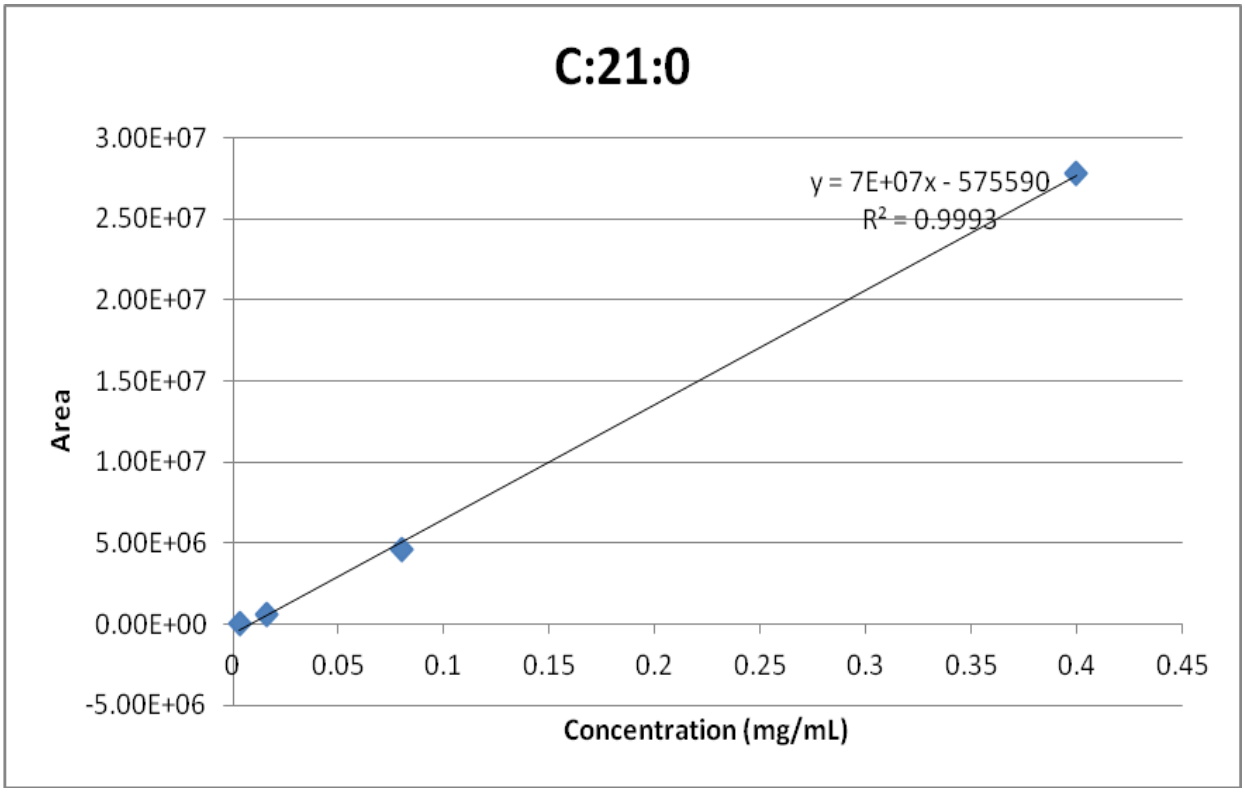

Figure 41: C_4-C_{24} Standard FAME C:21:0 Calibration Curve

The response factor was calculated for each analyte in all four serial dilutions with the following equation (2). See Table 6.

$$RF=(A_{FA}/C_{FA})/(A_{IS}/C_{IS}) \quad (2)$$

RF= Response Factor

A_{FA}= Area of Fatty Acid Methyl Ester

C_{FA}= Concentration of Fatty Acid Methyl Ester

A_{IS}= Area of Internal Standard (Naphthalene)

C_{IS}= Concentration of Internal Standard (Naphthalene)

The use of a response factor was necessary because the mass spectrometer generally will have a different response to each component analyzed [32]. The concentration of the internal standard and the FAME may be the same but the peak areas of each analyte may differ. The known response factor was then used to calculate the concentration of the FAME in the transesterification extract (Tables 7 and 8).

Table 6: C_4-C_{24} Standard FAME with Internal Standard Response Factor Values

C:12:0	
Dilution	RF
1	5.24E-01
2	2.31E-01
3	3.69E-01
4	n/a
Mean	**3.75E-01**
SD	**1.47E-01**

C:13:0	
Dilution	RF
1	1.05E+00
2	8.88E-01
3	7.87E-01
4	n/a
Mean	**9.08E-01**
SD	**1.32E-01**

C:14:0	
Dilution	RF
1	8.29E-01
2	3.70E-01
3	6.20E-01
4	n/a
Mean	**6.06E-01**
SD	**2.30E-01**

C:14:1	
Dilution	RF
1	6.41E-01
2	6.89E-01
3	3.75E-01
4	n/a
Mean	**5.69E-01**
SD	**1.69E-01**

C:15:0	
Dilution	RF
1	9.70E-01
2	8.23E-01
3	6.89E-01
4	n/a
Mean	**8.27E-01**
SD	**1.40E-01**

C:16:0	
Dilution	RF
1	1.21E+00
2	5.44E-01
3	8.83E-01
4	6.52E-01
Mean	**8.22E-01**
SD	**2.95E-01**

C:16:1	
Dilution	RF
1	8.46E-01
2	6.58E-01
3	4.53E-01
4	n/a
Mean	**6.52E-01**
SD	**1.96E-01**

C:17:0	
Dilution	RF
1	1.32E+00
2	5.75E-01
3	7.98E-01
4	n/a
Mean	**8.98E-01**
SD	**3.82E-01**

C:18:0	
Dilution	RF
1	1.59E+00
2	7.15E-01
3	1.14E+00
4	7.64E-01
Mean	**1.05E+00**
SD	**4.04E-01**

C:20:0	
Dilution	RF
1	1.95E+00
2	9.16E-01
3	1.35E+00
4	9.03E-01
Mean	**1.28E+00**
SD	**4.94E-01**

C:20:5	
Dilution	RF
1	9.78E-01
2	2.82E-01
3	1.02E+00
4	n/a
Mean	**7.59E-01**
SD	**4.14E-01**

C:21:0	
Dilution	RF
1	2.01E+00
2	8.66E-01
3	9.55E-01
4	n/a
Mean	**1.28E+00**
SD	**6.37E-00**

C:18:1 (48.18)	
Dilution	RF
1	7.44E-01
2	4.81E-01
3	5.89E-01
4	n/a
Mean	6.04E-01
SD	1.32E-01

C:18:1 (48.33)	
Dilution	RF
1	4.23E-01
2	2.62E-01
3	4.49E-01
4	3.61E-01
Mean	3.73E-01
SD	8.31E-02

C:18:2 (48.02)	
Dilution	RF
1	3.05E+00
2	4.81E-01
3	5.89E-01
4	7.21E-01
Mean	1.21E+00
SD	1.23E+00

C:18:2 (47.72)	
Dilution	RF
1	1.02E+00
2	4.15E-01
3	2.01E+00
4	n/a
Mean	1.15E+00
SD	0.803975

Calculation of Concentration of Fatty Acid for C:18:0

$RF=(A_{FA}/C_{FA})/(A_{IS}/C_{IS})$

$1.05=(3.70E6/C_{FA})/(1.73E5/5.01E-3)$

C_{FA}=9.39E-2

9.39E-2 mg/mL*1.0 ml of hexane =9.39E-2 mg C:18:0/1252.9 mg algae

Weight % = 0.00749 %

Table 7: Concentration of Fatty Acids in Transesterification Sample

Cmpd	Apex RT	Area	%Area	%Height	Conc. (mg/mL)	Wt %
C:14:0	30.43	1.11E+08	13.03	11.96	4.88E+00	3.89E-01
C:15:0	35.17	1.84E+06	0.22	0.35	5.92E-02	4.72E-03
C:16:1	38.99	1.77E+07	2.08	2.83	7.22E-01	5.77E-02
C:16:0	40.13	5.91E+07	6.94	8.24	1.92E+00	1.53E-01
C:17:0	43.35	4.01E+06	0.47	0.67	1.19E-01	9.51E-03
C:18:3	47.15	1.28E+08	15.03	12.72	*	*
C:18:4	47.4	5.34E+07	6.28	8.07	*	*
C:18:2	47.99	1.54E+08	18.07	15.26	*	*
C:18:1	48.32	2.14E+08	25.15	22.47	*	*
C:18:0	49.19	3.70E+06	0.44	0.69	9.39E-02	7.49E-03
C:20:5	54.71	3.56E+07	4.18	5.59	1.25E+00	9.98E-02
C:21:0	61.84	2.60E+04	0.00	0.10	5.42E-04	4.33E-05

Table 8: Estimated Concentration of Fatty Acids in Transesterification Sample

Cmpd	Apex RT	Area	%Area	%Height	Conc. (mg/mL)	Wt %
C:18:3	47.15	1.28E+08	15.03	12.72	3.41E+00	2.72E-01
C:18:4	47.4	5.34E+07	6.28	8.07	1.43E+00	1.14E-01
C:18:2	47.99	1.54E+08	18.07	15.26	4.10E+00	3.27E-01
C:18:1	48.32	2.14E+08	25.15	22.47	5.71E+00	4.56E-01

*The concentrations for these compounds were estimated using an RF value of 1.00.

The composition of high quality microalgal biodiesels should have an equal mixture of saturated and unsaturated fatty acids to maintain high oxidative stability and low temperature property [4]. Also, according to European Standards for quality biodiesel, the linolenic acid (C:18:3) content cannot exceed 12% of the total fatty acids [4]. The linolenic acid limit is not met and unfortunately the amount of lipids produced using the growing conditions described in Section 2.2 are too minute for *Chromulina* to be considered a good source of biodiesel.

Two different methods were used to dry the same batch of algae, a drying oven and a freeze dryer. The transesterification method described in Section 2.2.3 was used to extract the lipids from each sample. The oven dried (OD) and freeze dried (FD) transesterification extracts were analyzed via GC-MS with the parameters described in section 2.2.1. Figures 42 and 43 are the EI chromatograms for the OD and FD transesterification extracts, respectively. The retention times (RT) of the FAME were the same in the GC-MS analysis but the relative abundance of each compound differed. The relative abundance of C:14:0, C:15:0, C:16:0, and C:16:1 was decreased but the C:18 unsaturates and C:20:5 relative abundance was increased in the FD EI analysis. The CI analysis illustrated similar results (see Figure 44 and Figure 45). Table 9 is the ratio of the area and height of each FAME from the freeze dry to the oven dry method.

Table 9: Ratio of Freeze Dry (FD) Peak Area and Height vs. Oven Dry (OD) Peak Area and Height

Compound	FD/OD RT	FDa/ODa	FDh/ODh
C:14:0	30.32/30.23	0.91	0.78
C:15:0	35.16/35.37	0.28	0.26
C:16:1	38.95/38.93	0.87	0.77
C:16:0	40.10/40.05	0.81	0.66
C:18:3	47.09/46.95	1.23	0.87
C;18:2	47.36/47.21	2.03	1.67
C:18:1	47.75/47.67	1.40	0.78
C:20:5	54.67/54.60	1.55	1.35

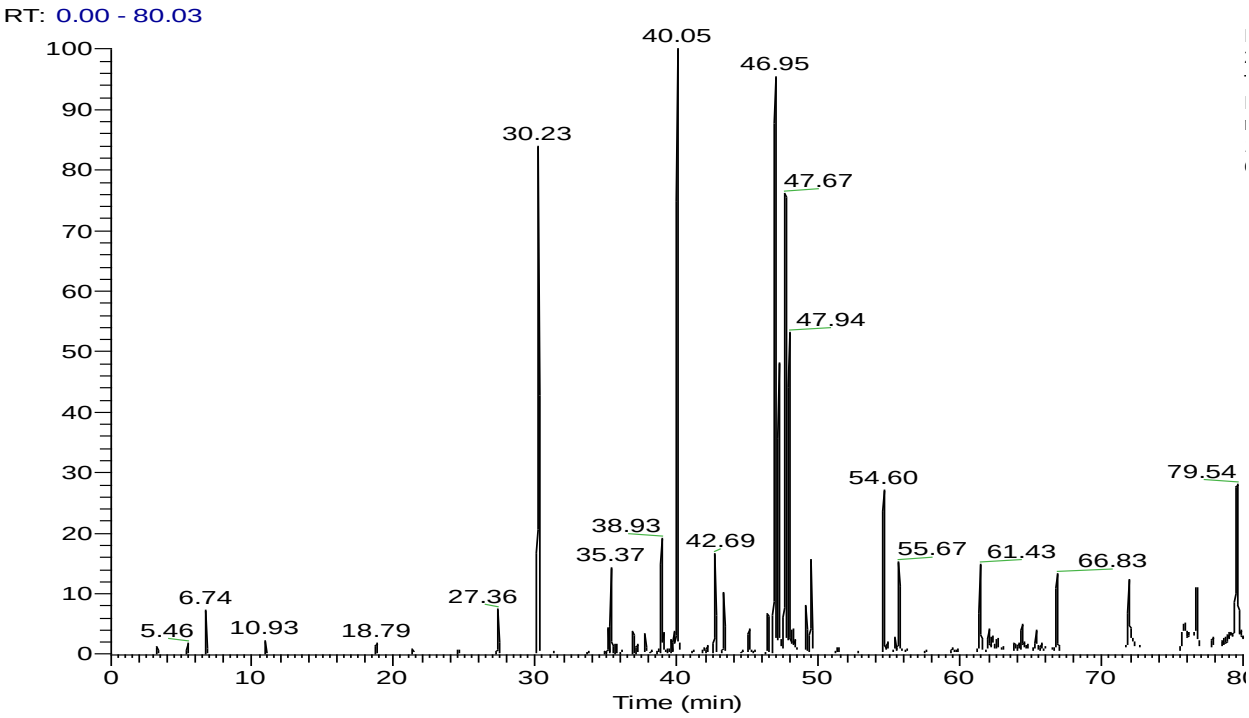

Figure 42: EI Chromatogram of Transesterification Sample from Oven Dried *C. freiburgensis*

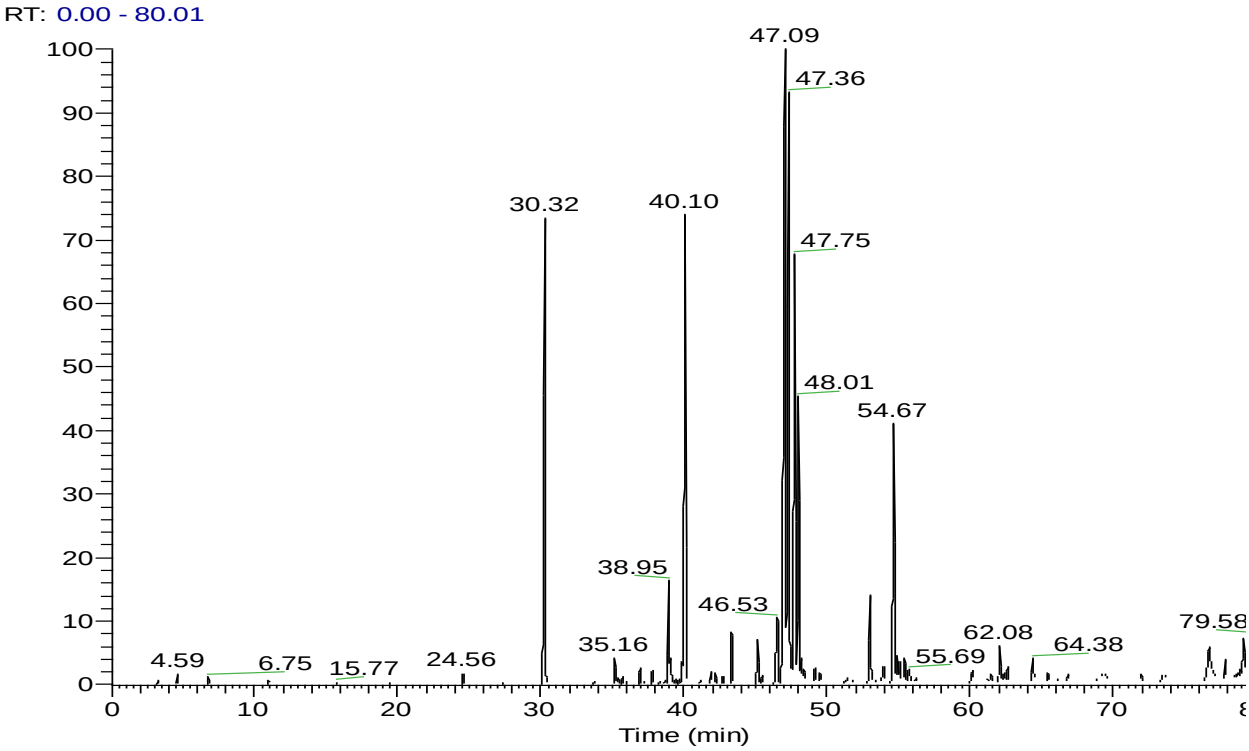

Figure 43: EI Chromatogram of Transesterification Sample from Freeze Dried *C. freiburgensis*

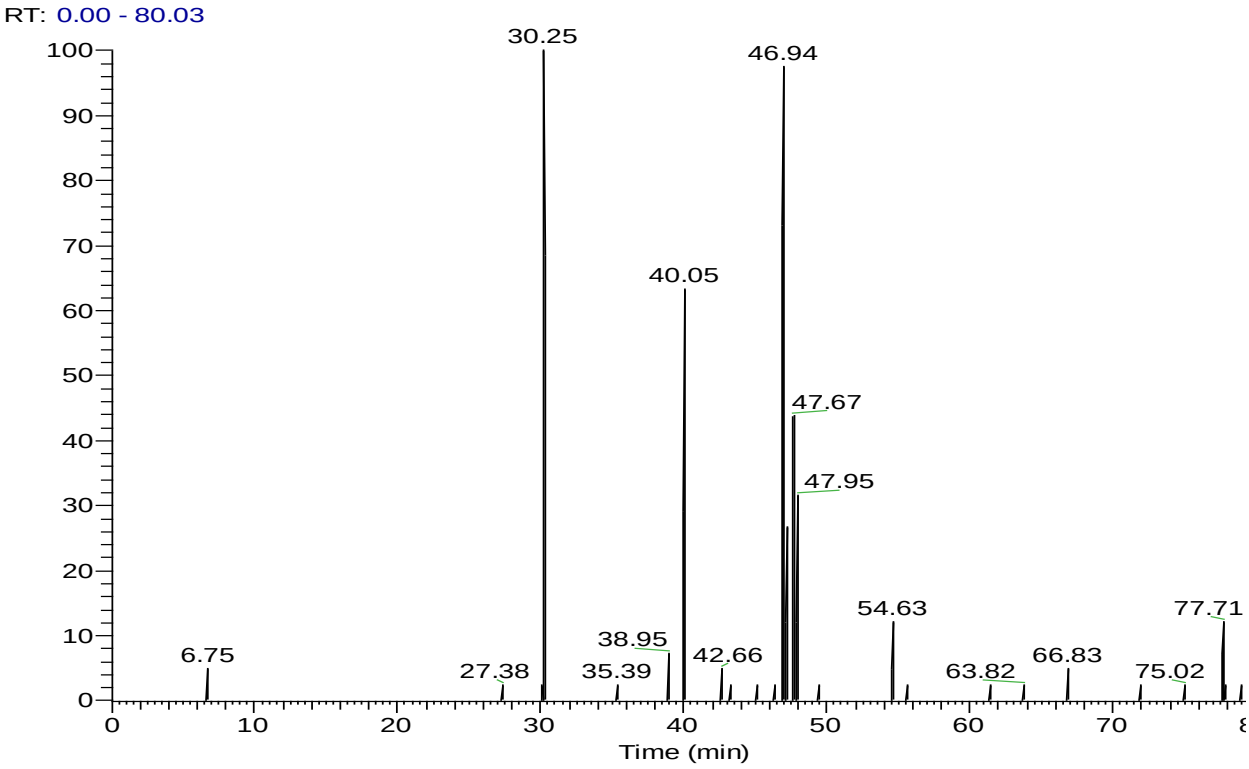

Figure 44: CI Chromatogram of Transesterification Sample from Oven Dried *C. freiburgensis*

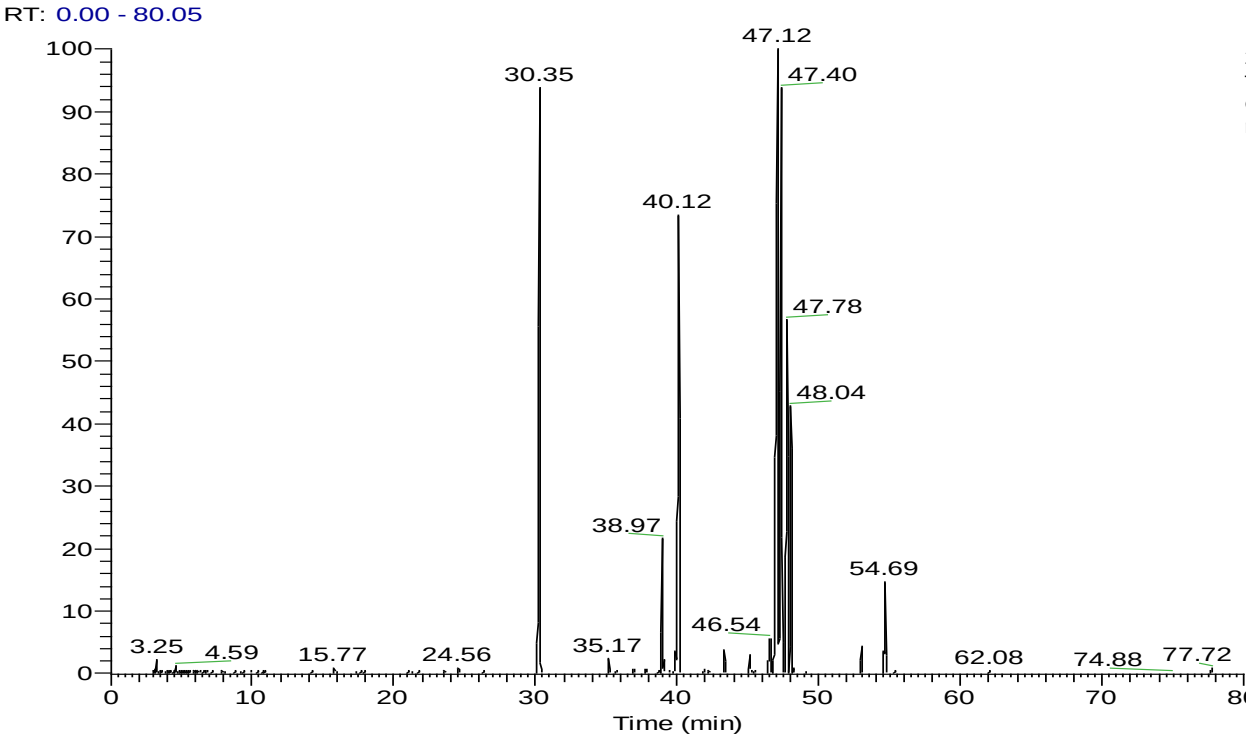

Figure 45: CI Chromatogram of Transesterification Sample from Freeze Dried *C. freiburgensis*

4. Conclusion

C. freiburgensis was isolated from the Berkeley Pit in Butte, Montana by Grant Mitman and successfully grown in MAM in pure culture. *Chromulina* does not appear to produce any free fatty acids under the growing conditions described in Section 2.2.1. This conclusion is based on not finding any detectable FAMEs from the Bligh and Dyer and Ether extraction methods. Methyl myristate (C:14:0), pentadecanoate (C:15:0), palmitate (C:16:0), palmitoleate (C:16:1), heptadecanoate (C:17:0), stearate (C:18:0), oleate (C:18:1), linoleate (C:18:2), linoleneate (C:18:3), arachidate (C:20:0), and eicosapentaenoate (C:20:5) were extracted using the transesterification method. The FAMES were identified and quantified by comparison to a C_4-C_{24} FAME standard.

Using the growing conditions in this study, *C. freiburgensis* did not produce enough fatty acid methyl esters to be used as a biofuel source. Microalgae that are currently being used to make biodiesel have a lipid content that is at least 25 % of their dry weight [4]. The most abundant lipids produced were methyl myristate (C:14:0), palmitic acid methyl ester (C:16:0), and saturated and unsaturated octadecanoic acid methyl esters (C:18:0, C:18:1, C:18:2, C:18:3, C:18:4). Most microalgal biodiesels are composed of unsaturated fatty acids such as palmitoleate, linoleate, and linoleneate and saturated fatty acids such as palmitate and oleate [33].

5. Future Work

The algal stocks used in this work were obtained from a mixture of organisms growing in Berkeley Pit water. The date of sample water extraction from the Berkeley Pit is unknown. A new sample must be collected from the waters of the Pit. Proper culturing techniques should be employed and freezer stocks should be made to ensure the cells are not continually changing. The genetics of the new *Chromulina* stock must to be compared to the previous sample to make sure the organism has not mutated since its original extraction.

The preliminary data (not shown) obtained from the polysaccharide extraction was promising. Further extraction, identification, and quantification of polysaccharides is crucial in determining the potential of *C. freiburgensis* as a source for biofuels. Polysaccharides have a high molecular weight; therefore, the polysaccharide extracts need to be analyzed via electrospray ionization.

Varying the growth conditions of *C. freiburgensis* to determine any resulting change in composition needs to be further explored. Changing the temperature and decreasing the nitrogen and phosphorous concentrations in the growth media may produce a larger quantity or alter the distribution of lipids [4]. *Chromulina* should also be grown in large scale and analyzed to determine any differences in lipid and polysaccharide production.

Lastly, repeat analyses of the freeze dry method should be performed. The data obtained thus far indicate that the drying method does not have a significant effect on lipid quantities but should be further investigated.

References Cited

1. Huang, G., et al., *Biodiesel Production by Microalgal Biotechnology.* Applied Energy, 2010. **87**: p. 38-46.
2. Hahn-Hagerdal, B., et al., *Bioethanol-the fuel of tomorrow from the residues of today.* TRENDS in Biotechnology, 2006. 24 (12): p. 549-556.
3. Hongjin, Q. and W. Guangce, *Effect of carbon source on growth and lipid accumulation in Chlorella sorokiniana.* Chinese Journal of Oceanology and Linmology, 2009. 27: p. 762-768.
4. Mutanda, T., S. Karthikeyan, and F. Bux, *The utilization of post-chlorinated municipal domestic wastewater for biomass and lipid production by Chlorella spp. under batch conditions.* Applied Biochemistry and Biotechnology, 2011. 164(7): p. 1126-1138.
5. *Oilgae*. 2011 [cited 2011 February 23]; Available from: http://www.oilgae.com/algae/algae.html.
6. Wu, L.F., et al., *The feasibility of biodiesel production by microalgae using industrial wastewater.* Bioresource Technology, 2012. 113: p. 14-18.
7. *Algae Biofuels for the Future*. [cited 2011 February 23]; Available from: http://www.alternative-energy-news.info/algae-biofuels-future/.
8. El-Sarraf, W.M. and G. El-Shaarawy, *Chemical composition of some marine algae from the Mediterranean Sear of Alexandria, Egypt.* Bulletin of H.I.P.H., 1994. 24 (3): p. 523-534.
9. *United States Energy Information.Biofuels:Ethanol and Biodiesel Explained*. 2011 [cited 2011 June 10]; Available from: http://www.eia.gov/energyexplained/index.cfm?page=biofuel_home#tab2.
10. *Smithsonian National Museum of Natural History: Algae Research*. 2011 [cited 2011 February 23].
11. Wigmosta, M.S., et al., *National Microalgae Biofuel Production Potential and Resource Demand.* Water Resources Research, 2011. 47: p. 1-13.
12. Cheng, J.J. and G.R. Timilsina, *Status and barriers of advanced biofuel technologies: A review.* Renewable Energy, 2011. 36: p. 3541-3549.
13. Hill, J., et al., *Environmental, economic, and energetic costs and benefits of biodiesel and ethanol biofuels.* Proc Natl Acad Sci U S A, 2006. 103 (30): p. 11206-10.

14. Mitman, G., *Algal Bioremediation of the Berkeley Pit Lake*. 1998, Montana Tech of the University of Montana: Butte, Montana.
15. Alberts, B., et al., *Molecular Biology of the Cell*. 4th ed. 2002, New York: Garland Science. 1463.
16. Campbell, N.A. and J.B. Reece, *Biology*. 6th ed. 2002, San Francisco: Pearson Education Inc. 1249.
17. Merchant, S.S., *The Chlamydomonas Genome Reveals the Evolution of Key Animal and Plant Functions.* Science, 2007. 318 (245): p. 245-251.
18. Merchant, S.S., et al., *TAG, You're It! Chlamydomonas as a reference organism for understanding algal triacylglycerol accumulation.* Current Opinion in Biotechnology, 2011. 23: p. 1-12.
19. Harwood, J.L. and I.A. Guschina, *The versatility of algae and their lipid metabolism.* Biochimie, 2009. 91: p. 679-684.
20. Dakel, S.M., *Bioremediative Potential of Chromuline freiburgensis in Culture from the Berkeley Pit*, in *Biological Sciences*. 2001, Montana Tech of the University of Montana: Butte.
21. Mitman, G., *Biological Survey of the Berkeley Pit Lake System*, in *Mine Waste Technology Program*. 1998, Montana Tech of the University of Montana: Butte, Montana.
22. *Biology Reference: Algae*. [cited 2011 February 23]; Biology Encyclopedia]. Available from: http://www.biologyreference.com/A-Ar/Algae.html.
23. Stewart, A., A. Mondloch, Editor. 2009, Montana Tech of the University of Montana: Butte.
24. Olaveson, M.M. and P.M. Stokes, *Responses of the acidophillic alga Euglena mutabilis (Euglenophyceae) to carbon enrichment at pH 3.* Journal of Phycology, 1989. 25: p. 529-539.
25. *Bold's Basal Medium*. The Provasoli-Guillard National center for Culture of Marine Phytoplankton [cited 2011 June 9]; Available from: https://ccmp.bigelow.org/index.php?q=node/71.
26. Xu, D.J., et al., *Molecular weight and monosaccaride composition of Astragalus polysaccharides.* Molecules, 2008. 13: p. 2408-2415.

27. Bligh, E.G. and W.J. Dyer, *A rapid method of total lipid extraction and purification.* Canadian Biochem. Physiol., 1959. **37**: p. 911-917.
28. Ehimen, E.A., Z.F. Sun, and C.G. Carrington, *Variables affecting the in situ transesterification of microalgal lipids.* Fuel, 2010. 89 (677-684).
29. Yu, G., et al., *A comparative analysis of four kinds of polysaccarides purified from Furcellaria lumbricalis.* Journal of Ocean University China, 2007. **6**: p. 16-20.
30. Pelt, C.K.V., J.T. Brenna, and B.K. Carpenter, *Studies of structure and mechanism in acetonitrile chemical ioniation tandem mass spectrometry of polyunsaturated fatty acid methyl esters.* J Am Soc Mass Spectrum, 1999. 10: p. 1253-1262.
31. Pelt, C.V. and J.T. Brenna, *Acetonitrile chemical ionization tandem mass spectrometry to locate double bonds in polyunsaturated fatty acid methyl esters.* Ananlytical Chemistry, 1999. 71: p. 1981-1989.
32. Sobrino, F.H., C.R. Monroy, and J.L. Perez, *Biofeuls and fossil fuels: Life cycle analysis (LCA) optimisation through productive resources maximization.* Renewable and Sustainable Energy Reviews, 2011. 15: p. 2621-2628.
33. Constenoble, O., et al., *Improvements needed for the biodiesel standard EN 14214.* Bioscopes, 2008: p. 1-171.

Appendix A:

Table A.1: CI Transesterification Peaks

CI Transesterification						
Apex RT	Start RT	End RT	Area	%Area	Height	%Height
15.78	15.73	15.92	37888.02	0.14	9532.55	0.31
21.35	21.30	21.49	20654.50	0.07	4523.78	0.15
30.41	30.12	30.47	3687728.21	13.31	399801.24	12.96
35.16	35.09	35.26	45987.22	0.17	9862.62	0.32
38.99	38.84	39.18	681681.61	2.46	116305.02	3.77
40.11	39.78	40.19	1682383.41	6.07	230360.11	7.47
43.35	43.25	43.45	81426.06	0.29	15295.98	0.50
54.70	54.48	54.80	1128524.73	4.07	181414.27	5.88
55.48	55.29	55.59	700241.23	2.53	119225.03	3.86
66.05	65.94	66.16	65359.31	0.24	12092.74	0.39

Table A.2: EI Transesterification Peaks

EI Transesterification						
Apex RT	Start RT	End RT	Area	%Area	Height	%Height
15.83	15.79	16.09	184314.43	0.02	27069.38	0.03
21.59	21.50	21.76	55766.07	0.01	5647.72	0.01
30.42	30.16	30.47	126072218.41	16.44	14375315.70	14.93
35.19	35.12	35.33	1232407.67	0.16	246290.08	0.26
38.99	38.85	39.19	14174312.10	1.85	2567944.60	2.67
40.13	39.80	40.24	54765377.26	7.14	8601021.65	8.93
43.36	43.26	43.49	3292439.66	0.43	588135.25	0.61
54.69	54.52	54.87	25349494.14	3.31	4177992.63	4.34
55.48	55.32	55.80	16940300.10	2.21	2799950.64	2.91
66.06	65.94	66.28	2301768.79	0.30	382243.54	0.40

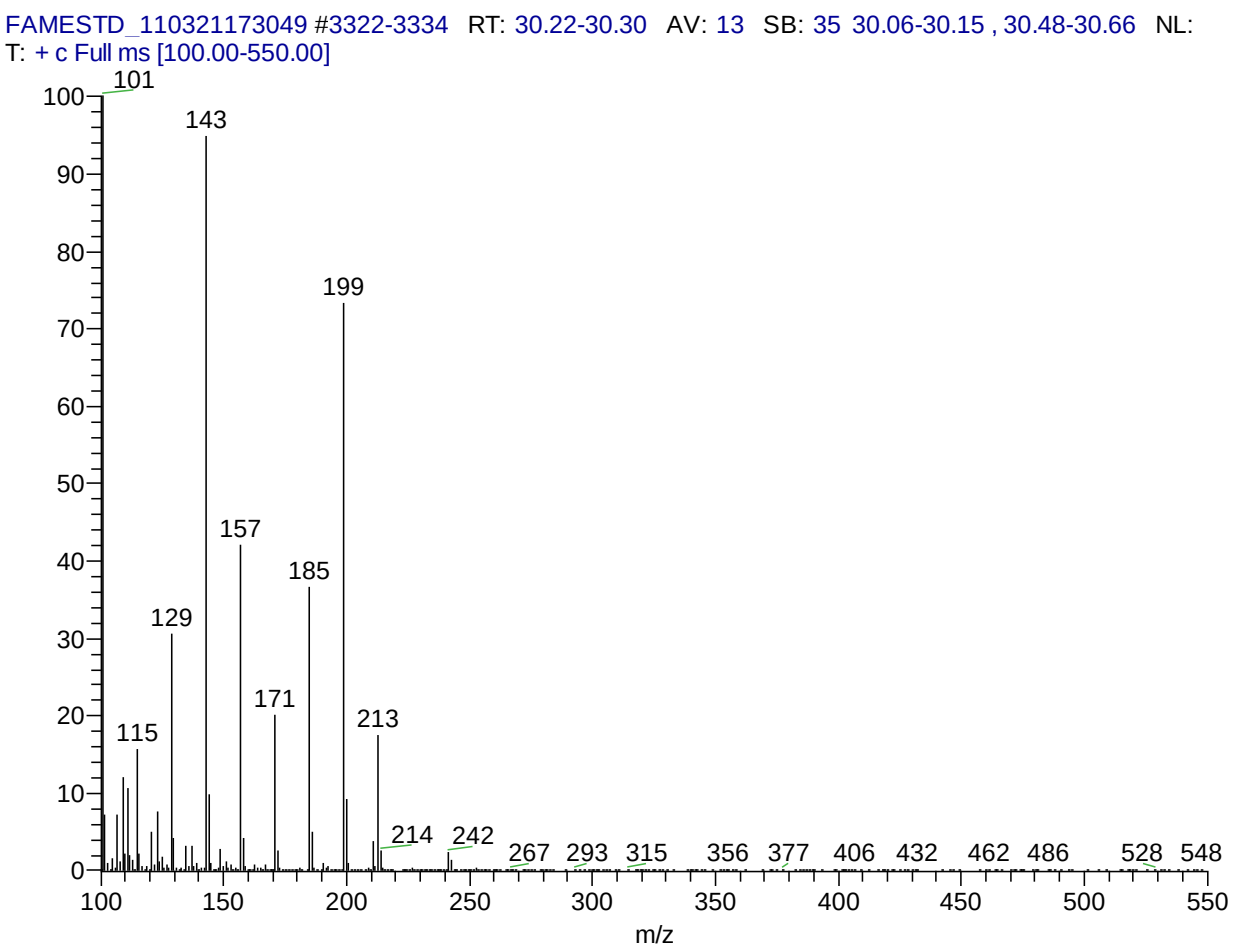

Figure A.1: FAME Standard EI Mass Spectrum at RT 30.25 minutes (C:14:0)

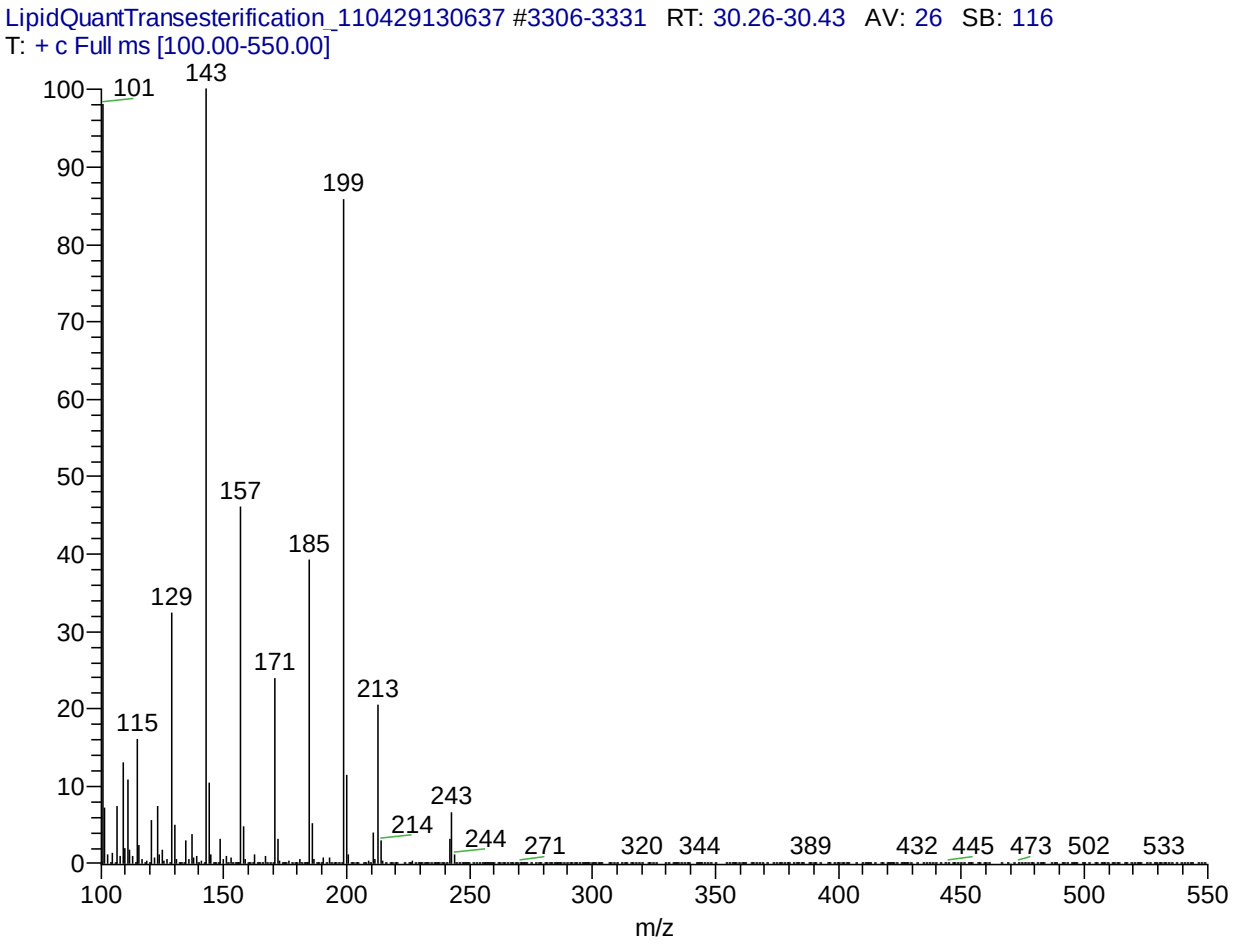

Figure A.2: Transesterification EI Mass Spectrum at RT 30.14 minutes (C:14:0)

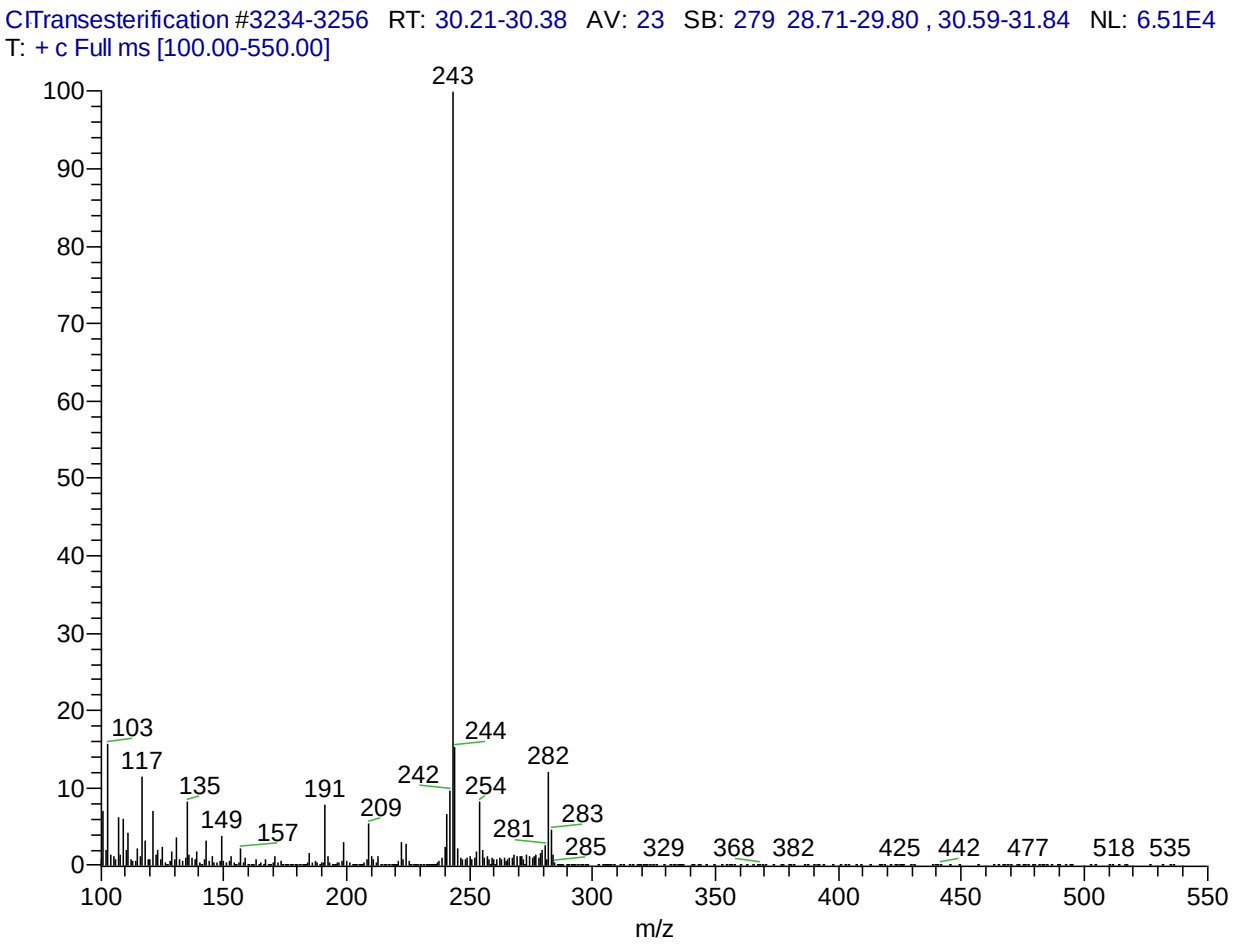

Figure A.3: Transesterification CI Mass Spectrum at RT 30.41 minutes (C:14:0)

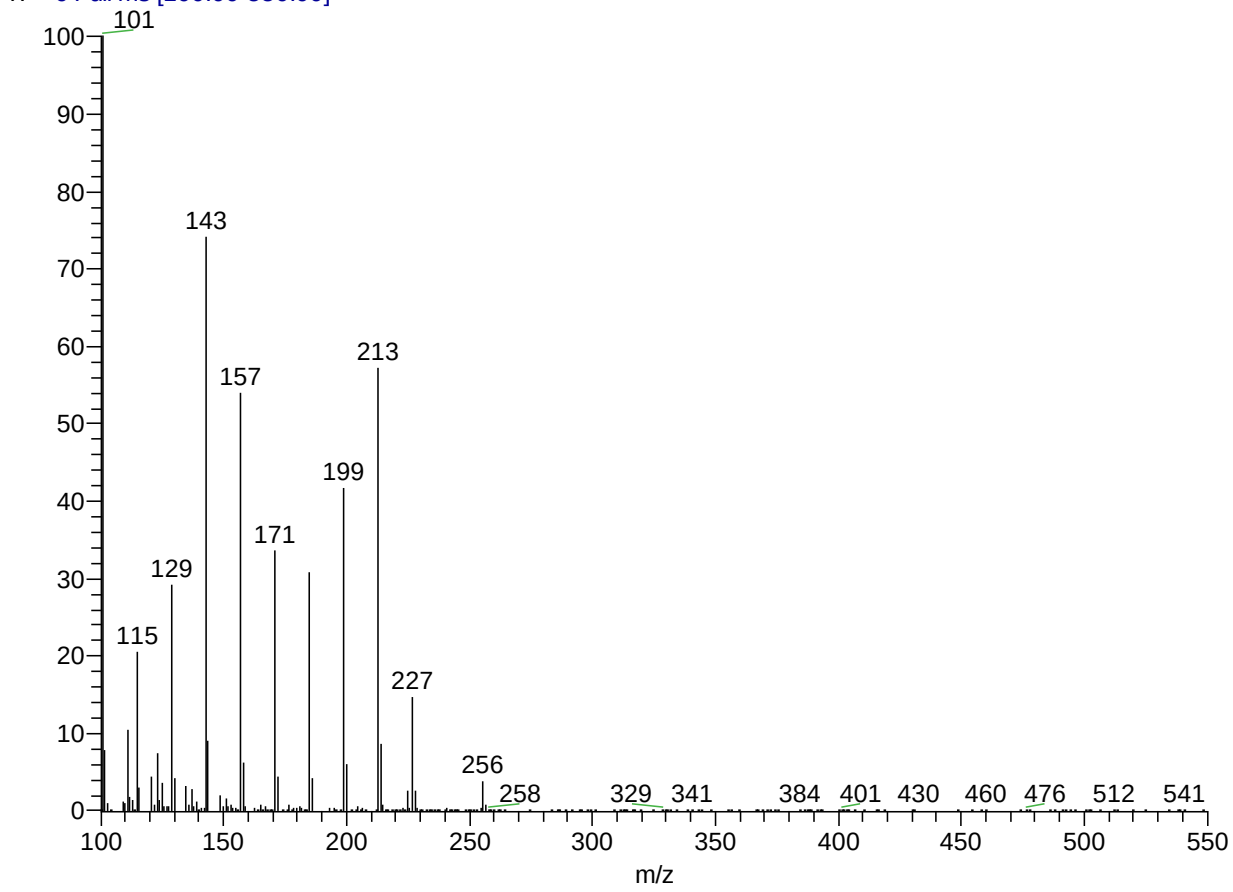

Figure A.4: FAME Standard EI Mass Spectrum at RT 35.24 minutes (C:15:0)

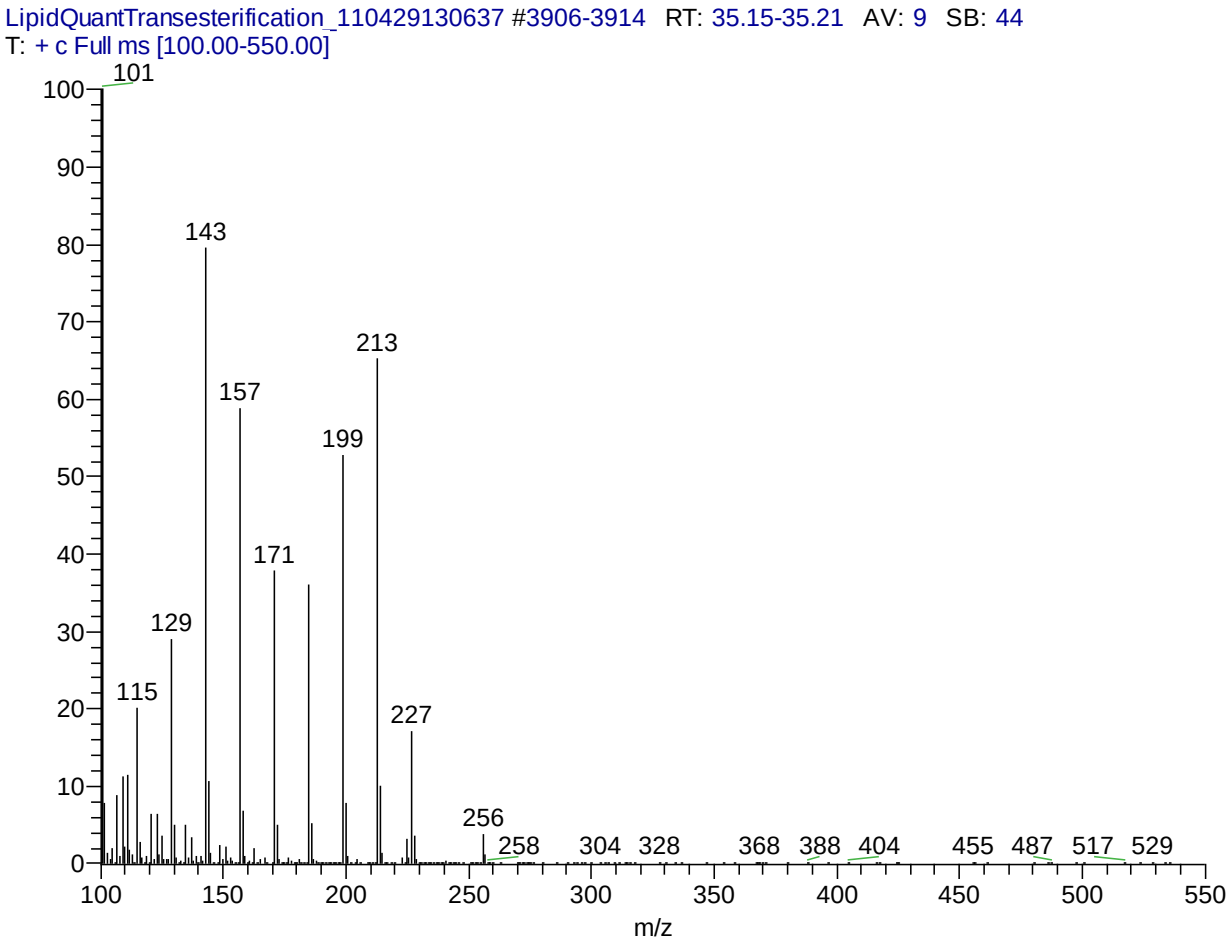

Figure A.5: Transesterification EI Mass Spectrum at RT 35.19 minutes (C:15:0)

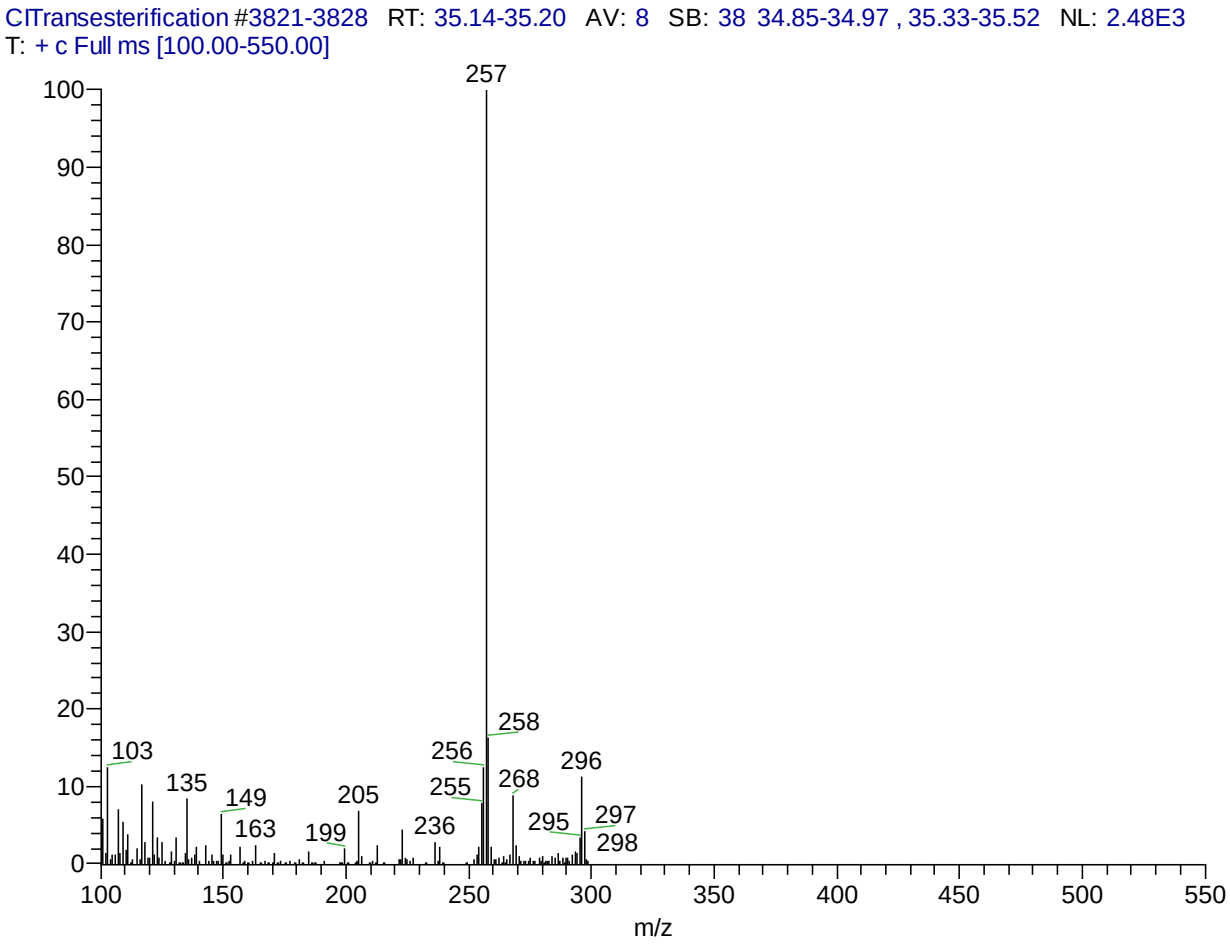

Figure A.6: Transesterification CI Mass Spectrum at RT 35.16 minutes (C:15:0)

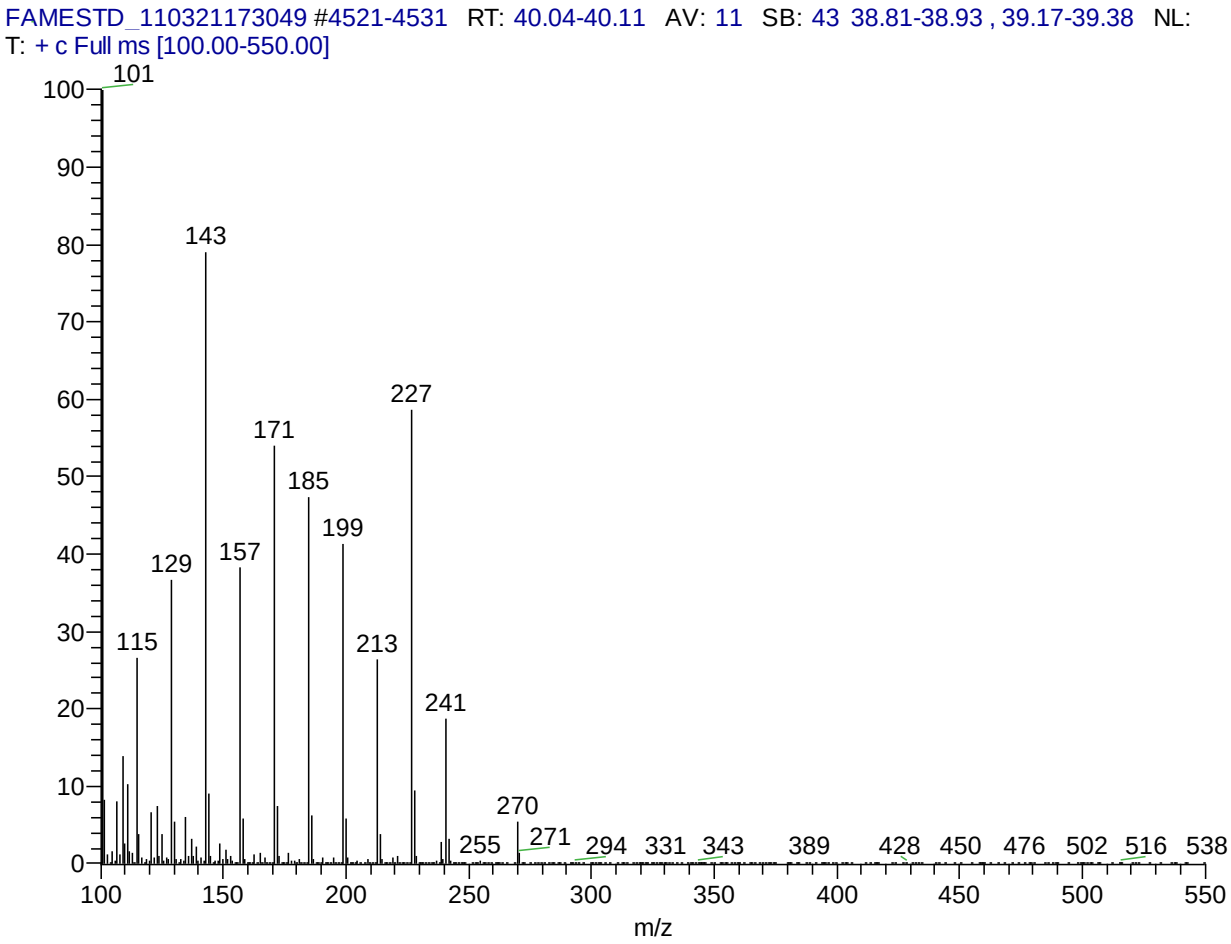

Figure A.7: FAME Standard EI Mass Spectrum at RT 39.02 minutes (C:16:0)

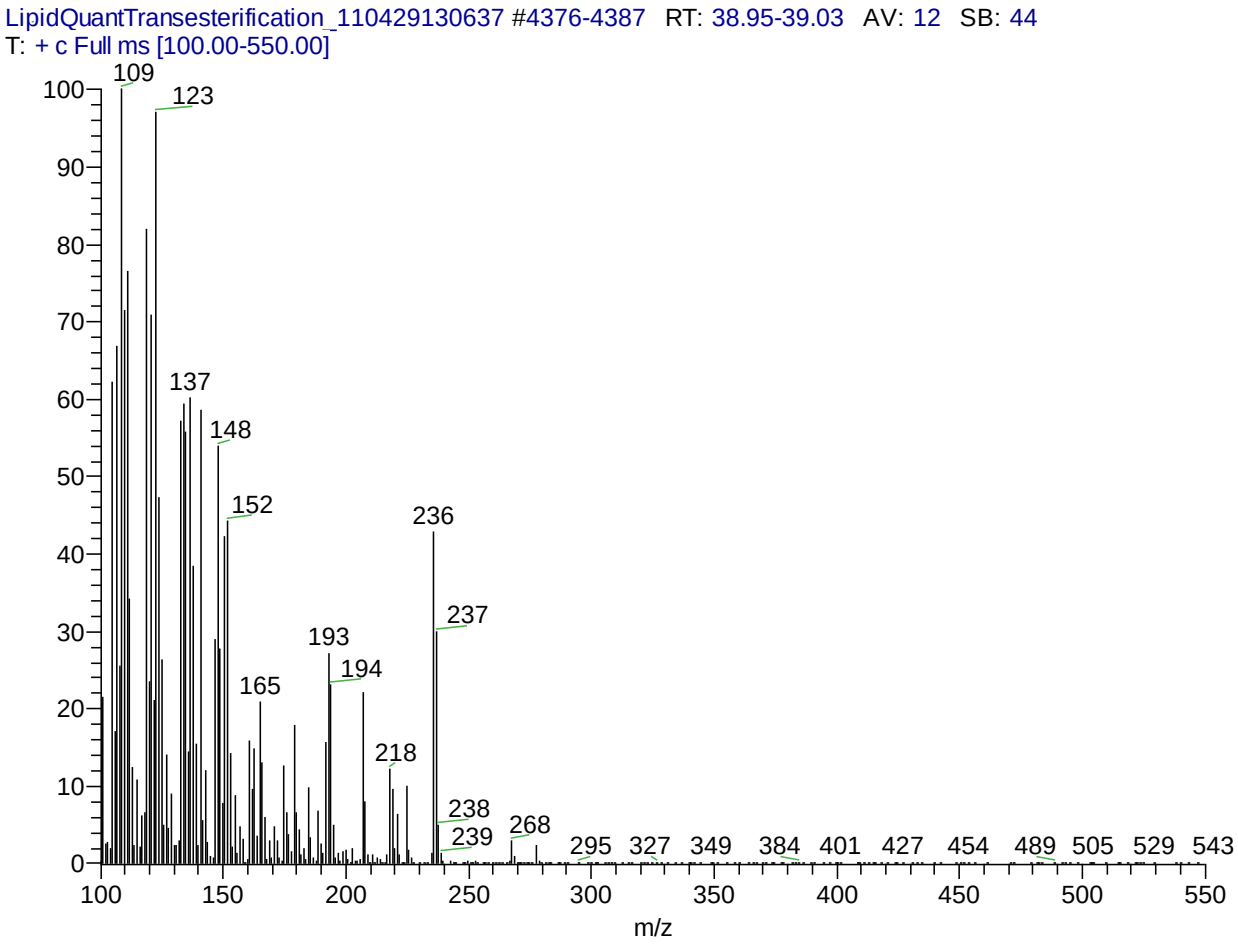

Figure A.8: Transesterification EI Mass Spectrum at RT 38.99 minutes (C:16:1)

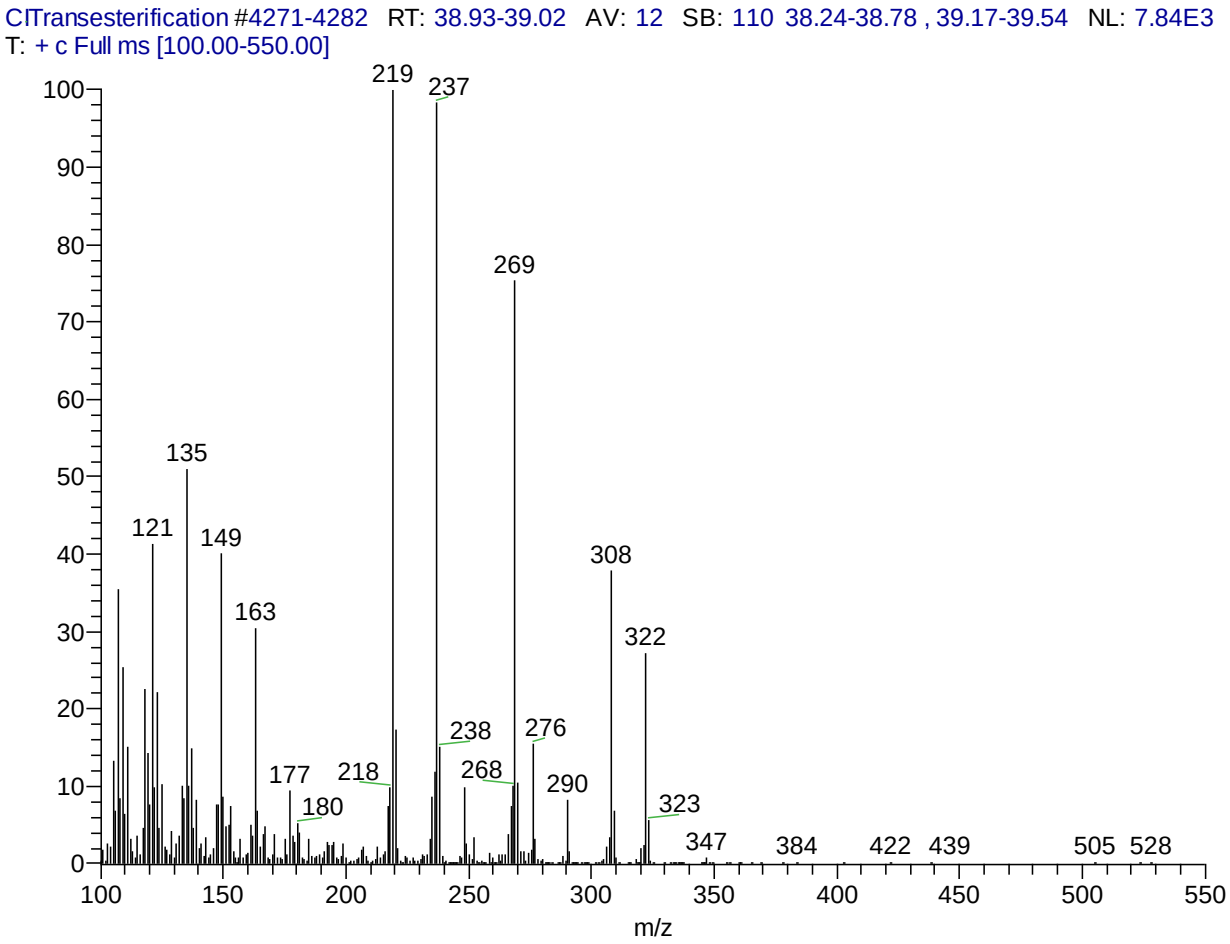

Figure A.9: Transesterification CI Mass Spectrum at RT 38.99 minutes (C:16:1)

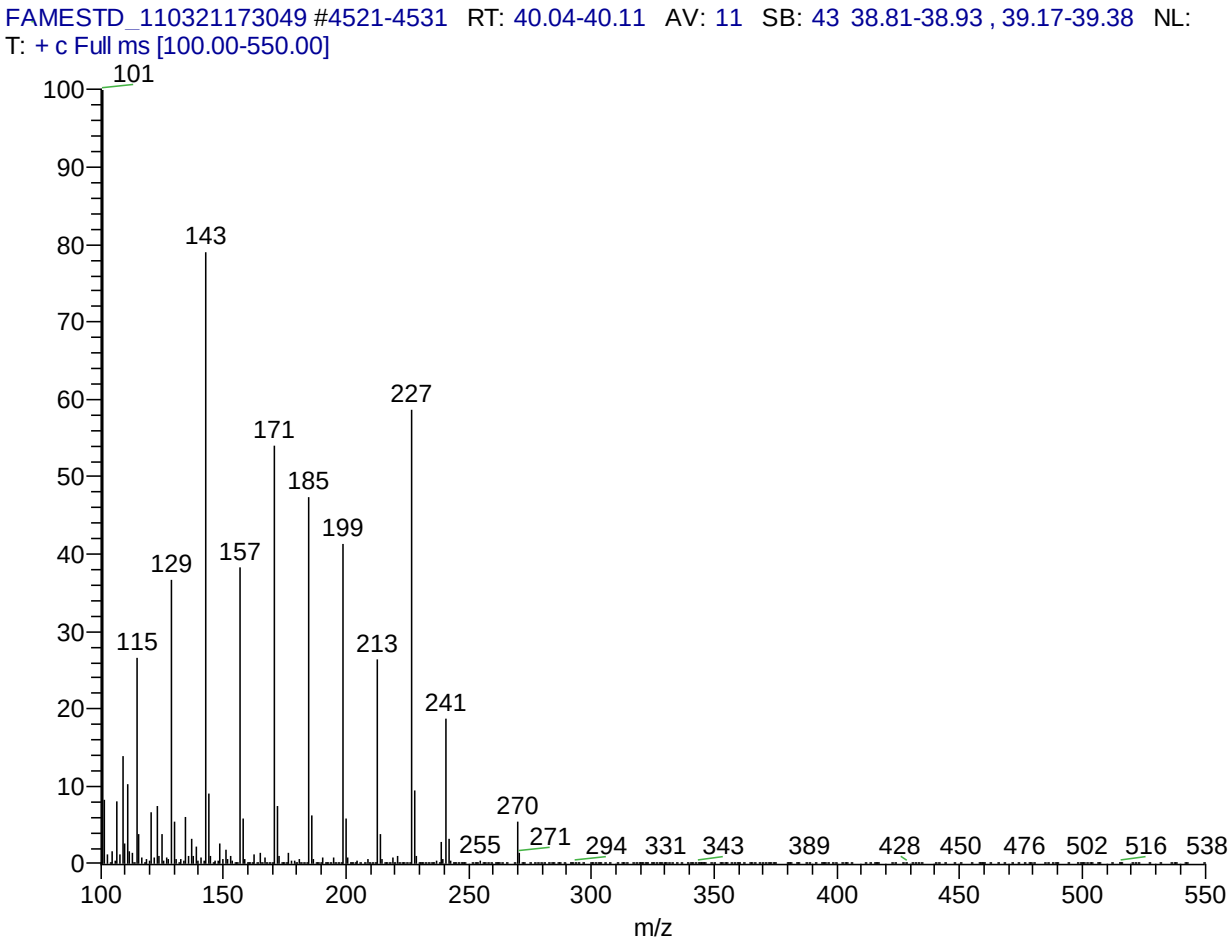

Figure A.10: FAME Standard EI Mass Spectrum at RT 40.09 minutes (C:16:0)

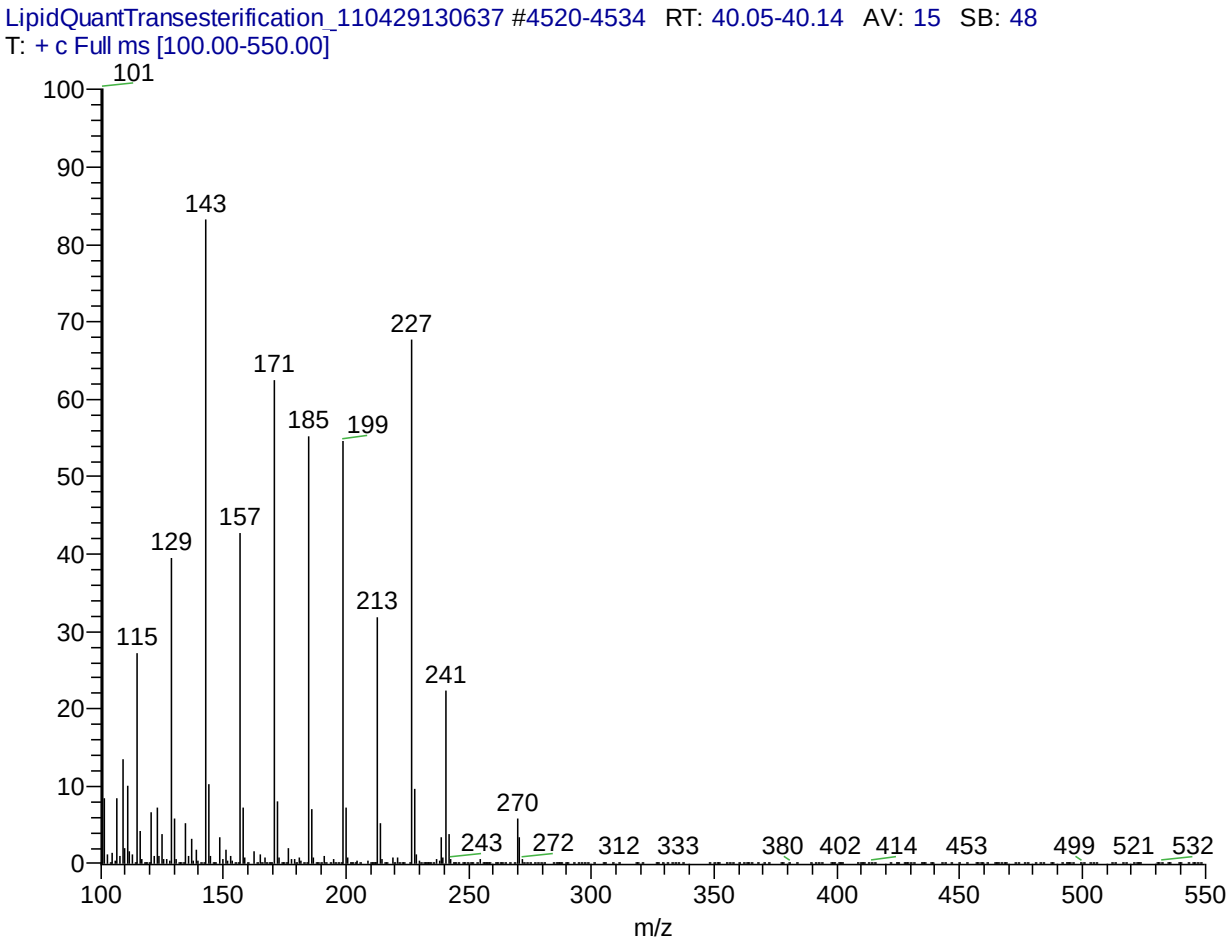

Figure A.11: Transesterification EI Mass Spectrum at RT 40.13 minutes (C:16:0)

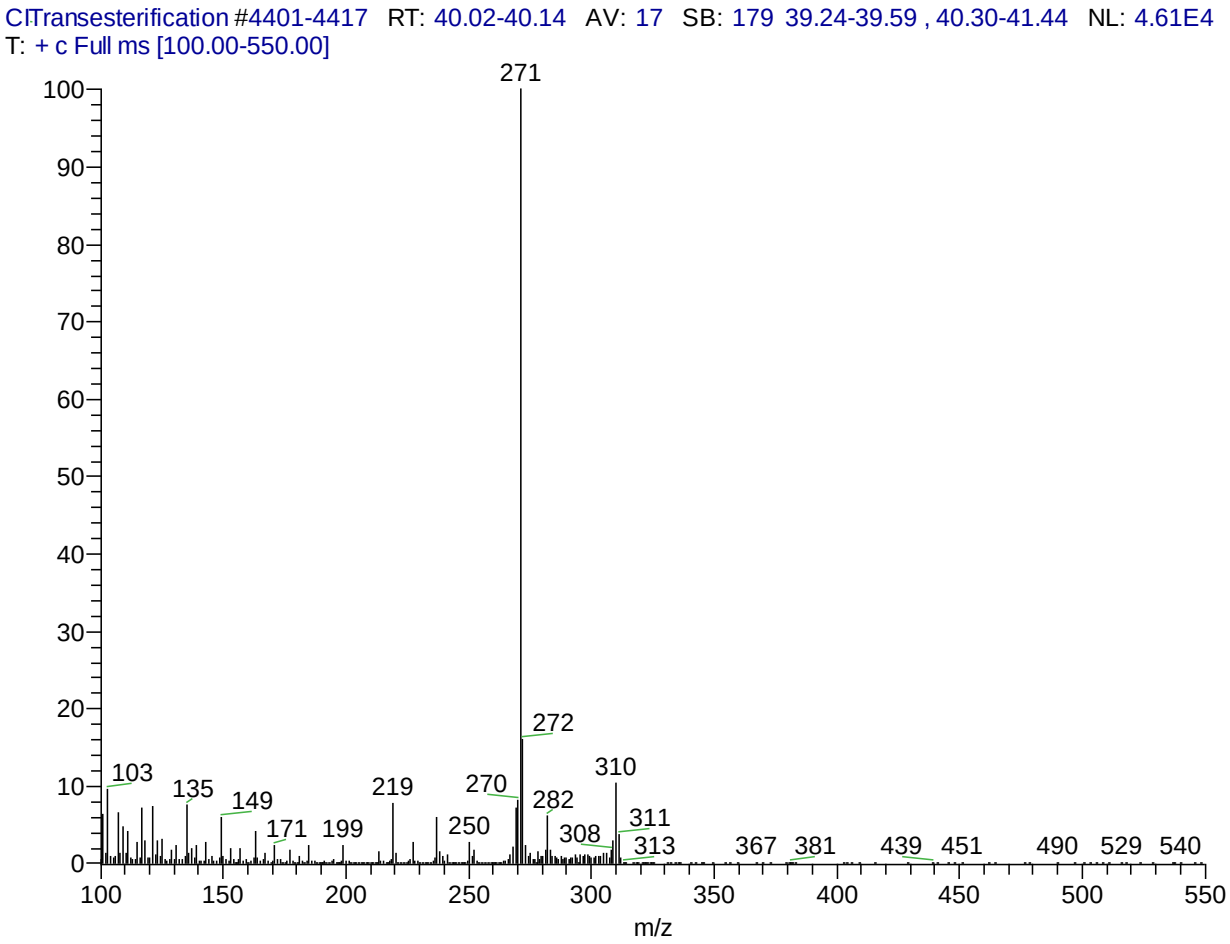

Figure A.12: Transesterification CI Mass Spectrum at RT 40.11 minutes (C:16:0)

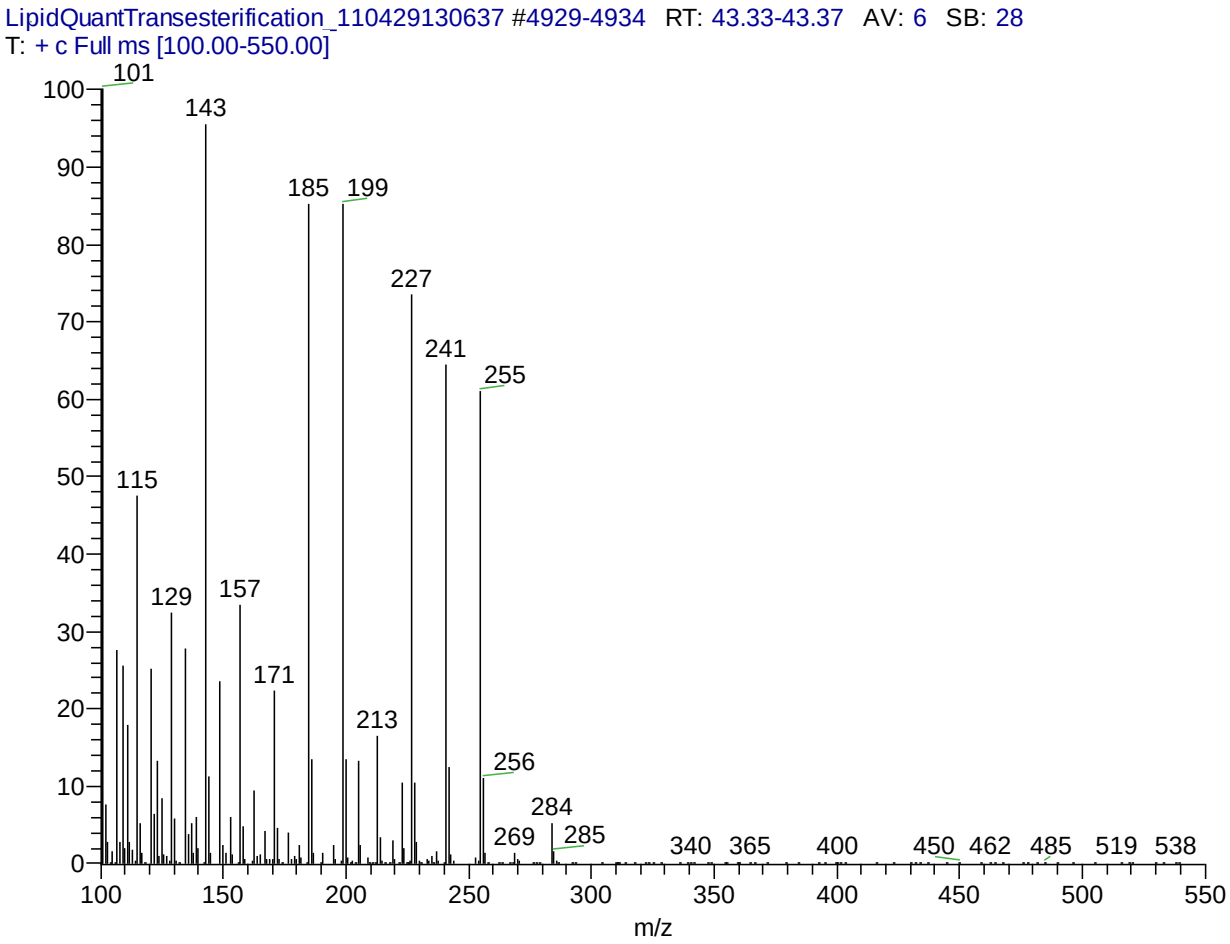

Figure A.13: Transesterification EI Mass Spectrum at RT 43.36 minutes (C:17:0)

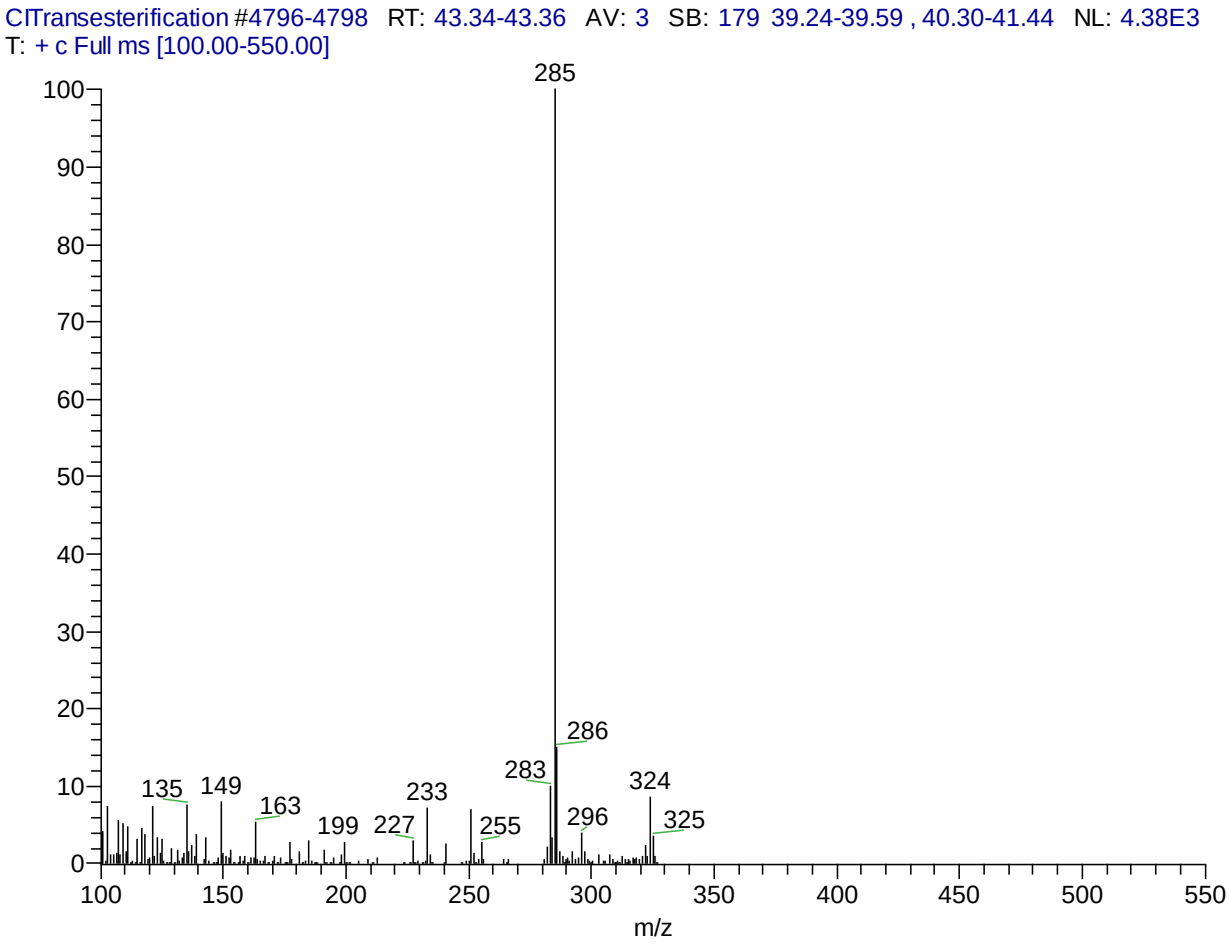

Figure A.14: Transesterification CI Mass Spectrum at RT 43.35 minutes (C:17:0)

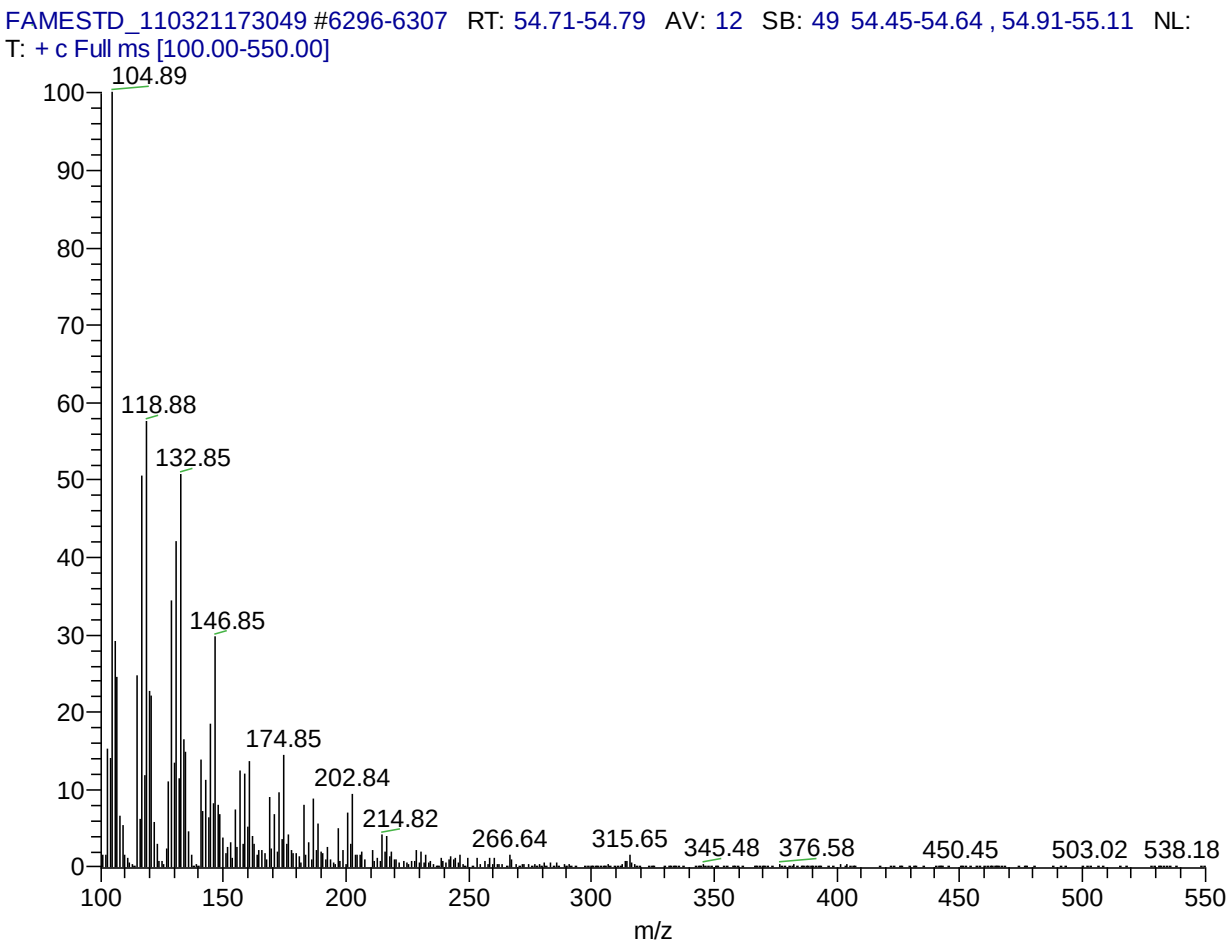

Figure A.15: FAME Standard EI Mass Spectrum at RT 54.54 minutes (C:20:5)

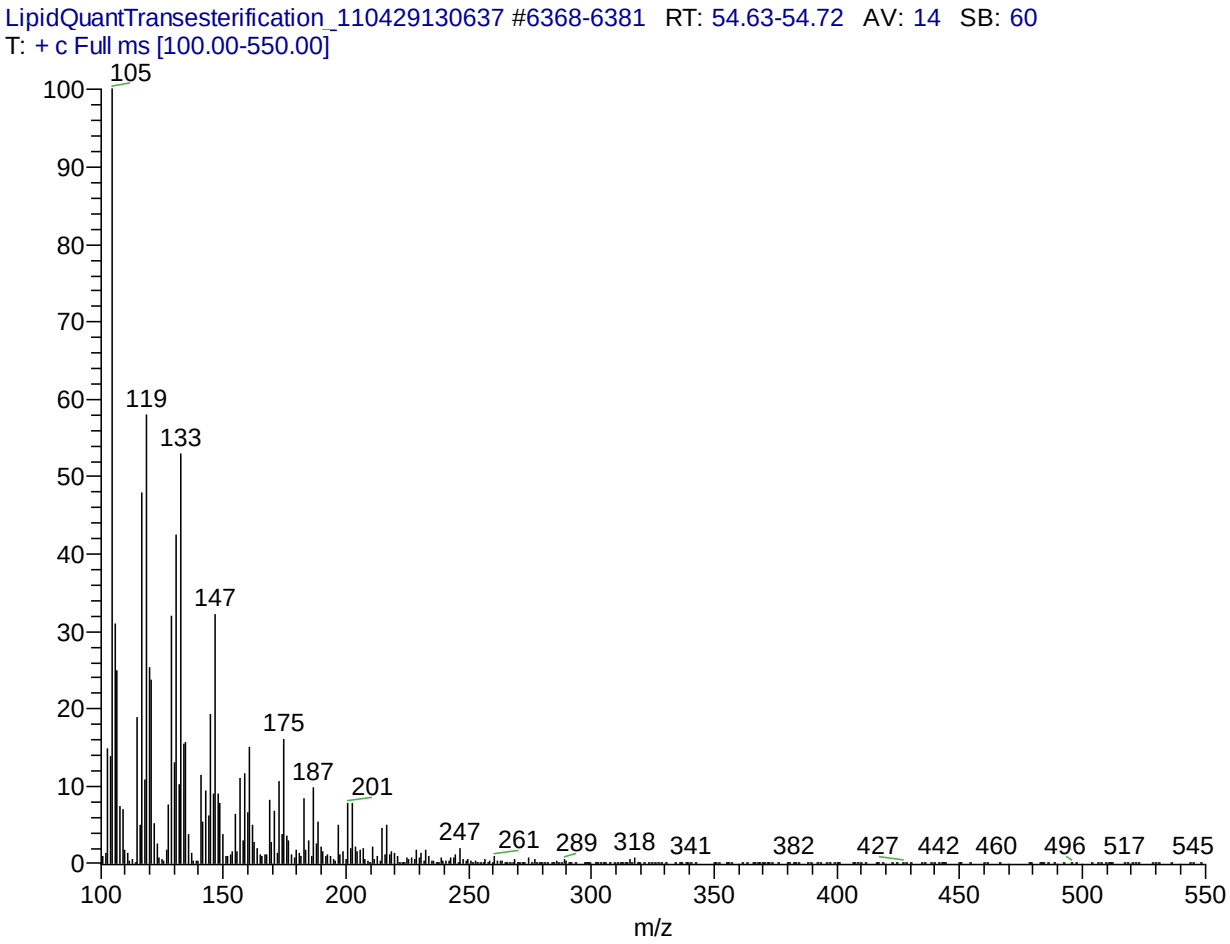

Figure A.16: Transesterification EI Mass Spectrum at RT 54.69 minutes (C:20:5)

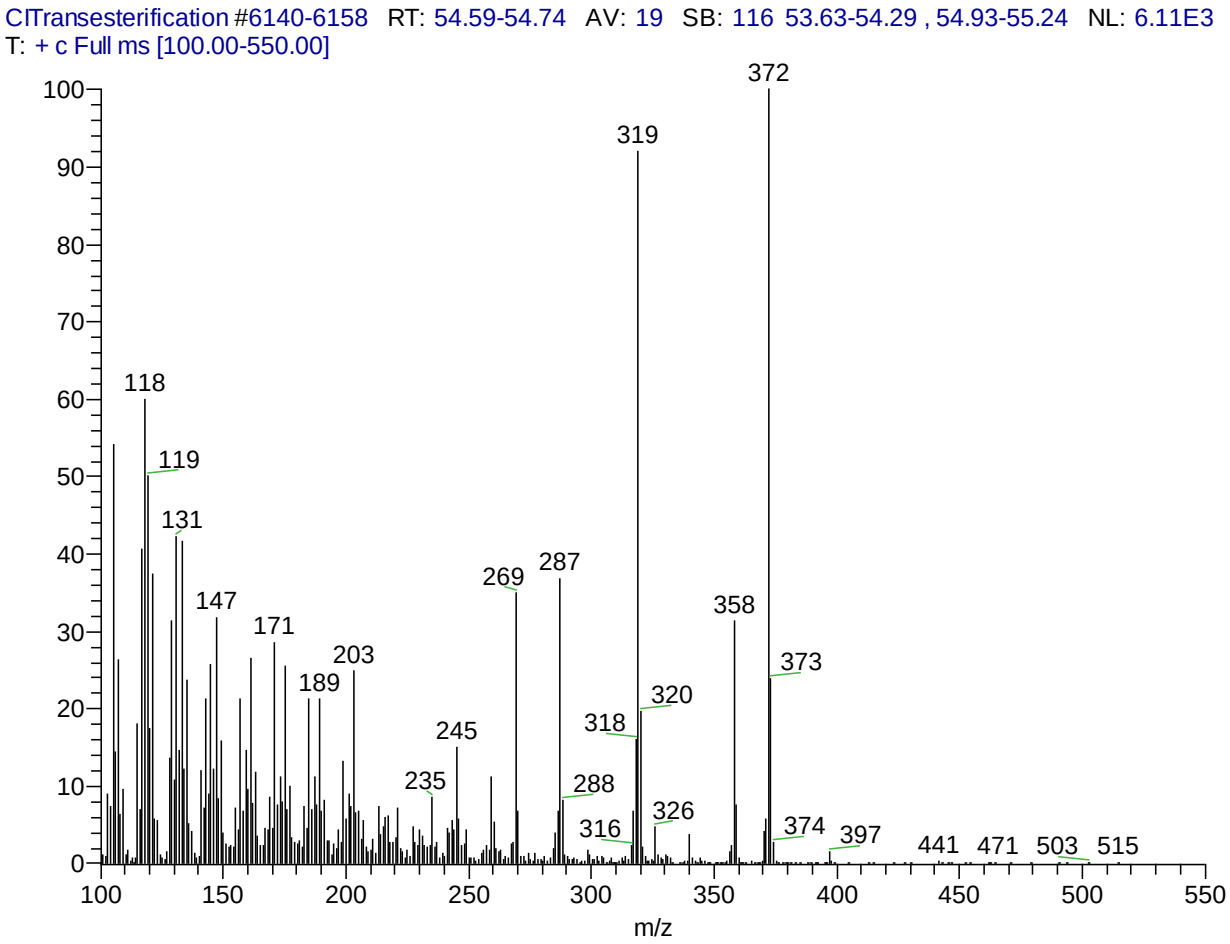

Figure A.17: Transesterification CI Mass Spectrum at RT 54.70 minutes (C:20:5)

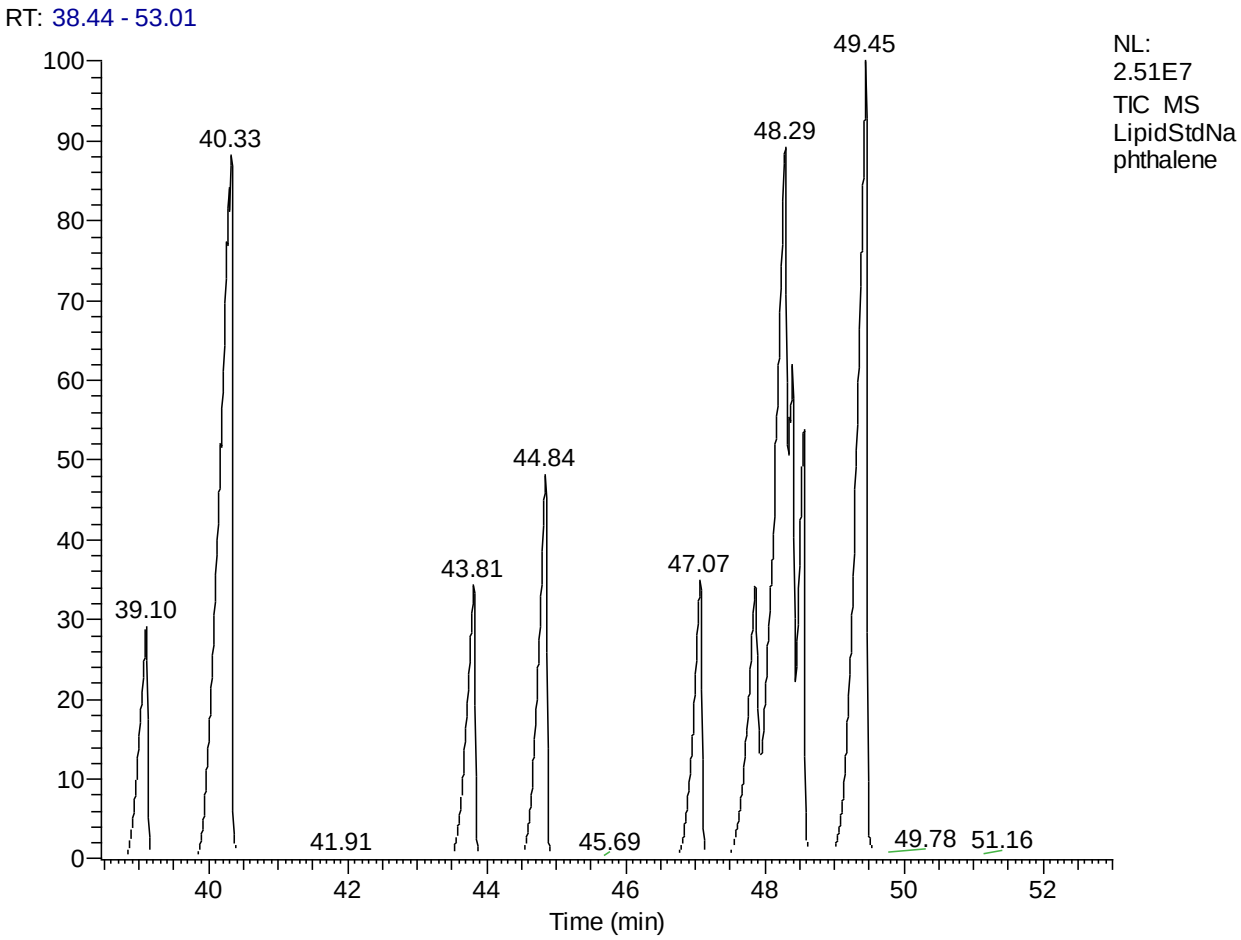

Figure A.18: EI Chromatogram of C:14-C:20

Figure A.21: *C. freiburgensis* in three different media; Left- BP water & NaNO3, Center- MAM, Right- Acidified Bold Basal Medium

Figure A.22: *C. freiburgensis* in MAM in culture chamber.

Table A.3: Modified Acid Medium Recipe

Modified Acid Medium (MAM)						
Chemical	**Formula**	**M.W.**	**Stock Solution**		**Final Concentration**	
Macronutrients			weight (g/L)	addition (mL/L)	mg/L	mM
Ammonium sulphate	$(NH_4)SO_2$	131.70	20.00	10.00	200.46	1.52
Calcium chloride	$CaCl_2$ *2(H_2O)	146.99	0.80	10.00	7.99	0.06
Magnesium sulphate	$MgSO_4$*7(H_2O)	246.36	50.00	10.00	499.91	2.03
Potassium phosphate	KH_2PO_4	139.09	30.00	1.00	29.99	0.22
Sodium chloride	NaCl	58.44	2.40	10.00	23.99	0.41
Na-EDTA		372.24	1.60	10.00	16.00	0.04
Potassium sulphate	K_2SO_4	174.25	19.20	9.00	172.80	1.10
Micronutrients						
Ammonium molybdate	$(NH_4)_6Mo_7O_{24}$*4(H_2O)	1145.57	10.00	1.00	10.22	0.01
Boric Acid	H_3BO_3	61.83	10.00	1.00	10.00	0.16
Colbalt chloride	$CoSO_4$*6(H_2O)	237.90	30.00	1.00	29.89	0.13
Copper sulphate	$CuSO_4$*5(H_2O)	249.81	60.00	1.00	59.99	0.24
Ferrous ammonium sulphate	$Fe(NH_4)2(SO_4)_2$*6(H_2O)	392.04	1170.00	1.00	1169.42	2.93
Manganese sulphate	$MnSO_4$*4(H_2O)	223.05	690.00	1.00	689.66	3.09
Sodium vanadate	$NaVO_3$	121.93	2.00	1.00	2.00	0.02
Zinc sulphate	$ZnSO_4$*7(H_2O)	287.54	370.00	1.00	370.07	1.29
Vitamins						
Thiamine-HCl B1		337.27	50.00	0.67	100.00	0.30
Cyanocobalamin B12				1.30	1.00	

*Combine 10 ml of each micronutrient to make a stock solution. Add 10 ml of stock micronutrients solution to a 9476 ml of de-ionized water. Add 10 ml of each macronutrient except KH_2PO_4 and K_2SO_4. Add 10 ml of KH_2PO_4 and 90 ml of K_2SO_4. Weigh 0.03 g of B_1 and add to solution. Add 13.0 ml of B_{12} to bottle and mix well.

SIGNATURE PAGE

This is to certify that the thesis prepared by Amanda Mondloch entitled "Analysis of Lipids from *Chromulina freiburgensis* for their Potential Use as Biofuels" has been examined and approved for acceptance by the Department of Interdisciplinary Sciences, Montana Tech of The University of Montana, on this 2nd day of March, 2012.

Doug Cameron, Phd, Professor of Analytical Chemistry and
Department Head
Department of Chemistry & Geochemistry
Chair, Examination Committee

Marisa Pedulla, Phd, Associate Professor
Department of Biological Sciences
Member, Examination Committee

Grant Mitman, Phd, Professor
Department of Biological Sciences
Member, Examination Committee

Katie Hailer, Phd, Assistant Professor
Department of Chemistry & Geochemistry
Member, Examination Committee